1993

The gas-phase thermal chemistry of tetralin and related model systems

James Louis Malandra
Iowa State University

Order Number 9321193

The gas-phase thermal chemistry of tetralin and related model systems

Malandra, James Louis, Ph.D.

Iowa State University, 1993

U·M·I
300 N. Zeeb Rd.
Ann Arbor, MI 48106

The gas-phase thermal chemistry of tetralin and related model systems

by

James Louis Malandra

A Dissertation Submitted to the
Graduate Faculty in Partial Fulfillment of the
Requirements for the Degree of
DOCTOR OF PHILOSOPHY

Department: Chemistry
Major: Organic Chemistry

Approved:

Signature was redacted for privacy.

In Charge of Major Work

Signature was redacted for privacy.

For the Major Department

Signature was redacted for privacy.

For the Graduate College

Iowa State University
Ames, Iowa

1993

TABLE OF CONTENTS

LIST OF FIGURES

LIST OF TABLES

PAPER 2

PAPER 5

GENERAL INTRODUCTION

For the past decade, workers in the Trahanovsky research group have been studying the gas-phase thermal decomposition of simple organic molecules as model systems of various features of coal structure. The hydrocarbon tetralin, the simplest hydroaromatic compound, has been studied as a model of this important structural feature of coal. Previous studies on the decomposition of tetralin have shown that tetralin decomposes to produce the dehydrogenation products 1,2-dihydronaphthalene and naphthalene, the ethylene-loss products benzocyclobutene and styrene, and other products such as indene and *o*-allyltoluene in smaller amounts. Pyrolysis studies in the literature using conventional heating techniques produced primarily dehydrogenation products, while in laser-induced decomposition and shock tube experiments ethylene loss predominated. It has been suggested that catalytic dehydrogenation is occurring using the conventional pyrolysis techniques. Our purpose has been to clarify these discrepancies and to determine to what extent, if any, heterogeneous surface catalysis is involved in the decomposition of tetralin. Additionally, we have been interested in the mechanism of tetralin decomposition and have designed several model compounds to probe the viability of various mechanistic pathways. The five papers in this dissertation describe our studies of tetralin decomposition and related model systems using the techniques of laser-induced decomposition, flash vacuum pyrolysis (FVP), and flow pyrolysis.

In paper 1, studies of the gas-phase thermal decomposition of tetralin itself are presented. This paper is part of a collaborative project with Professor Edward S. Yeung and the experimental work involving laser-induced decomposition is part of the Ph.D. dissertation of Jianzhong Zhu (Iowa State University, 1989). Paper 2 contains the

results of the decomposition of two systems related to tetralin, ketone 3-benzocycloheptenone and sulfone 1,3,4,5-tetrahydro-2-benzothiepin-2,2-dioxide. In papers 3 and 4, the FVP of bis(*o*-allylbenzyl) oxalate and 1,4-diphenylbutane, respectively, are described. Paper 5 concerns the FVP of *o*-allyltoluene, a primary product in tetralin decomposition.

Explanation of Dissertation Format

This dissertation consists of five complete papers in the style suitable for publication in journals published by the American Chemical Society. As such, each section has its own numbering system and reference section following the text. Detailed analytical data are contained in an appendix following each section. The research described in the results and experimental sections was done by the author unless otherwise indicated. Paper 1 is the result of a collaborative project as described above. The material in paper 1 that is part of the Ph.D. dissertation of Jianzhong Zhu (Iowa State University, 1989) is indicated with a footnote. A general summary follows the final paper.

PAPER 1. THE GAS-PHASE THERMAL DECOMPOSITION OF TETRALIN

INTRODUCTION

Our recent research efforts have been directed toward understanding the gas-phase thermal chemistry of tetralin (**1**). In previous work, **1** has been used as a hydrogen-donor solvent for coal liquefaction processes[1] and, as the simplest hydroaromatic compound, has been studied as a model of this important structural feature of coal.[2] The gas-phase chemistry of **1** at elevated temperatures has been examined under static, flow, and vacuum pyrolysis conditions,[3,4] through sensitized laser-induced thermal decomposition,[5,6] and in single-pulse shock tube experiments.[7] The major products of tetralin thermal decomposition (Scheme I) include primary products 1,2-dihydronaphthalene (**2**), benzocyclobutene (**3**), and *o*-allyltoluene (**4**). Secondary products, naphthalene (**5**) from **2**, styrene (**6**) from **3**, 2-methylindan (**7**)[8] from **4**, and indene (**8**) primarily from **7**, have been identified along with various minor products.

Analysis of the complex tetralin product mixtures is simplified by treating the "hydrogen-loss" or dehydrogenation products 1,2-dihydronaphthalene (**2**) and naphtha-

Scheme I

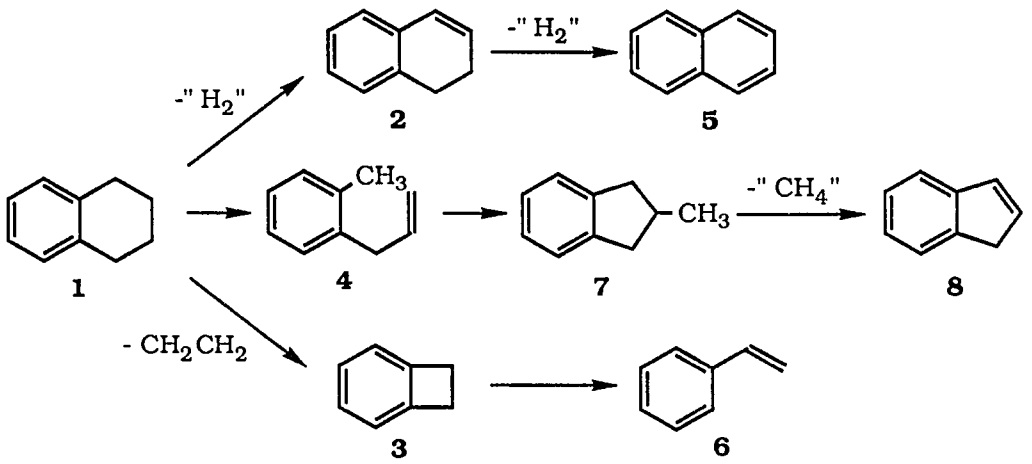

lene (**5**) together. Similarly, benzocyclobutene (**3**) and styrene (**6**) are also considered as a group and referred to as "ethylene-loss" products. The ratio of dehydrogenation to ethylene loss will be used to evaluate tetralin pyrolysis mixtures.

Gas-phase pyrolysis[4] of **1** has been reported to give primarily dehydrogenation, while laser-induced decomposition[5] and single-pulse shock tube studies[7] gave primarily ethylene loss. It has been suggested that surface catalytic effects have influenced the pyrolysis results.[5b] In this paper, we report our reexamination of the thermal decomposition of **1** under both laser-induced and pyrolysis conditions.

In our experiments, the laser-sensitized decomposition of **1** produced primarily dehydrogenation. These results are at variance with those previously reported;[5] however, our gas-phase pyrolysis results confirm that the lowest energy unimolecular decomposition reaction of **1** is ethylene loss. We show that the excess dehydrogenation observed is not the result of a surface catalytic effect. We believe a bimolecular reaction sequence produces excess dehydrogenation under some conditions.

RESULTS

Primary Pathways in Tetralin Decomposition

Laser-induced decomposition[6]

We have studied the laser-induced decomposition of tetralin (**1**) under reaction conditions and analytical procedures that were chosen to match closely those reported earlier.[5] Three types of laser-induced decomposition experiments were performed: direct multiphoton dissociation (MPD),[10] sensitized thermal decomposition by pulsed IR laser,[11] sensitized thermal decomposition by continuous wave (cw) IR laser.

In the MPD of **1** (Table I), ethylene loss to form benzocyclobutene (**3**) and styrene (**6**) is clearly the major reaction pathway. This result is in agreement with the previous study.[5]

The laser-induced sensitized pyrolysis of **1** has also been examined. In our experiments, no part of the cell felt warm to the touch even at the highest laser powers used

Table I. Products and dehydrogenation to ethylene loss ratio from MPD of tetralin (**1**) [a,b]

			yield, % [c]					
pulses	conversion, % [d]	ratio $\frac{(2+5)}{(3+6)}$	**2**	**5**	**3**	**6**	**4**	other prods.
950	1.3	0.45	25.1	4.4	54.1	11.0	—	5.4
2812	2.3	0.61	26.0	8.9	48.2	9.0	7.5	0.4

[a] MPD conditions: laser energy = 1.6 J pulse^{-1}, $\bar{\nu}$ = 944.2 cm^{-1}, cell = 10- x 2-cm (id), **1** = 0.325 torr. [b] Amounts determined by GC with a known quantity of biphenyl added as standard. [c] Moles of product divided by total moles of products. [d] One minus moles of recovered starting material divided by moles of starting material used.

so that reactions on hot surfaces can be neglected. No decomposition products were found when the reaction mixture was left in the cell for 28 hours without laser irradiation.

A representative selection of the results of the pulsed laser sensitized decomposition of **1** is shown in Table II. The pulse energies for SF_6 and SiF_4 sensitization cannot be compared directly, since the absorption coefficients of the sensitizers are quite different. Regardless of the sensitizer, at low excitation energies and low conversions, dehydrogenation is the dominant reaction. At higher pulse energies, the ratio of dehydrogenation to ethylene loss is *ca.* 1. This is in contrast to earlier reports,[5] where ethylene loss was found to be the major dissociation channel. No fluorinated hydrocarbons were found in the GCMS analysis indicating the sensitizer acts only as a heat-transfer agent.

The results of cw laser-induced thermal decomposition is shown in Table III. Invariably, the major products are associated with dehydrogenation. Longer reaction times are required with SiF_4 to achieve similar conversions because of the difference in absorption coefficients for SiF_4 and SF_6. As expected, substantial conversion to secondary products (**5** and **8**) occurs when the reaction yields are high. The two studies involving SF_6 show that energy density, and not just total energy deposited, is important to the extent of reaction and the "maximum temperature", as was pointed out in the previous work.[5b] No fluorinated hydrocarbons were found in the GCMS analysis indicating the sensitizer acts only as a heat-transfer agent in tetralin decomposition.

To assess the contributions of surface reactions to the overall decomposition process, we studied the dependence of the absolute yields of products on the size and shape of the sample cell at a fixed input laser power of 9 W. Under these conditions, the major

Table II. Products and dehydrogenation to ethylene loss ratio from sensitized pulsed laser-induced decomposition of tetralin (**1**) [a]

laser energy, J pulse^{-1}	pulses	sensitizer (P, torr)	conversion, % [c]	ratio $\frac{(2+5)}{(3+6)}$	yield, % [b]						
					2	**5**	**3**	**6**	**4**	**8**	other prods.
0.04	3420	SF_6 (3) [d]	0.1	>30	75.8	24.2	—	—	—	—	—
0.26	5	SF_6 (3) [d]	0.7	1.0	19.1	22.7	14.9	24.5	12.4	1.6	4.8
0.09	2000	SiF_4 (6) [e]	0.4	>20	63.4	36.5	trace	trace	—	—	0.1
0.11	2500	SiF_4 (6) [e]	3.8	0.99	49.7	trace	50.3	—	—	—	—

[a] See Table I, footnote *b*. [b] See Table I, footnote *c*. [c] See Table I, footnote *d*. [d] Laser-induced pyrolysis conditions: cell = 10- x 2-cm (id), **1** = 0.325 torr. [e] Laser-induced pyrolysis conditions: cell = 5- x 2-cm (id), **1** = 0.325 torr.

Table III. Products and dehydrogenation to ethylene loss ratio from sensitized cw laser-induced decomposition of tetralin (**1**) [a,b]

laser power, W	time	sensitizer (P, torr)	conversion, % [d]	ratio (2+5)/(3+6)	yield, % [c]						
					2	**5**	**3**	**6**	**4**	**8**	other prods.
5.0	12 h	SiF_4 (6)	2.1	>20	100	trace	trace	—	—	—	—
6.6	5 min	SF_6 (3)	1.1	5.8	70.6	14.6	14.7	—	—	—	0.1
14.5	1 min	SF_6 (3)	58.2	1.7	3.1	55.5	1.8	31.9	7.6	0.5	—

[a] Laser-induced pyrolysis conditions: cell = 5- x 2-cm (id), **1** = 0.325 torr. [b] See Table I, footnote *b*. [c] See Table I, footnote *c*. [d] See Table I, footnote *d*.

reaction products are **2** and **5**. For cylindrical cells of length (cm) x internal diameter (cm) of 4 x 3.8, 4 x 2.8, 2 x 2.8, and 1 x 2.8, the measured formation rates (10^{-12} mol s^{-1}) for **2** plus **5** are 121, 52, 1.9, and 0.21, respectively.

Deuterium labeling studies were done to provide additional insight into the mechanism of cw laser sensitized dehydrogenation. In these experiments, the total conversion was kept low to avoid secondary pyrolysis products. Dehydrogenation of **1** was the main reaction observed. Two types of studies were performed. In the first series of experiments, the deuterium distribution in **2** was determined for the pyrolysis of 1,1,4,4-d_4-tetralin. The relative amounts of d_0, d_1, d_2, d_3, and d_4 in **2** were found to be 2.0%, 0.8%, 10.9%, 80.2%, and 6.2%, respectively. These distributions are comparable to those obtained in the pulsed laser sensitized pyrolysis of 1,1,4,4-d_4-tetralin.[5]

In a second set of experiments, the deuterium distribution in the hydrogen gas formed during the pyrolysis of 1:1 mixtures of **1** and d_{12}-**1** were measured. The relative amounts of H_2, HD, and D_2 were found to be 53:35:12 at laser power 8.6 W with a 3 min irradiation time. These results are also consistent with those reported earlier.[5]

To assess the importance of hydrogen atom chain reactions, we studied the effect of potential chain terminators on the cw pyrolysis of **1**. Table IV shows sets of experiments involving the addition of potential chain terminators. Ideally, the species added should be in large excess; however, the maximum temperature may vary due to a change in the effective thermal conductivity of the gas.[12] Conversion was maintained low enough to avoid secondary pyrolysis reactions yet sufficiently high to allow reliable analysis of the products.

Table IV shows that the addition of toluene as a potential chain terminator[13] to the pyrolysis mixture slightly lowered the fraction of dehydrogenation products. There is a noticeable decrease in the total conversion that is consistent with a decrease in tem-

Table IV. Products and dehydrogenation to ethylene loss ratio from sensitized cw laser-induced decomposition of tetralin (**1**) in the presence of hydrogen atom chain terminators [a,b]

chain terminator (P, torr)	time (s)	conversion, % [d]	ratio (2+5)/(3+6)	yield, % [c]						
				2	**5**	**3**	**6**	**4**	**8**	other prods.
none (—)	120	2.7	2.1	56.6	6.6	19.2	11.0	4.8	1.8	—
toluene (1.0)	120	0.9	1.4	53.5	4.7	35.7	6.0	—	—	—
HI (0.2)	60	0.8	3.9	70.0	9.2	11.2	9.2	—	—	—
HI (1.0)	60	1.0	2.3	70.0	trace	30.0	trace	—	—	—
iodine (0.25)	60	0.2	73	50.7	44.0	1.3	—	—	—	3.6 [e]

[a] Laser-induced pyrolysis conditions: laser power = 9.0 W, cell = 4.0- x 3.5-cm (id), **1** = 0.325 torr, SF_6 = 6.0 torr. [b] See Table I, footnote *b*. [c] See Table I, footnote *c*. [d] See Table I, footnote *d*. [e] Two products with retention times longer than **5** whose structures were not determined, but are likely to be iodine substitution products.

perature of the heated gas due to the higher thermal conductivity of toluene. The simultaneous decrease in the transmission of laser light through the cell independently confirms this.[12]

When HI is used as a potential chain terminator, Table IV shows that the total conversion decreases, presumably due to a decrease in reaction temperature. The contribution of dehydrogenation to the overall reaction is however increased relative to ethylene loss. We found that deposits of I_2 are visible on the cell walls after these pyrolysis experiments. Laser excitation of a mixture of HI and SF_6 alone did not produce any observable I_2 deposits under similar conditions.

Then I_2 was used as a potential chain terminator and as a check to determine if the I_2 produced in the HI experiments above had biased the results. Table IV shows that the amount of dehydrogenation increased markedly. This is likely due to an iodine atom induced dehydrogenation. The direct production of iodine atoms at room temperature by laser photolysis of I_2 (45 mW, 576.601 nm, 20 min)[14] did not produce any dissociation in **1**. This is not unexpected since there should exist a reasonable energy barrier for the reaction of iodine atom with **1**.

We also studied the effect of potential hydrogen-atom assisted dissociation of **1**. Hydrogen atoms can be produced either by room temperature laser photolysis or by cw laser sensitized reaction at high temperatures. Photolysis of HI at 308 nm produces visible deposits of I_2 on the cell walls, indicating dissociation of HI to generate hydrogen atoms. A mixture of **1** (0.325 torr), SF_6 (6.0 torr) and HI (3.7 torr) was laser irradiated (308 nm, 147 mJ $pulse^{-1}$, 3000 pulses) in the gas cell used in the laser sensitized experiments after quartz windows were installed. Only four product peaks were found by GCMS analysis, giving a total conversion of 1.4% of **1**. These have *m/e* of 134 (30%), 136

(10%), 136 (10%), and 138 (50%), respectively. These clearly are hydrogen addition products of **1**. 1,2-dihydronaphthalene (**2**) was not detected.

We have also studied the reaction between hydrogen atoms and **1** at elevated temperatures (cw laser-sensitized reaction). Hexamethylethane decomposes to produce hydrogen atoms as an intermediate.[13] Isobutene (6.5%) was identified when a mixture of hexamethylethane (2.0 torr) and SF_6 (6.0 torr) was irradiated by a cw laser (944.2 cm^{-1}, 5.0 W, 180 s), indicating that hydrogen atoms are indeed produced under these conditions. When hexamethylethane (2.0 torr) was copyrolyzed with **1** (0.30 torr), butylbenzene (m/e = 134) was the primary product (1.1%). Only a trace of **2** was found. In the absence of hexamethylethane, only a trace of **2** was found in the product analysis of the sensitized pyrolysis of **1** under identical conditions.

Flash vacuum and flow pyrolysis

The yields of key flash vacuum pyrolysis (FVP) products of tetralin (**1**) vary with experimental conditions. Product yields are not only effected by the oven temperature but other experimental conditions, such as system pressure and sample temperature, as well.

In the FVP of **1** at 10^{-5} torr, the ratio of 1,2-dihydronaphthalene (**2**) and naphthalene (**5**) to benzocyclobutene (**3**) and styrene (**6**) remains *ca.* 1 (0.90–1.03) from 850 to 950 °C and finally drops to 0.73 at 1000 °C (Table V, Figure 1). On the other hand, when **1** is pyrolyzed at 0.10 torr a distinct drop in the dehydrogenation to ethylene loss ratio, from 2.70 to 0.72 (Table VI, Figure 1), with increasing pyrolysis temperature is observed. In Figure 1, conversion was plotted rather than oven temperature because the former is a better indicator of the actual reaction temperature.

Table V. Total recovery of material, conversion, and dehydrogenation to ethylene loss ratio from FVP of tetralin (**1**) at 10^{-5} torr and various oven temperatures [a,b,c]

oven temp., °C	recovery, % [d]	conversion, % [e]	ratio (**2**+**5**)/(**3**+**6**)
850	90.0	4.8	0.90
900	85.6	17.2	1.03
950	80.4	34.4	0.92
1000	76.2	65.4	0.73

[a] FVP conditions: system pressure = 1 x 10^{-5} torr, sample temperature = 0 °C. [b] See Table I, footnote *b*. Data represent the average of triplicate runs. [c] See Table A-I in the Appendix of Paper 1, this dissertation, for a more detailed analysis. [d] Total moles of recovered material divided by moles of starting material used. [e] Total moles of recovered material minus moles of recovered starting material divided by total moles of recovered material.

The influence of sample temperature on the pyrolysis of **1** was also investigated at three sample temperatures from -30 °C to room temperature (900 °C, 10^{-5} torr). These data are presented in Table VII and clearly show a low sample temperature results in lower conversion and less dehydrogenation relative to ethylene loss.

The possibility that bimolecular or surface reactions were responsible for the above results lead to some additional experiments. To minimize collisions between hot tetralin molecules with each other and with the quartz surface of the oven, tetralin vapor was mixed with a large amount of argon (*ca.* 4500:1 mole ratio of argon to tetralin). This mixture was introduced into an evacuated pyrolysis oven through a flow system (Figure 2).

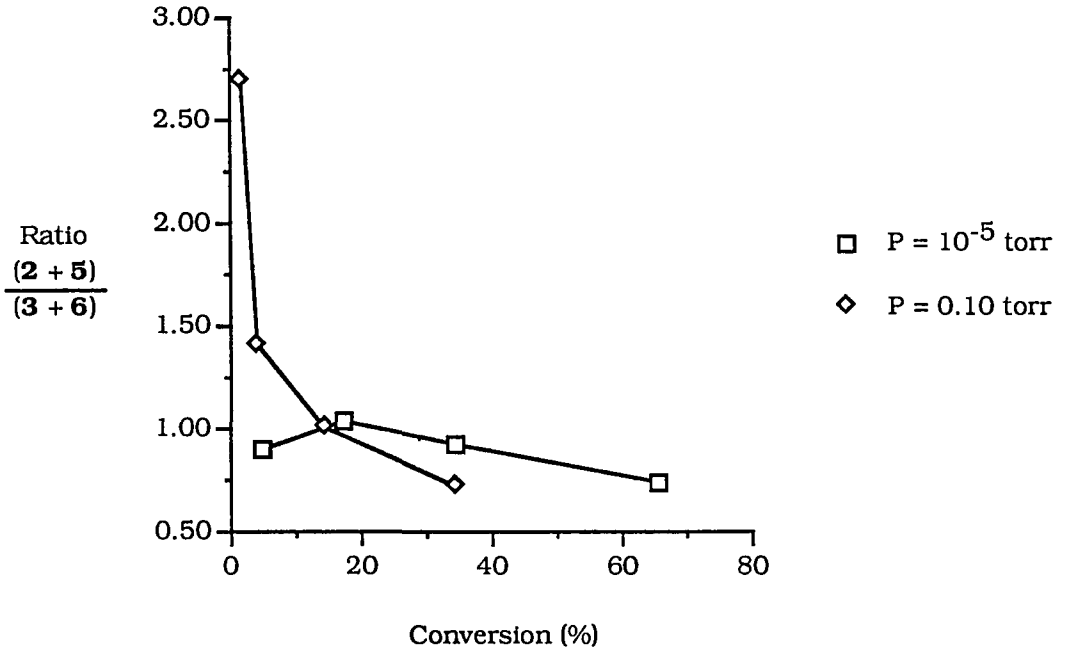

Figure 1. The dehydrogenation to ethylene loss ratio vs. conversion at two system pressures (sample temperature, 0 °C)

Table VI. Total recovery of material, conversion, and dehydrogenation to ethylene loss ratio from FVP of tetralin (**1**) at 0.10 torr and various oven temperatures [a,b,c]

oven temp., °C	recovery, % [d]	conversion, % [e]	ratio **(2+5)/(3+6)**
750	91.8	1.4	2.70
800	92.0	3.7	1.41
850	83.8	14.3	1.01
900	85.2	34.3	0.72

[a] FVP conditions: system pressure = 0.10 torr, sample temperature = 0 °C. [b] See Table V, footnote *b*. [c] See Table A-II in the Appendix of Paper 1, this dissertation, for a more detailed analysis. [d] See Table V, footnote *d*. [e] See Table V, footnote *e*.

Table VII. Total recovery of material, conversion, and dehydrogenation to ethylene loss ratio from FVP of tetralin (**1**) at 10^{-5} torr and various sample temperatures [a,b,c]

sample temp., °C	recovery, % [d]	conversion, % [e]	ratio (**2**+**5**)/(**3**+**6**)
-30	85.2	13.4	0.39
0	86.7	20.7	0.84
RT	80.8	30.2	2.09

[a] FVP conditions: oven temperature = 900 °C, system pressure = 1 x 10^{-5} torr. [b] See Table V, footnote *b*. [c] See Table A-III in the Appendix of Paper 1, this dissertation, for a more detailed analysis. [d] See Table V, footnote *d*. [e] See Table V, footnote *e*.

When **1** is pyrolyzed under flow conditions (Table VIII), the major products are benzocyclobutene (**3**) and styrene (**6**). In fact, ethylene loss exceeds dehydrogenation by a ratio of between 3 and 5 to 1, over a wide temperature and conversion range.

Secondary Pathways in Tetralin Decomposition

To develop a complete picture of tetralin thermal decomposition, it was necessary to examine the chemistry of some of the other products. *o*-Allyltoluene (**4**) is produced in the flow pyrolysis of tetralin (**1**) at 800 °C (Table VIII), along with the other initially formed products, 1,2-dihydronaphthalene (**2**), benzocyclobutene (**3**), and styrene (**6**). At higher temperatures, increasing amounts of styrene (**6**), 2-methylindan (**7**), indene (**8**), and naphthalene (**5**) are present. To clarify the origin of some to these secondary products, *o*-allyltoluene (**4**) and 1,2-dihydronaphthalene (**2**) were pyrolyzed separately.

When **4** is pyrolyzed in the flow apparatus (Table IX), the major reaction observed is isomerization of **4** to **7**. At higher temperatures, **7** is further converted to **8**. Numerous other products are produced in smaller amounts, including **1**, **2**, **3**, **5**, and **6**. Although small amounts of **3**, **5**, and **6** appear to be produced directly from **4** below 800 °C, it is likely that most of the **2**, **3**, **5**, and **6** observed at higher temperatures result from secondary pyrolysis of **1**.

1,2-Dihydronaphthalene (**2**) was also pyrolyzed under conditions similar to those used for the flow pyrolysis of **1** and **4**. These results are summarized in Table X. As expected, the major product is **5**. Even at high temperatures, products other than **5** constitute only a small percentage of the pyrolysate.

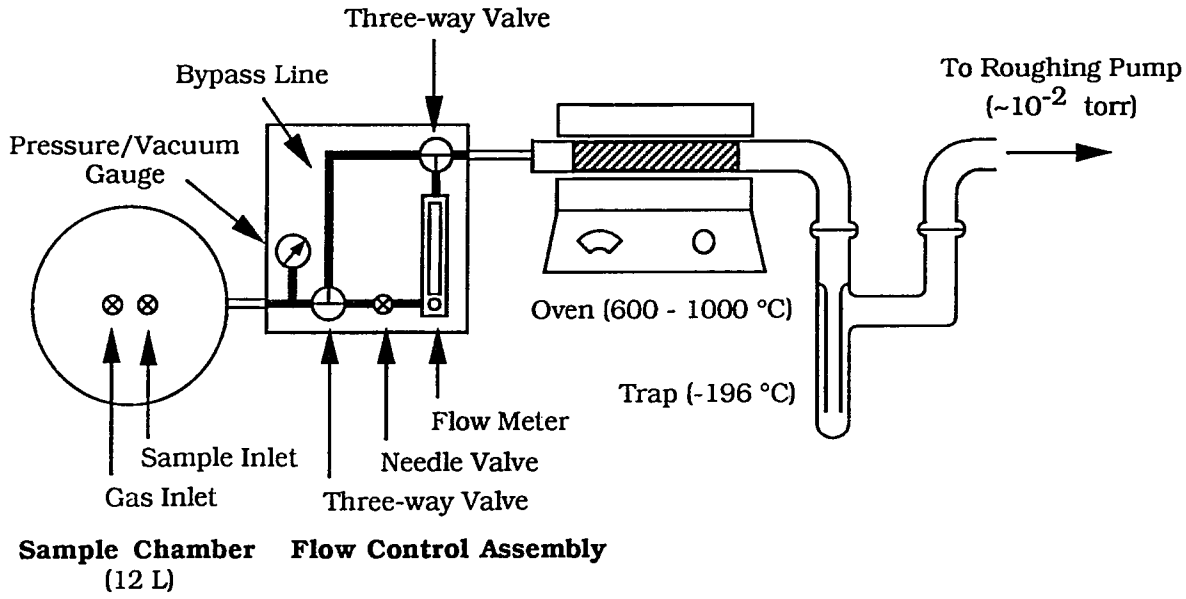

Figure 2. Schematic diagram of flow pyrolysis apparatus

Table VIII. Products and recovered starting material and dehydrogenation to ethylene loss ratio from flow pyrolysis of tetralin (**1**) at various oven temperatures [a,b]

oven temp., °C	recovery, % [d]	conversion, % [e]	ratio (2+5)/(3+6)	yield, % [c]								
				1	**2**	**5**	**3**	**6**	**4**	**7**	**8**	other prods.
800	89.0	1.5	0.40 [f]	98.5	0.4 [f]	—	0.9	<0.1	0.2	—	—	—
850	89.2	9.3	0.28	90.7	1.1	0.5	4.7	1.1	1.1	0.6	0.2	—
900	93.4	22.7	0.22	77.3	1.7	1.4	9.9	4.6	1.9	1.7	1.0	0.3 [g]
950	85.3	53.9	0.21	46.1	2.2	5.0	13.9	20.7	2.2	2.9	4.3	2.8 [g]

[a] Flow pyrolysis conditions: system pressure = 1 x 10^{-2} torr, flow rate = 24 mL min^{-1} (Ar), residence time = 0.31 s. [b] See Table V, footnote *b*. Data at 850 °C represent the average of six runs. [c] Moles of product divided by total moles of recovered material. [d] See Table V, footnote *d*. [e] See Table V, footnote *e*. [f] At low conversion, the peak for **2** is on the tail of the large peak for **1**, enhancing the apparent amount of **2**. [g] See Table A-IV in the Appendix of Paper 1, this dissertation, for a more detailed analysis.

Table IX. Products and recovered starting material from flow pyrolysis of *o*-allyltoluene (**4**) at various oven temperatures [a,b]

	yield, % [c]					
entry	700 °C	750 °C	800 °C	850 °C	900 °C	950 °C
o-allyltoluene (**4**) [d]	94.0	83.6	71.0	30.9	12.7	5.8
2-methylindan (**7**)	2.1	8.4	17.8	34.8	28.7	13.1
indene (**8**)	0.7	1.4	2.0	9.7	23.9	39.9
tetralin (**1**)	0.3	0.8	2.0	5.2	5.4	3.9
1,2-dihydronaphthalene (**2**)	0.6	1.4	0.5	1.0	0.8	0.5
naphthalene (**5**) [d]	0.1	0.3	0.1	0.9	1.1	2.5
benzocyclobutene (**3**)	—	0.2	0.5	1.4	2.8	2.2
styrene (**6**)	—	—	—	0.4	2.3	5.7
other products	2.4 [e]	3.9 [e]	6.3 [e]	15.9 [e]	22.4 [e]	26.8 [e]
recovery [f]	84.0	81.2	88.3	74.0	80.1	69.8
conversion [g]	6.0	16.4	29.0	69.1	87.3	94.2

[a] Flow pyrolysis conditions: system pressure = 1 x 10^{-2} torr, flow rate = 24 mL min^{-1} (Ar), residence time = 0.31 s. [b] See Table V, footnote *b*. [c] See Table VIII, footnote *c*. [d] Starting material (yield, %): *o*-allyltoluene (98.1), *m*/*p*-allyltoluene (1.6), naphthalene (0.3). [e] See Table A-V in the Appendix of Paper 1, this dissertation, for a more detailed analysis. [f] See Table V, footnote *d*. [g] See Table V, footnote *e*.

Table X. Products and recovered starting material from flow pyrolysis of 1,2-dihydronaphthalene (**2**) at various oven temperatures [a,b]

	yield, % [c]		
entry	800 °C	850 °C	900 °C
1,2-dihydronaphthalene (**2**) [d]	89.9	73.2	31.1
naphthalene (**5**)	8.7	23.4	61.7
other products	1.4 [e]	3.4 [e]	7.1 [e]
recovery [f]	80.1	90.3	83.1
conversion [g]	10.1	26.8	68.9

[a] Flow pyrolysis conditions: system pressure = 1 x 10^{-2} torr, flow rate = 22 mL min^{-1} (Ar), residence time = 0.31 s. [b] See Table V, footnote *b*. [c] See Table VIII, footnote *c*. [d] Starting material (yield, %): 1,2-dihydronaphthalene (99.7), tetralin (0.3). [e] See Table A-VI in the Appendix of Paper 1, this dissertation, for a more detailed analysis. [f] See Table V, footnote *d*. [g] See Table V, footnote *e*.

DISCUSSION

Dehydrogenation vs. Ethylene Loss in Tetralin Decomposition

Laser-induced decomposition[6]

In the multiphoton dissociation (MPD) of tetralin (**1**), ethylene loss to form benzocyclobutene (**3**) and styrene (**6**) is clearly the major reaction pathway (Table I). The results for the MPD of **1** in this work agree with those in the previous study.[5] It is difficult to compare the fluence of these MPD experiments with those used earlier[15] but considering the beam properties and the optical arrangements, we believe they are comparable. Though we observe no indene (**8**) and more 1,2-dihydronaphthalene (**2**) is observed here than previously reported, the conclusion that ethylene loss is the main decomposition channel in MPD is confirmed.

In this work, the predominant reaction of **1** in the continuous wave (cw) and pulsed laser-induced sensitized decompositions (Table II, Table III) is dehydrogenation to form 1,2-dihydronaphthalene (**2**) and naphthalene (**5**). These results are in disagreement with the previous study,[5] which found that ethylene loss was the main decomposition reaction. Since the MPD results from the two studies agree, it is unlikely that the discrepancies in the pulsed laser sensitized experiments are due to differences in the tetralin purity or analytical procedures used, nor do nonhomogeneous reactions provide a satisfactory explanation.

In the pulsed laser decomposition of **1** shown in Table II, the amount and fraction of ethylene loss increases with laser energy. In the two SiF_4 sensitized pyrolyses, the difference in laser powers is responsible for the results. Though 0.11 J does not seem too different from 0.09 J, our laser shows large pulse-to-pulse variations

at the maximum output range. Although the average energy per pulse is 0.11 J, there are individual pulses as high as 0.15 J throughout the experiment. It is the pulses with the highest power that dominate the pyrolysis process, since yields are exponentially dependent on temperature. The substantially increased yield at 0.11 J also confirms a higher reaction temperature. Unfortunately, we were not able to obtain still higher output levels from our laser at the SiF_4 wavelength to observe a clear-cut cross-over of the two reaction channels.

Tetralin decomposition sensitized by SiF_4 or SF_6 based on cw IR laser excitation has not been reported previously. A major consideration is that one can control the power levels and the power densities much more reliably than with the corresponding pulsed lasers.[16] One expects to find a steady-state temperature gradient starting at a high level at the center of the laser beam (due to cumulative absorption), dropping quickly outside the irradiated region, and eventually equilibrating to the cell walls along a slower temperature gradient than for the pulsed laser.[12] The results in Table III show that the major decomposition reaction of **1** under cw laser-induced sensitized conditions is dehydrogenation.

To assess the contributions of surface reactions to the overall decomposition process, we studied the dependence of the absolute yields of products on the size and shape of the sample cell. The KBr windows in every case should contribute roughly the same amount of surface reactions since the contact areas as well as the distances from the hot gas column are comparable. In fact, since less depletion of laser light and less area for thermal conduction exist in the smallest cell, surface temperatures at the windows there should be the highest. The decomposition rates decrease substantially in the series of experiments from large to small cells indicating that surface reactions at the cell windows cannot be important in the cw laser-induced decomposition.

As for the Pyrex cell walls, the first two absolute yields (4- x 3.8-cm (id) cell, 121 x 10^{-12} mol s^{-1}; 4- x 2.8-cm (id) cell, 52 x 10^{-12} mol s^{-1}; $R_1:R_2 \approx 2:1$) show a decrease in the rate of formation of 1,2-dihydronaphthalene (**2**) and naphthalene (**5**) (the only major products) that is better explained by the difference in the volume of gas heated ($V = \pi r^2 h$, $V_1:V_2 = (3.8)^2:(2.8)^2 \approx 2:1$) than by the decrease in available surface area ($S = 2\pi rh$, $S_1:S_2 = 3.8:2.8 \approx 1:1$). The Pyrex surface area decreased by a factor of four in the last three cells (4- x 2.8-cm (id) cell, 52 x 10^{-12} mol s^{-1}; 2- x 2.8-cm (id) cell, 1.9 x 10^{-12} mol s^{-1}; 1- x 2.8-cm (id) cell, 0.21 x 10^{-12} mol s^{-1}) but the yields decreased by a factor of 360.

It has been shown[12] that smaller cells provide shorter distances for heat conduction from the center of the cell to the cell walls. We confirmed that the smallest cell (1- x 2.8-cm) did feel hot to the touch during laser pyrolysis compared to the larger cells. Since the cell walls are close to room temperature, the heated gas column has a lower temperature in smaller cells for the same incident laser power and this accounts for the dramatic decrease in absolute rates in these experiments. One can therefore conclude that neither the Pyrex cell walls nor the KBr windows contribute to the dehydrogenation of **1** through surface reactions.

Our deuterium labeling results indicate that 1,2-elimination is the primary mode (*ca.* 80%) of dehydrogenation but that *ca.* 10% 1,4- and 10% 2,3-elimination are also involved. However, it is not possible to conclude whether the loss of hydrogen from **1** involves intermolecular processes (e.g., abstraction) or whether isotopic scrambling occurs after decomposition.

The large amount of HD produced in the pyrolysis of a 1:1 mixture of **1** and d^{12}-**1** indicates that at least 80% of the hydrogen is formed by intermolecular pathways. Previous workers[5b] also studied the decomposition of deuterated tetralin

derivatives and concluded that the hydrogen loss was consistent with an 80% stepwise process.

The observation of an excess of dehydrogenation products (**2** and **5**) over ethylene-loss products (**3** and **6**) at low temperatures in itself cannot confirm that the former is the unimolecular decomposition reaction with the lower energy barrier. It is possible that dehydrogenation products are formed as a result of radical chains, which magnify the contributions from that channel. We have already shown above that surface-catalyzed reactions are not important in the production of **2** and **5**. The isotopic studies indicate that hydrogen atoms are formed during pyrolysis. Presumably these can cycle (by reaction with **1**) to produce more dehydrogenation products.

Although chain-induced dehydrogenation may be occurring under our laser-induced pyrolysis conditions, it is not clear why such chains should be more important here than in the previous work.[5] In pulsed laser experiments, the hot zone quickly expands and is cooled by the surrounding gas to quench long chain processes. In cw laser experiments, gases in the heated zone migrate outwards and are also cooled by the surrounding gas. Although the temperature profiles are different in the two cases, the time periods involved for migration from the heated zone to the cold walls are quite similar.

The implication is that the earlier pulsed laser-sensitized study[5] was performed at an effective temperature higher than either the pulsed or cw laser experiments reported here. The sensitizer is excited to high vibrational levels following multiphoton absorption (pulsed experiments). Since V $\rightarrow$ V energy transfer to the reactant is highly favored (compared to V $\rightarrow$ T), the calculated maximum temperature[5b] for pulsed experiments does not adequately describe the non-Boltzmann excitation of the reactants.

Flash vacuum and flow pyrolysis

The interpretation of the results of the FVP of tetralin (**1**) at different system pressures and sample temperatures are not clear-cut. In the initial FVP of **1**, there was a marked difference in the chemistry of the pyrolysis at 10^{-5} torr and 0.10 torr. Changing the system pressure results in different amounts of dehydrogenation relative to ethylene loss at comparable conversions.

The system pressure is one of the factors that determines the residence time of sample molecules in the pyrolysis oven. However, a change in the residence time of **1** in the pyrolysis oven should have no effect on the relative amounts of dehydrogenation and ethylene loss at a given effective temperature if both of the pathways are unimolecular processes. If both 1,2-dihydronaphthalene (**2**) and benzocyclobutene (**3**) had been produced by the unimolecular decomposition of **1**, the dehydrogenation to ethylene loss ratio would have been determined by the ratio of the rate constants for their formation. If this were the case, one might expect the curve representing the ratio of dehydrogenation to ethylene loss (Figure 1) to show the same trend regardless of the system pressure. This is clearly not the case. At low conversion, there is a marked difference between the almost 3 to 1 excess of dehydrogenation to ethylene loss observed at 0.10 torr and the 1 to 1 ratio observed at 10^{-5} torr.

Ultimately, this leads to the conclusion that a substantial portion of either the dehydrogenation or the ethylene-loss products are not produced in an unimolecular gas-phase reaction of **1**. However, it is difficult to imagine how surface catalytic effects or bimolecular reactions would effect ethylene loss. Only catalytic or bimolecular dehydrogenation remain as possible explanations of the variable results from the FVP of **1** with different system pressures and sample temperatures. Catalytic dehydrogenation on the quartz surface should be favored under conditions that maximize surface contact

and minimize collisions between sample molecules, while bimolecular decomposition should be favored under conditions that increase the probability of collisions between sample molecules.

Surface catalytic dehydrogenation would be minimized by short residence time at low system pressure (10^{-5} torr). This could explain the smaller amounts of dehydrogenation products 1,2-dihydronaphthalene (**2**) and naphthalene (**5**) produced when **1** was pyrolyzed at 10^{-5} torr (Table V, Figure 1) as compared to 0.10 torr (Table VI, Figure 1). However, surface effects cannot explain the prevalence of dehydrogenation at high tetralin sample temperature (Table VII). Catalysis on the quartz surface should be most evident when collisions between tetralin molecules are at a minimum; i.e., when the tetralin vapor pressure is low (at low sample temperature). Contrary to this explanation, Table VII shows that high tetralin vapor pressure (at high sample temperature) favors dehydrogenation. Surface catalytic dehydrogenation is also inconsistent with the results from laser pyrolysis, *vide supra*.

A bimolecular reaction neatly explains the prevalence of dehydrogenation at high tetralin pressures (Table VII). The increased probability of collisions between sample molecules should favor a bimolecular reaction; therefore, more dehydrogenation and increased conversion will result from the high tetralin pressure at high sample temperatures. Rationalizing the system pressure effect with bimolecular dehydrogenation is less straightforward. The residence time could be insufficient for significant bimolecular collisions to occur at low system pressure (10^{-5} torr). At high system pressure (0.10 torr), bimolecular reactions are important at low temperature but the unimolecular gas-phase reaction of **1**, i.e., ethylene loss, overcomes bimolecular dehydrogenation at higher temperatures, producing the change in the relative amounts of dehydrogenation to ethylene loss observed (Figure 1).

Flow pyrolysis of **1** was performed to eliminate both surface catalytic and bimolecular reactions and to determine the actual unimolecular decomposition products of **1**. In the flow pyrolysis experiment, energy is transferred from the oven walls to the argon and then to the tetralin through collisions. Surface effects are minimized because wall to tetralin collisions should be minor. The high dilution reduces collisions between hot tetralin molecules and other tetralin molecules or reactive species from its' decomposition; therefore, bimolecular reactions should be minimized under these conditions. The experiments (Table VIII) show that ethylene loss to form **3** and **6** is the lowest energy gas-phase unimolecular decomposition reaction of **1**.

Thus, it is likely that a bimolecular dehydrogenation reaction is responsible for the excess production of **2** and **5** observed at low temperature and conversion under some FVP conditions and in the laser-induced decomposition of **1**. The combined evidence from the laser-induced and flash vacuum pyrolysis experiments reported here is inconsistent with heterogeneous surface catalysis.

Primary Pathways in Tetralin Decomposition

We can propose two mechanisms for the bimolecular dehydrogenation of tetralin (**1**). The first is an autocatalytic intramolecular hydrogen atom transfer (Scheme II). The key step in the first proposed mechanism is the intermolecular transfer of a hydrogen atom from the benzylic position of **1** to a double bond conjugated to an aromatic ring. Unimolecular decomposition products or impurities, such as 1,2-dihydronaphthalene (**2**) and styrene (**6**), could initiate the process to produce radicals **9** and **10**, both of which undergo cleavage of a ß hydrogen to regenerate **2** and **6**, respectively. The

Scheme II

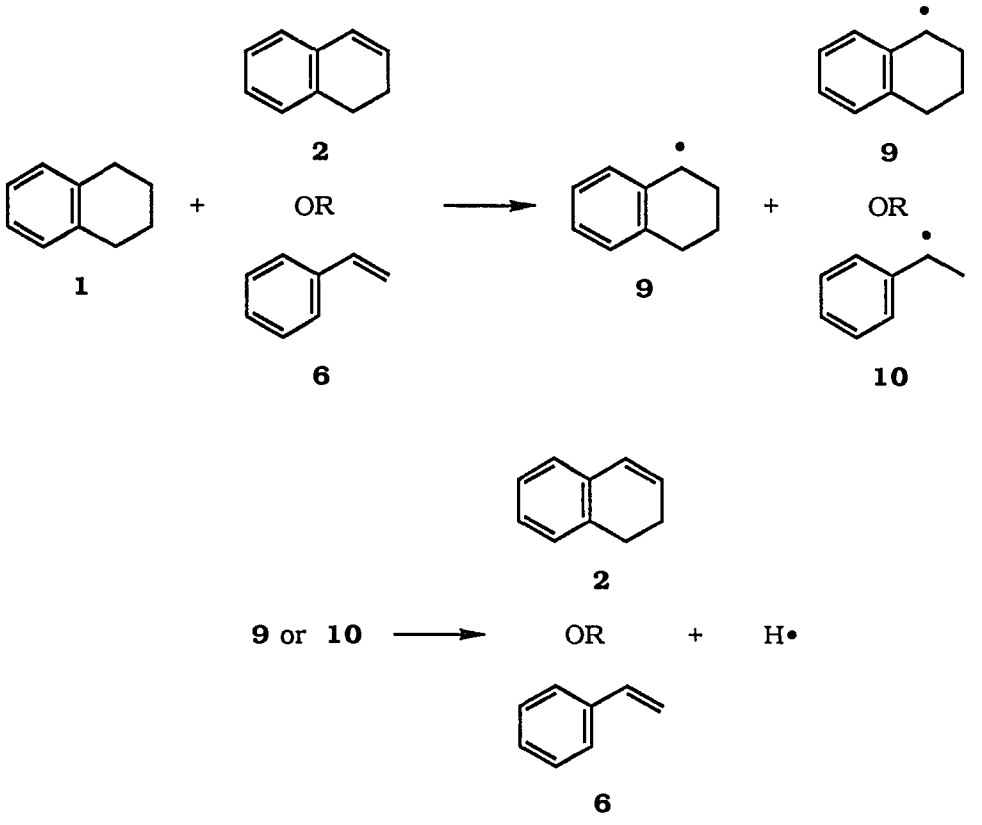

production of **2** would then be autocatalytic. The calculated[17] $\Delta H°$ for this hydrogen atom transfer reaction is between 31-34 kcal mol^{-1}, which is not unreasonable in this temperature range. Two other examples of this type of reaction are found in the disproportionation of 1,2-dihydronaphthalene (**2**)[3,18e] and 9,10-dihydroanthracene.[3,19]

A second possible mechanism is the hydrogen atom chain in Scheme III. The hydrogen atom is sufficiently reactive to abstract either the α or ß hydrogen from **1** to form the 1-tetryl (**9**) and 2-tetryl (**11**) radicals. Previous examples of this type of chain reaction have been observed in the decomposition of toluene[20] and in the disproportionation of **2**[3,18] at higher temperatures.

Scheme III

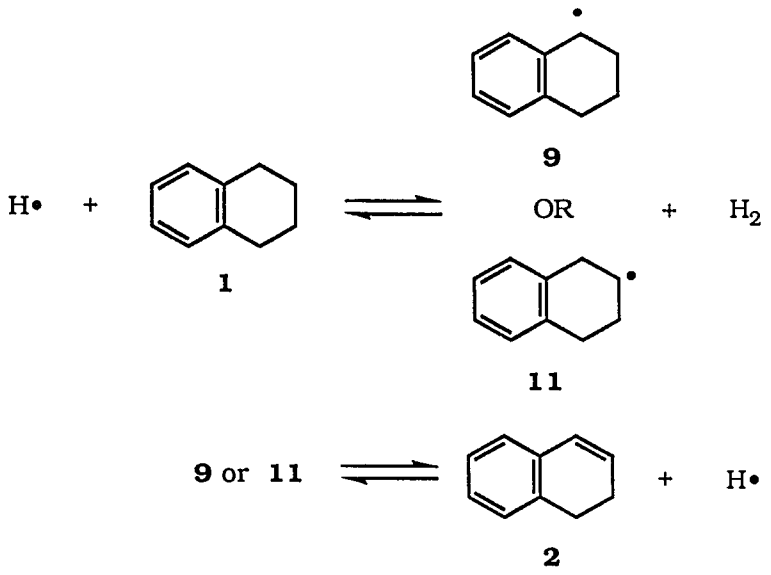

There is some evidence for the presence of a hydrogen atom chain operating under the conditions of the experiments reported here. In the laser-induced pyrolysis of **1** (Table IV), there was a small, though not dramatic, reduction in the relative portions of dehydrogenation to ethylene-loss products in the presence of toluene. However, addition of the chain terminators to the sample cell also reduces the temperature and complicates the analysis of these experiments. A substantial increase in the dehydrogenation of **1** occurs in the presence of I_2. This increase in the amount of **2** and **5** is consistent with either iodine atom initiated dissociation (I• + **1** → **9** + HI) or competition with the recombination of tetryl radicals with hydrogen atoms (I_2 + H• → HI + I• or I• + **9** → HI + **2**).

On the other hand, the observation of only hydrogen addition products from the laser-induced decomposition of **1** in the presence of hydrogen atoms is reported in this paper. These results would seem to indicate that abstraction by hydrogen atom,

required for the chain decomposition, is not a favored process. In the room temperature photolysis of HI, the expected *ipso* addition of hydrogen atom to **1** leads to the formation of radical **12** (Scheme IV). Cleavage of **12** and subsequent trapping of the primary radical **13** by HI, leads to the formation of butylbenzene (**14**). Trapping of radical **12** by HI would lead to 1,2,3,4,4a,5,6,8a-octahydronaphthalene (**15**), 1,2,3,4,4a,5,8,8a-octahydronaphthalene (**16**), and decalin (**17**). This scheme is consistent with the molecular weights of the observed products (one of *m/e* 134, two with *m/e* 136, and one with *m/e* 138).

In the high temperature laser-induced decomposition of **1** in the presence of hexamethylethane, **14** was the major product observed. Little or no **2**, formed from ß-hydrogen loss from 1-tetryl radical (**9**), was found in either laser experiment. The previously reported[7] shock tube decomposition of **1** in the presence of hexamethylethane, however, resulted in increased dehydrogenation. The discrepancy between hydrogen atom addition to **1** in our laser studies, on the one hand, and abstraction in the shock

Scheme IV

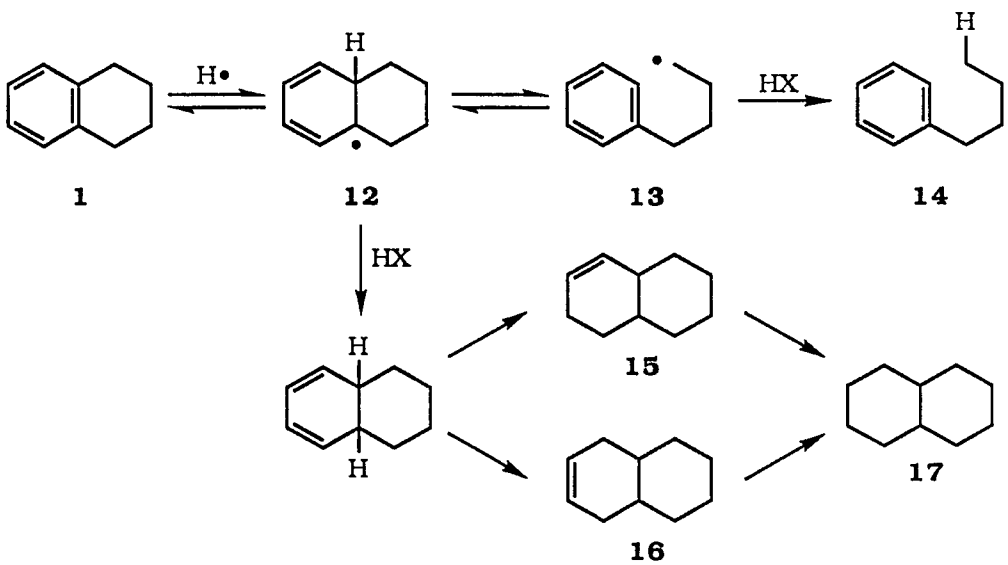

tube results, on the other, can be reconciled as follows. In the studies reported here, a large excess of hydrogen atoms was used, while in the shock tube experiments **1** was in excess. It is possible that, with a large excess of hydrogen atoms, any **2** produced by abstraction is consumed by the readdition of hydrogen atom to the double bond. Alternately, if hydrogen atom addition is reversible, a large excess of hydrogen atoms may be required to favor addition.

Although the evidence is not overwhelming, we can state that hydrogen atom chains (Scheme III) are involved in tetralin decomposition under some conditions. We cannot, however, rule out the first bimolecular mechanism (Scheme II). It is possible that under some conditions both mechanisms operate, as was found to be the case for the disproportion of **2**.[22e]

In the flow pyrolysis of tetralin (**1**), there is a residual amount of dehydrogenation so we must entertain the possibility of a unimolecular dehydrogenation pathway. The most likely intermediate is the diradical **18** (Scheme V) formed from breaking the benzylic carbon-carbon bond, the weakest bond in **1**. Three possible reaction routes are possible for diradical **18**. To produce a net hydrogen-loss product, cleavage of the ß-carbon-hydrogen bond of **18** is required. This would lead to the formation of *o*-allylbenzyl radical (**19**), which could close either to the kinetically favored 2-indanylmethyl radical (**20**) or the thermodynamically more stable 2-tetryl radical (**11**). The cyclization of **19** should be reversible at these temperatures and products from **11** should predominate. The major product formed by cleavage of the ß hydrogen of **11** is **2**. To confirm this, we produced radical **19** by the pyrolysis of the bis oxalate ester of *o*-allylbenzyl alcohol.[21] When this oxalate is pyrolyzed, the major product is 1,2-dihydronaphthalene (**2**).

A second reaction of diradical **18** is intramolecular disproportionation to form *o*-allyltoluene (**4**). This intramolecular hydrogen atom abstraction is likely to occur if **18**

Scheme V

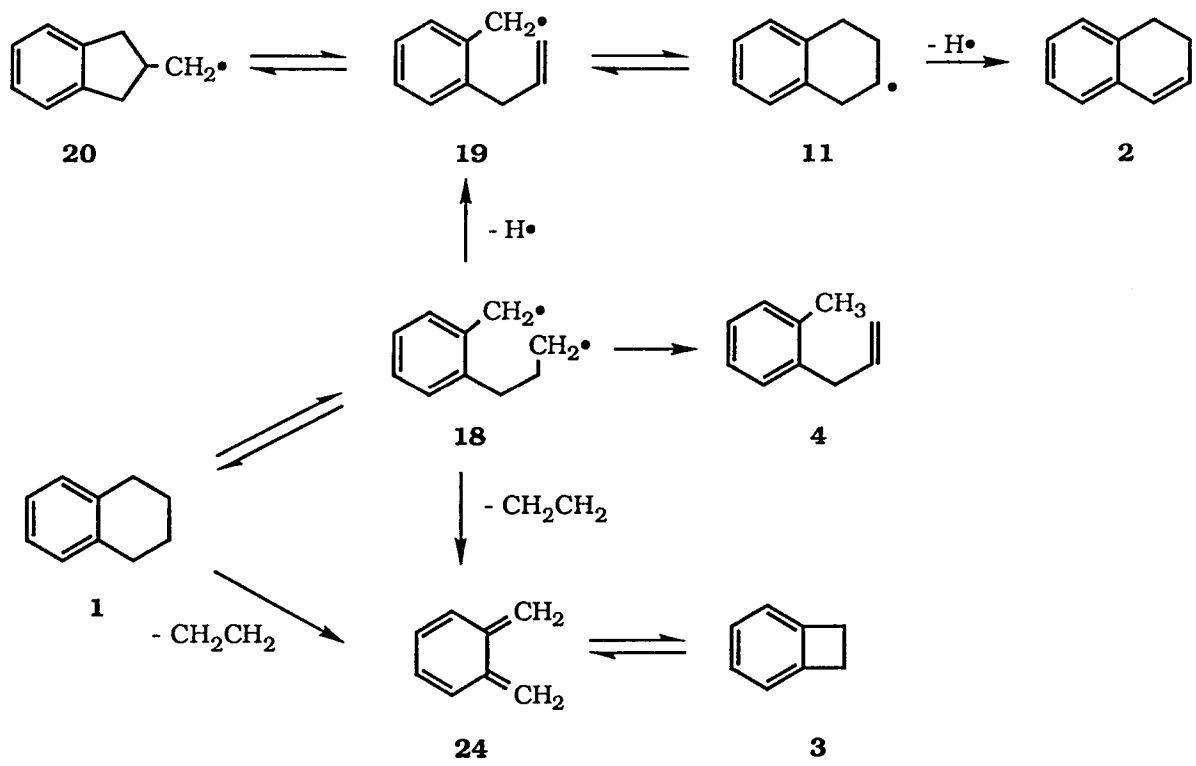

is formed. The product **4** was formed in the decomposition studies reported here. Additionally, **4** was also observed in the pyrolysis of 9-methylenespiro[3.5]nona-5,7-diene (**21**),[22] 3-benzocycloheptenone (**22**),[23] and 1,3,4,5-tetrahydro-2-benzothie-

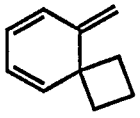

21

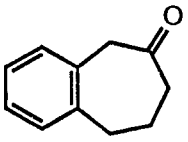

22

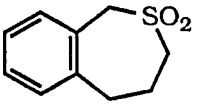

23

pin-2,2-dioxide (**23**),[23] model systems expected to produce **18**. *o*-Allyltoluene (**4**) was also formed in room temperature photolysis of **22**.[23]

The third possible reaction path for diradical **18** is cleavage of the ß-carbon-carbon bond leading to the formation of *o*-xylylene (**24**) and ultimately to benzocyclobutene (**3**). The cleavage of a carbon-carbon bond is thermodynamically more favorable than ß-hydrogen loss in normal alkyl radicals; however, geometric constraints required to form **24** and the resulting loss of aromaticity may make the carbon-carbon bond cleavage of **18** less favorable than in other systems. Additionally, the loss of cyclohexene from *cis*- and *trans*-1,2,3,4,4a,9,9a,10-octahydroanthracene appears to be concerted.[41] Although the loss of cyclohexene from these precursors may not be a good model for the loss of ethylene from tetralin (**1**), we must at least entertain the possibility that ethylene loss from **1** is concerted.

None of the above model systems (**21**, **22**, or **23**) for the formation of diradical **18**, produces ethylene-loss products. If **18** is formed, clearly the loss of ethylene is not favorable. However, we cannot be certain that **18** is actually formed in the pyrolysis of **21**, **22**, or **23**; although, as noted above, the formation of **4** is consistent with the presence of this radical. The activation parameters for the loss of ethylene from **1** do not preclude concerted ethylene loss. We do not believe there is enough evidence to make a definitive conclusion on this matter.

Secondary Pathways in Tetralin Decomposition

We have also examined the decomposition of the primary pyrolysis products of tetralin (**1**). The primary ethylene-loss product, benzocyclobutene (**3**), decomposes to styrene (**6**). This transformation has been studied previously.[24] Nothing unusual was found in the pyrolysis of 1,2-dihydronaphthalene (**2**). Naphthalene (**5**) was the major product (Table X) with only minor amounts of other products observed.

In the flow pyrolysis of *o*-allyltoluene (**4**), isomerization to 2-methylindan (**7**) was observed (Table IX). Loss of a methyl from **7** results in the formation of indene (**8**). Although there are numerous minor products (<2%), **4**, **7**, and **8** constitute *ca.* 60% of the product mixture even at 950 °C. At this temperature, over 90% of the *o*-allyltoluene (**4**) has been converted to products. Clearly **4** is the primary source of **8** produced in the pyrolysis of **1**.

We have proposed[25] an intramolecular hydrogen atom transfer to account for the transformation of **4** to **7**. Transfer of the benzylic hydrogen of **4** to the terminal end of the double bond would form the diradical **25**, which would close to form **7** (Scheme VI). Transfer of the benzylic hydrogen to the internal end of the double bond of **4** would form diradical **18**. Closure of this radical should form tetralin (**1**), which is the highest yield minor product found. Many of the minor products formed in the pyrolysis of **4** probably result from the secondary pyrolysis of **1**. This can be seen by examining the data in Table IX. The amount of **1** produced increases steadily up to 850 °C, levels off at 900 °C and drops at 950 °C. At the same time the major decomposition products of **1**, benzocyclobutene (**3**) and styrene (**6**) are produced in substantial amounts only above 850 °C.

Scheme VI

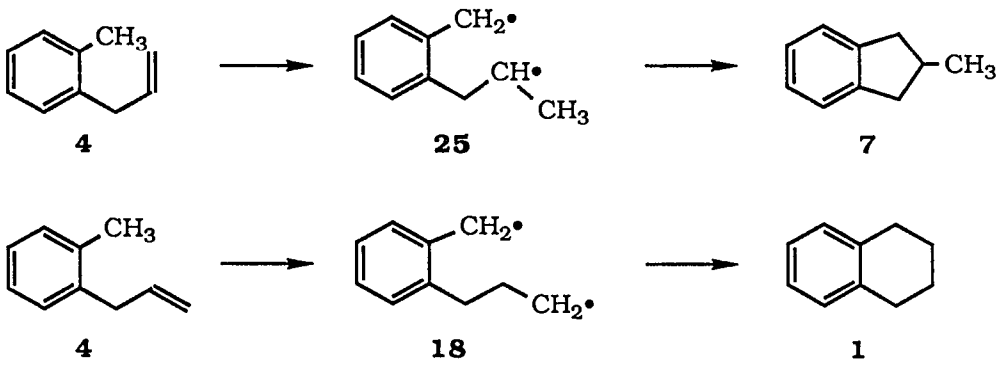

CONCLUSION

In this paper, we present new results on the thermal decomposition of tetralin (**1**) under sensitized laser-induced pyrolysis conditions under both cw and pulsed laser excitation. We have found dehydrogenation to predominate at low temperatures in these experiments. We have also examined the thermal chemistry of **1** under FVP and flow pyrolysis conditions. Our flow experiments show that the lowest energy unimolecular gas-phase decomposition channel for **1** is ethylene loss. A bimolecular dehydrogenation reaction, possibly a hydrogen atom chain, is responsible for greater amounts of hydrogen-loss products observed under some conditions in the decomposition of **1**. In none of our pyrolysis experiments, whether laser-induced or under standard pyrolysis conditions, did we find any evidence of heterogeneous catalytic reactions on surfaces. We can conclude that MPD favors the lowest energy unimolecular decomposition channel while laser-sensitized pyrolysis (cw or pulsed) can lead to homogenous bimolecular reactions as well.

We have observed the facile transformation of *o*-allyltoluene (**4**) to 2-methylindan (**7**), which we propose occurs through an intramolecular hydrogen atom transfer from the benzylic methyl group to the double bond of **4**. Loss of a methyl from **7** leads to the formation of indene (**8**). We have identified the transformation **4** to **7** to **8** as the major source of **8** in the gas-phase thermal decomposition of **1**.

EXPERIMENTAL SECTION

General Procedures

Apparatus

Laser-induced pyrolysis[6] The experimental arrangements were very similar for the three types of laser studies: infrared pulsed laser sensitized pyrolysis, infrared pulsed laser multiphoton dissociation (MPD), infrared continuous wave (cw) laser sensitized pyrolysis. A schematic diagram of the experimental arrangement for the pulsed laser sensitized pyrolysis is shown in Figure 3. A grating-tuned TEA CO_2 laser (Lumonics, Model 102) was used as the pulsed laser. The laser beam was defined with a 0.8-cm pinhole. The intensity profile was tophat shaped with variations of 30% across the beam. The laser pulse had a 150-ns peak and a 2-μs tail. The unattenuated energy of the laser beam was 0.11 J pulse^{-1} at 1027.4 cm^{-1}, and 0.26 J pulse^{-1} at 944.2 cm^{-1} and 933.0 cm^{-1}. The pulse-to-pulse variation was ± 15% at 1027.4 cm^{-1} and ± 5% at the other two lines. The pulsed laser beam was attenuated by a 10-cm cell filled with 0–10 torr of SF_6 or SiF_4 depending on the wavelength used. The laser beam was unfocused. Around 10% of the laser energy was directed into a power meter (Laser Precision, Model RJ7200) for monitoring the laser energy continually during the pyrolysis. The incident laser energy (I_0) was measured with no pyrolysis cell in the beam path.

For MPD, a BaF_2 lens with a 6.0-cm focal length was placed before the pyrolysis cell and no pinhole or attenuation cell was used. The laser beam was focused in the center of the pyrolysis cell. The P(20) line at 944.2 cm^{-1} was used with a square beam of 1.6 cm and an energy of 1.6 J pulse^{-1}. The energy density at the focal point was not evalu-

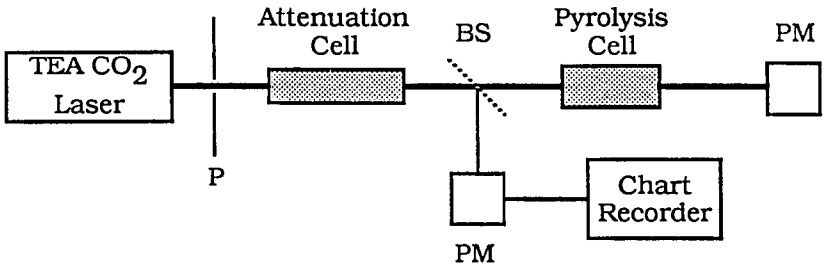

Figure 3. Schematic diagram of the experimental arrangement for the sensitized pulsed laser-induced pyrolysis (P = pinhole, BS = beam splitter, PM = power meter)

ated. The pulsed laser was operated at 0.4 Hz for all experiments. Higher repetition rates produce poor pulse-to pulse reproducibility.

The cw laser sensitized pyrolysis was performed with a Molectron C250 grating-tuned CO_2 laser. The experimental setup was similar to the pulsed laser sensitized pyrolysis shown in Figure 3, except that no attenuation cell was used. The laser power was controlled directly by the laser operating current. The laser beam was near Gaussian in profile with power levels stable to ± 1% throughout the experiment. The maximum power obtained was 18 W at 933.0 cm^{-1}, 21 W at 944.2 cm^{-1} and 5 W at 1027.4 cm^{-1}. The laser power was measured by a power meter (Coherent, 1 W = 1 mV).

For both the pulsed and cw lasers, the wavelength was calibrated by a spectrum analyzer (Optical Engineering). The transmission was about 20–40% in a 4- x 3.8-cm (id) cell with 6.0 torr of SF_6. Higher laser powers resulted in a greater fraction of the light transmitted. A chart recorder (Fisher 5000) was used to monitor the laser power throughout the experiment.

Several Pyrex sample cells fitted with KBr windows at normal incidence were used as the pyrolysis cell. MPD experiments were carried out in a 10- x 2-cm (id), 4- x 3.8-cm (id), or 4- x 3.5-cm (id) cell. The windows were attached with a 5-min epoxy

(Devcon). A 2.8-cm (id) Pyrex cell with an adjustable length of 1, 2, or 4 cm was used to study the surface effects. All the cells were fitted with two stopcocks and two O-ring joints, one connected to a 2- x 0.2-cm (id) glass sampling tube and the other connected to the vacuum line. In the kinetic study with cyclopropane, the sampling tube was 3 x 0.7 cm (id) and fitted with a gas-sampling septum.

A dye laser (Spectra-Physics, Model 380) pumped by an argon ion laser was used for I_2 excitation at 576.601 nm. The wavelength was monitored by a wavemeter (Burleigh). The I_2 absorption was confirmed by the strong reddish fluorescence from a second (low pressure) I_2 cell that was placed in the laser path during irradiation.

In the UV photolysis experiments, HI was excited by an excimer laser (Lambda Physik) at 308 nm. The laser beam was focused with a BaF_2 lens (focal length = 15 cm). For both HI and I_2 photolysis experiments, the 4- x 3.8-cm (id) cell with two quartz windows was used.

Flash vacuum pyrolysis Flash vacuum pyrolysis (FVP) was performed on the previously described apparatus.[27]

Flow pyrolysis A flow apparatus (Figure 2) was designed to fit the commercially available pyrolysis apparatus[27] in place of the usual sample head. The flow apparatus has two parts: a sample chamber and a flow control assembly. The sample chamber consists of a 12-L Pyrex glassblowers' flask (Ace 6870-24) fitted with a Pyrex to stainless steel ISO size NW 40 vacuum adapter (VWR AC50900NW040). Attached to the side of the flask are two 90° Teflon needle valve stopcocks (Ace 8193-04) with 14/20 inner joints. One of the stopcocks functions as a gas inlet, the other as a sample inlet. The entire assembly was enclosed in a wooden box with clear Lexan sides.

The flow control assembly was constructed with stainless steel parts and consists of a Bourdon type pressure/vacuum gauge (Omega PGS-25B-30V/15) connected to

switchable bypass or flow control lines between two three-way ball valves (Witey SS-43XS4). The flow control line consists of a needle valve (Nupro SS-SS4) connected to a flow meter (Air Products E21-A-41504 with flow tube E29-M-150MM3). All connections are with $\frac{1}{4}$" tubing and compression fittings (Swagelok). The pressure/vacuum gauge, three-way ball valves, needle valve and flow meter were mounted on a stainless steel panel.

The flow control assembly is connected to the sample chamber with $\frac{1}{4}$" stainless steel tubing, a $\frac{1}{4}$" Swagelok to $\frac{1}{4}$" NPT fitting and a $\frac{1}{4}$" NPT to ISO size NW 40 vacuum adapter (VWR 55009-155). The connection from the flow control assembly to the pyrolysis apparatus is identical to the one with the sample chamber except for the addition of a Pyrex to stainless steel ISO size NW 40 vacuum adapter (VWR AC50900NW040) fitted with a Pyrex 40/35 outer joint.

Methods and materials

Capillary gas chromatographic analysis of condensable pyrolysis products was performed using a Hewlett-Packard HP5840A gas chromatograph equipped with a 30-m (0.25-μm film thickness) DB-1701 capillary column (J & W Scientific) using nitrogen carrier gas and flame ionization detector. GCMS analysis was performed on a Finnegan 4000 mass spectrometer. H_2, HD, and D_2 isotopic analysis was performed on a Kratos MS50 mass spectrometer. HPLC was done on an ISCO Model 2350 instrument equipped with a Model 2360 Gradient Programmer and a Spectra-Physics SP4270 integrator using a semiprep C_{18} reversed-phase column (25 cm, 10 mm diameter, 5 μm particle size). ^1H NMR spectra were recorded on a Nicolet NT-300 spectrometer. Chemical shifts are reported in ppm (δ) relative to tetramethylsilane. All materials were commercially available and used as received, except as indicated below.

Tetralin (**1**) purified by the method of Bass.[26] As an alternate purification, **1** was washed with H_2SO_4 until the acid layer was no longer colored and was successively washed with deionized H_2O, 10% Na_2CO_3 and deionized H_2O and then dried with $MgSO_4$. Finally, **1** was fractionally distilled from CaH_2.

Sulfuric acid washed **1** was purified by HPLC in small portions as needed. 250 μL of a 25% w/v solution of **1** in HPLC grade CH_3OH was injected and a solvent of 90% CH_3OH and 10% H_2O with a flow rate of 3.0 mL min^{-1} was used. Fractions were collected with the UV detector at 254 nm. The combined fractions were diluted with saturated NaCl solution (*ca.* $\frac{1}{2}$ total volume) and deionized H_2O (*ca.* $\frac{1}{2}$ total volume) and extracted with fractionally distilled certified grade hexanes. The combined hexanes fractions were washed with deionized H_2O, dried with $MgSO_4$ and the solvent was removed *in vacuo*. HPLC purified **1** was stored under Ar at -40 °C until use. Concentrated samples (50 mg mL^{-1}) analyzed by GC indicate the purity of the sample exceeds 99.8%.

1,2-Dihydronaphthalene (**2**) was purified by HPLC as described for **1**.

Benzocyclobutene (3) Benzocyclobutene (**3**) was prepared by FVP[27] of α-chloro-*o*-xylene at 790 °C and 0.010 torr.[28] ^1H NMR ($CDCl_3$) δ 7.2–7.0 (m, 4H), 3.19 (s, 4 H) [lit.[5b] ^1H NMR ($CDCl_3$) δ 7.01 (m, 4 H), 3.11 (s, 4 H)]; GCMS (70 eV) *m/e* (% base peak) 104 (100), 103 (54.0), 78 (49.6), 51 (39.1) [lit.[5b] MS (50 eV) *m/e* (% base peak) 104 (100), 103 (53), 78 (59), 51 (52)].

***o*-Allyltoluene (4)** *o*-Allyltoluene (**4**) was prepared by the previously published procedure[29] and was purified by HPLC as described for **1**. ^1H NMR ($CDCl_3$) δ 7.12 (s, 4 H), 5.94 (qt, J_q = 10.3 Hz, J_t = 6.4 Hz, 1 H), 5.04 (dq, J_d = 10.1 Hz, J_q = 1.6 Hz, 1 H), 4.98 (dq, J_d = 17.0 Hz, J_q = 1.7 Hz, 1 H), 3.36 (dt, J_d = 6.3 Hz, J_t = 1.6 Hz, 1 H), 2.28 (s, 3 H) [lit.[5b] ^1H NMR (CCl_4) δ 6.94 (s, 4 H), 5.79 (qt, J_q = 11.3 Hz, J_t = 6.5 Hz, 1 H), 4.93 (m, 1 H), 4.79 (dq, J_d = 11.3 Hz, J_q = 2.1 Hz, 1 H), 3.24 (dt, J_d = 6.0 Hz, J_t = 1.8 Hz, 2 H),

2.20 (s, 3H)]; GCMS (70 eV) *m/e* (% base peak) 132 (77.5), 117 (100), 115 (42.3), 91 (35.6), 65 (31.6) [lit.[5b] MS (50 eV) *m/e* 132 (parent), 117 (base)].

2-Methyl-1*H*-indene 2-Methyl-1*H*-indene was synthesized using the literature preparation.[30] ^{1}H NMR ($CDCl_3$) δ 7.38–7.04 (m, 4 H), 6.47 (s, 1 H), 3.29 (s, 2 H), 2.18 (s, 3 H) [lit.[31] ^{1}H NMR ($CDCl_3$) δ 7.11–7.05 (m, 4 H), 6.50 (s, 1 H), 3.30 (s, 2 H), 2.18 (s, 3 H)]; GCMS (70 eV) *m/e* (% base peak) 130 (100), 129 (61.1), 128 (30.1), 115 (76.1) [lit.[30] MS (70 eV) *m/e* (% base peak) 130 (100), 115 (70)].

2-Methylindan (7) 2-Methylindan was prepared according to the literature.[30] ^{1}H NMR ($CDCl_3$) δ 7.27–7.05 (m, 4 H), 3.10–2.97 (m, 2 H), 2.58–2.47 (m, 3 H), 1.14 (d, J = 6.2 Hz, 3 H) [lit.[30] ^{1}H NMR ($CDCl_3$) δ 7.24–7.04 (m, 4 H), 3.12–2.92 (m, 2 H), 2.60–2.40 (m, 3 H), 1.13 (d, J = 6 Hz, 3 H)]; GCMS (70 eV) *m/e* (% base peak) 132 (63.8), 117 (100), 115 (30.8) [lit.[32] MS (70 eV) *m/e* 132 (parent), 117 (base)].

3-Methyl-1*H*-indene 3-Methyl-1*H*-indene was prepared according to the literature procedure.[30] ^{1}H NMR ($CDCl_3$) δ 7.49–7.17 (m, 4 H), 6.21–6.18 (m, 1 H), 3.33–3.29 (m, 2 H), 2.18–2.15 (m, 3 H) [lit.[30] ^{1}H NMR ($CDCl_3$) δ 7.45–7.05 (m, 4 H), 6.18 (s, 1 H), 3.30 (s, 2 H), 2.18 (s, 3 H)]; GCMS (70 eV) *m/e* (% base peak) 130 (100), 129 (75.6), 128 (43.5), 115 (76.7) [lit.[30] MS (70 eV) *m/e* (% base peak) 130 (34), 115 (64), 77 (41)].

1-Methylindan 1-Methylindan was prepared according to the previously published procedure.[30] ^{1}H NMR ($CDCl_3$) δ 7.24–7.10 (m, 4 H), 3.25–3.10 (m, 1 H), 2.97–2.75 (m, 2 H), 2.36–2.23 (m, 1 H), 1.67–1.52 (m, 1H), 1,29 (d, J = 6.6, 3 H) [lit.[30] ^{1}H NMR ($CDCl_3$) δ 7.32–7.08 (m, 4 H), 3.28–2.78 (m, 3 H), 2.40–1.52 (m, 2 H), 1.28 (d, J = 7 Hz, 3 H)]; GCMS (70 eV) *m/e* (% base peak) 132 (27.8), 117 (100), 115 (19.1) [lit.[33] MS (70 eV) *m/e* (% base peak) 132 (24), 131 (11), 128 (5), 117 (100), 115 (24), 91 (13), 77 (7), 65 (8), 63 (9)].

Laser-induced pyrolysis[6] Samples were prepared in a turbomolecular pump (Pfeiffer, TPU 40) vacuum system, with grease-free stopcocks and O-ring joint connections. The base pressure was less than 10^{-6} torr. The pyrolysis cell and the vacuum manifold were heated by a heat gun to clean the walls before the sample was prepared. Pressure was measured by a manometer (MKS 221 AHS-F) with 10-torr full scale.

The sample preparation was the same in both cw and pulsed laser sensitized pyrolyses. Initially, freshly purified **1**, stored in a side arm of the vacuum manifold, was frozen with liquid N_2 and the air was evacuated. Sensitizer was then expanded into the sample cell and was frozen into the sample tube. Next, the stopcock to the sample tube was closed and the cell was evacuated. Then **1** was allowed to expand into the cell until the pressure was 0.325 torr. The sensitizer was then warmed up to expand back into the cell as the stopcock was opened. Five minutes was allowed for equilibration of the gases before irradiation. When an additional gas was required for the sample mixtures, it was usually introduced after the sensitizer and was condensed in the sample tube before **1** was introduced. For MPD experiments, the cell contains only 0.325 torr of **1**.

The pyrolysis cell was irradiated immediately after sample preparation. The reaction time was 1–2 h for a pulsed laser experiment and 1–5 min for a cw laser experiment. After the reaction, the condensable materials were frozen into the sample tube. Then the sample tube was warmed up with a Dry Ice/2-propanol bath and the sensitizer was evacuated. The tube was then detached from the cell. 50 μL of hexanes (HPLC grade) with biphenyl added as an internal standard was introduced along the wall with a 50-μL syringe (Hamilton). GC analysis was done immediately. The non-condensable gas mixtures were taken to a mass spectrometer for H_2, HD, and D_2 analysis in a continuous flow system, as needed.

After the experiment was complete, the pyrolysis cell was cleaned with HNO_3, H_2O and acetone. Following the I_2, HI, or deuterium experiments, the KBr windows were repolished.

The infrared spectra of **1** and SF_6 for the laser experiments were taken by FTIR with 0.3 cm^{-1} resolution with a 4- x 3.8-cm (id) cell. Both **1** (0.325 torr) and SF_6 (6.0 torr) were at the same pressure as in the pyrolysis experiment.

Flash vacuum pyrolysis The pyrolysis oven was equilibrated at the desired temperature before pyrolysis. A weighed sample (*ca.* 10–25 mg) was placed in a 50-mL 24/40 round-bottom flask and connected to the pyrolysis apparatus fitted with a right angle sample adapter (40/35 outer 90° to 24/40 inner). The entire system was flushed with N_2 and the sample frozen with liquid N_2. The system was evacuated with the roughing pump to *ca.* 0.1 torr and the pyrolysis trap was frozen with liquid N_2. If the diffusion pump was used, the system was then evacuated to 10^{-5} torr. The sample was warmed to the desired temperature with an appropriate bath. A sample temperature of 0 °C was maintained with an ice/water bath for all pyrolysis experiments except for those at -30 °C (Dry Ice/$CaCl_2$/H_2O) and room temperature (water). After the pyrolysis was complete, the system was filled with N_2 and the trap was allowed to warm to near room temperature. 1.0 mL of *ca.* 2 mg mL^{-1} solution of biphenyl in CH_2Cl_2 and an additional 1.0 mL of CH_2Cl_2 was added to the trap. The trap was thoroughly rinsed with the solution, which was immediately analyzed by GC.

Flow pyrolysis The flow pyrolysis apparatus (Figure 2) was filled with Ar and evacuated several times and then allowed to pump down at least 12 h (flow assembly on bypass). A weighed sample in a 5-mL 14/20 round-bottom flask flushed with Ar was attached to the sample inlet, frozen with liquid N_2 and the sample inlet was opened. After the system had returned to the original pressure (30–60 min), the sample inlet was

closed and the sample allowed to warm to room temperature. The sample was refrozen with liquid N_2 and opened to the system for an additional 15–30 min. The sample chamber was isolated from the flow assembly and pyrolysis apparatus. The sample inlet was opened and the sample was allowed to warm to room temperature. No liquid sample remained in the flask. The sample chamber was filled with Ar to atmospheric pressure through the gas inlet and the gas mixture was allowed to equilibrate for 15 min. The pyrolysis trap was cooled with liquid N_2. The flow of gas mixture into the pyrolysis apparatus was maintained at a fixed rate of 20–25 mL min^{-1} (Ar/1 atm) until the sample chamber was evacuated to *ca.* $\frac{1}{2}$ atmospheric pressure. The sample chamber and flow control assembly were isolated from the pyrolysis apparatus that was then filled with N_2. After the trap had warmed to near room temperature, 0.5 mL biphenyl in CH_2Cl_2 (*ca.* 2 mg mL^{-1}) and an additional 0.5 mL CH_2Cl_2 was added to the trap. The trap was thoroughly rinsed with the solution, which was immediately analyzed by GC. A clean trap was fitted to the pyrolysis apparatus and the entire assembly was filled with Ar and evacuated several times. The apparatus was allowed to pump down at least 12 h (flow assembly on bypass) before repeat use.

Product analysis The oven for capillary GC was initially programmed at 80 °C for 10 min, heated at 3 °C min^{-1} until the temperature reached 242 °C and held for 1 min. For the laser-induced decomposition samples, the oven was initially programmed at 80 °C for 10 min, heated at 3 °C min^{-1} for 15 min and then 15 °C min^{-1} until the temperature reached 250 °C. All compounds eluted before 35 min.

For the FVP and flow pyrolysis samples, 1 μL of CH_2Cl_2 solution was injected while 2 μL of a hexanes solution was used to analyze the laser-induced decomposition samples. Results agreed among injections within ± 3%. For FVP and flow pyrolysis experiments, the major products (**1**, **2**, **3**, **4**, **5**, **6**, **8**, toluene, ethylbenzene, *o*-xylene, and

o-ethyltoluene) were corrected for fid response to a known amount of added standard (biphenyl). Percentages reported are for moles of product relative to total moles of recovered material. In the laser experiments, the major products (**2**, **3**, **4**, **5**, **6**, and **8**) were corrected for fid response relative to **1**. Conversion was calculated from a known amount of added standard (biphenyl). Percentages reported are for moles of product relative to total moles of products. The reproducibility for the overall experiment was within ± 5%. Major products were identified by GC retention time of authentic samples (**1**, **2**, **3**, **4**, **5**, **6**, **7**, **8**, toluene, ethylbenzene, *o*-xylene, *o*-ethyltoluene, 1-methylindan, 2-methyl-1*H*-indene, and 3-methyl-1*H*-indene) and GCMS. The molecular weight of minor products was determined by GCMS.

Isotopic analyses for laser studies were done by GCMS. The responses of H_2 and D_2 were almost the same in a 1 to 1 H_2:D_2 mixture. HD was assumed to produce the same response.

REFERENCES

(1) Schlupp, K. F.; Wien, H. *Angew. Chem., Int. Ed. Engl.* **1976**, *15*, 341.

(2) Whitehurst, D. D. "Organic Chemistry of Coal," In *ACS Symposium Series 71*, Larson, J. W., Ed.; American Chemical Society: Washington, D. C., 1978; pp 1-35.

(3) Poutsma, M. L. *A Review of Thermolysis Studies of Model Compounds Relevant to Processing of Coal*; ORNL/TM-10673, Oak Ridge National Laboratory, Oak Ridge, TN 37831. This review is available from National Technical Information Service, U. S. Dept. of Commerce, 5285 Port Royal Rd., Springfield, VA 22161.

(4) (a) Badger, G. M.; Kimber, R. W. L. *J. Chem. Soc.* **1960**, 266. (b) Badger, G. M.; Kimber, R. W. L.; Novotny, J. *Aust. J. Chem.* **1962**, *15*, 616. (c) Loudon, A. G.; Maccoll, A.; Wong, S. K. *J. Chem. Soc. B* **1970**, 1733. (d) Penninger, J. M. L.; Slotboom, H. W. *Recl. Trav. Chim. Pays-bays* **1973**, *92*, 513. (e) Penninger, J. M. L.; Slotboom, H. W. *Ibid.* **1973**, *92*, 1089. (f) Tominaga, H.; Yahagi, U. *J. Fac. Eng., Univ. Tokyo, Ser. A* **1977**, *15*, 68. (g) Bredael, P.; Vinh, T. H. *Fuel* **1979**, *58*, 211. (h) Gangwer, T.; MacKenzie, D.; Casano, S. *J. Phys. Chem.* **1979**, *83*, 2013. (i) Cyprès, R.; Bredael, P. *Fuel Process. Tech.* **1980**, *3*, 297. (j) Trushkova, L. V.; Magaril, R. Z.; Korzun, N. V.; Bulatov, R. A. *Russ. J. Phys. Chem.* **1980**, *54*, 1062. (k) Takahashi, K.; Ogino, Y. *Fuel* **1981**, *60*, 975. (l) Trahanovsky, W. S.; Swenson, K. E. *J. Org. Chem.* **1981**, *46*, 2984. (m) Bajus, M.; Baxa, J. *Coll. Czech. Chem. Commun.* **1982**, *47*, 1838. (n) Penninger, J. M. L. *Int. J. Chem. Kinetics* **1982**, *14*, 761. (o) Hillebrand, W.; Hodek, W.; Kölling, G. *Fuel* **1984**, *63*, 756. (p) Korzun, N. V.; Trushkova, L. V. *Kinetics Catal.* **1985**, *26*, 195.

(5) (a) Berman, M. R.; Comita, P. B.; Moore, C. B.; Bergman, R. G. *J. Amer. Chem. Soc.* **1980**, *102*, 5692. (b) Comita, P. B.; Berman, M. R.; Moore, B. C.; Bergman, R. G. *J. Phys. Chem.* **1981**, *85*, 3266.

(6) Zhu, J. Ph.D. Dissertation, Iowa State University of Science and Technology, 1989.

(7) Tsang, W.; Cui, J. P. *J. Amer. Chem. Soc.* **1990**, *112*, 1665.

(8) In the liquid-phase pyrolysis of **1**, the major ring-contracted product has been identified as 1-methylindan,[9] but we have conclusively identified the major methylindan in gas-phase pyrolysis of **1** as the 2-methyl isomer (**7**). Some

workers have incorrectly reported 1-methylindan as the gas-phase pyrolysis product.[4d,e,n]

(9) Benjamin, B. M.; Hagaman, E. W.; Raaen, V. F.; Collins, C. J. *Fuel* **1979**, *58*, 386.

(10) (a) Rosenfield, R. N.; Brauman, J. I.; Barker, J. R.; Golden, D. M. *J. Amer. Chem. Soc.* **1977**, *99*, 8063. (b) Danen, W. C.; Koster, D. F.; Zitter, R. N. *J. Amer. Chem. Soc.* **1979**, *101*, 4281. (c) Reiser, C.; Lussier, F. M.; Jensen, C.; Steinfield, J. I. *J. Amer. Chem. Soc.* **1979**, *101*, 350. (d) Golden, D. M.; Rossi, M. J.; Baldwin, A. C.; Barker, J. R. *Acc. Chem. Res.* **1981**, *14*, 56.

(11) (a) Shaub, W. M.; Bauer, S. H. *Int. J. Chem. Kinetics* **1975**, *7*, 509. (b) Dai, H. L.; Specht, E.; Berman, M. R.; Moore, C. B. *J. Chem. Phys.* **1982**, *77*, 4494. (c) McMillen, D. F.; Lewis, K. E.; Smith, G. P.; Golden, D. M. *J. Phys. Chem.* **1982**, *86*, 709.

(12) Zhu, J.; Yeung, E. S. *J. Phys. Chem.* **1988**, *92*, 2184.

(13) Tsang, W. *Int. J. Chem. Kinet.* **1978**, *10*, 1119.

(14) Yappert, M. C.; Yeung, E. S. *J. Amer. Chem. Soc.* **1986**, *108*, 7529.

(15) The intensity profile here is tophat shape with variations of 30% across the beam, compared to a near Gaussian beam in the previous work.[5] A 6-cm focal length BaF_2 lens was used in these experiments, while a 15-cm focal length NaCl lens was used previously. The laser pulse here has a 150-ns peak and 2-μs tail, compared to a 100-ns peak and 1-μs tail in previous work.

(16) The cw laser beam is near Gaussian in profile with power levels stable to ± 1% throughout the experiment, compared to ± 5% pulse-to-pulse variations in the P(20) CO_2 line (MPD and SF_6 sensitization) and ± 15% pulse-to-pulse variations in the P(40) CO_2 line (SiF_4 sensitization).

(17) Benson, S. W. *Thermochemical Kinetics*, 2nd ed.; Wiley: 1976.

(18) (a) Gill, G. B.; Hawkins, S. *J. Chem. Soc., Chem. Commun.* **1974**, 742. (b) Heesing, A.; Müllers, W. *Chem. Ber.* **1980**, *113*, 9. (c) King, H-H.; Stock, L. M. *Fuel* **1981**, *60*, 748. (d) Allen, D. T.; Gavalas, G. R. *J. Chem. Kinetics* **1983**, *15*, 219. (e) Franz, J. A.; Camaioni, D. M.; Beishline, R. R.; Dalling, D. K. *J. Org. Chem.* **1984**, *49*, 3563.

(19) Billmers, R.; Griffith, L. L.; Stein, S. E. *J. Phys. Chem.* **1986**, *90*, 517.

(20) Robaugh, D.; Tsang, W. *J. Phys. Chem.* **1986**, *90*, 4159.

(21) Malandra, J. L.; Trahanovsky, W. S. *J. Org. Chem.* **1993**, *58*, 0000. [Paper 3, this dissertation]

(22) Gajewski, J. J.; Paul, G. C. *J. Org. Chem.* **1990**, *55*, 4575.

(23) Malandra, J. L.; Trahanovsky, W. S., manuscript in preparation. [Paper 2, this dissertation]

(24) (a) Chapman, O. L.; Tsou, U. P. E. *J. Amer. Chem. Soc.* **1984**, *106*, 7974. (b) Trahanovsky, W. S.; Scribner, M. E. *J. Amer. Chem. Soc.* **1984**, *106*, 7976.

(25) Trahanovsky, W. S.; Malandra, J. L.; Ferguson, J. M. *J. Amer. Chem. Soc.* **1993**, *115*, 0000. [Paper 5, this dissertation]

(26) Bass, K. C. *J. Chem. Soc.* **1964**, 3498.

(27) Trahanovsky, W. S.; Ong, C. C.; Pataky, J. G.; Weitl, F. L.; Mullen, P. W.; Clardy, J. C.; Hansen, R. S. *J. Org. Chem.* **1971**, *36*, 3575. Commercial apparatus is available from Kontes Scientific Glassware, Vineland, NJ 08360.

(28) Morello, M. J.; Trahanovsky, W. S. *Tetrahedron Lett.* **1979**, 4435.

(29) Hurd, C. D.; Bollman, H. T. *J. Amer. Chem. Soc.* **1934**, *56*, 447.

(30) Adamczyk, M.; Watt, D. S.; Netzel, D. A. *J. Org. Chem.* **1984**, *49*, 4226.

(31) Banks, H.; Ziffer, H. *J. Org. Chem.* **1982**, *47*, 3743.

(32) Douboudin, J. G.; Jousseaume, B.; Pinet-Vallier, M. *J. Organomet. Chem.* **1979**, *172*, 1.

(33) Finkel'shtein, E. S.; Mikaya, A. I.; Zaikin, V. G.; Vdovin, V. M. *Neftekhimiva* **1980**, *20*, 75; *Petrol. Chem. USSR* **1980**, *20*, 6.

APPENDIX 1

SUPPLEMENTARY DATA TABLES

Table A-I. Products and recovered starting material, total recovery of material, and conversion from the FVP of tetralin (**1**) at 10^{-5} torr and various oven temperatures [a,b]

	yield, % [c]				
entry	RT [d]	850 °C	900 °C	950 °C	1000 °C
toluene	—	—	—	0.10	0.65
TA	—	—	—	—	*e*
ethylbenzene	—	—	0.03	0.09	0.29
m/*p*-xylene	—	—	—	0.02	0.08
o-xylene	—	—	0.12	0.37	1.46
styrene (**6**)	—	0.41	2.09	5.80	18.62
benzocyclobutene (**3**)	—	1.67	4.52	7.73	9.40
allylbenzene	—	—	—	—	0.04
propylbenzene	—	—	—	—	0.04
o-ethyltoluene	—	—	0.02	0.07	0.12
o-methylstyrene	—	—	0.11	0.32	0.75
m/*p*-allyltoluene	—	—	—	—	0.10
o-allyltoluene (**4**)	—	0.47	1.15	1.66	1.54
indene (**8**)	—	0.15	1.08	3.00	8.02
2-methylindan (**7**)	—	0.14	0.59	1.10	1.21
1-methylindan	—	—	—	0.06	0.06

Table A-I continues on next page

Table A-I. Continued

entry	yield, % [c]				
	RT [d]	850 °C	900 °C	950 °C	1000 °C
TD-130 [$C_{10}H_{10}$]	—	—	0.04	0.12	0.37
TE-130 [$C_{10}H_{10}$]	—	—	—	0.03	—
TF-130 [$C_{10}H_{10}$]	—	—	0.04	0.07	0.07
o-(1-propenyl)toluene	—	—	0.13	0.32	0.50
TH-130 [$C_{10}H_{10}$]	—	—	0.05	0.08	0.09
TI-132 [$C_{10}H_{12}$]	—	—	—	0.05	0.08
TJ-132 [$C_{10}H_{12}$]	—	—	—	0.06	0.09
tetralin (**1**)	99.85	95.19	82.76	65.64	34.63
2-methyl-1*H*-indene	—	0.04	0.19	0.35	0.44
TK-130 [$C_{10}H_{10}$]	—	0.07	0.28	0.46	0.51
1,2-dihydronaphthalene (**2**)	0.06	1.36	4.13	5.37	4.24
TL-128 [$C_{10}H_8$]	—	—	0.03	0.04	0.14
1,4-dihydronaphthalene	0.05	—	—	0.02	—
TM	*e*	*e*	*e*	—	—
naphthalene (**5**)	0.05	0.51	2.66	7.04	16.27
TN	*e*	*e*	*e*	*e*	—
TO-148 [$C_{11}H_{16}$]	—	—	—	0.02	0.03
2-methylnaphthalene	—	—	—	—	0.09
1-methylnaphthalene	—	—	—	—	0.07
recovery [f]	92.90	90.02	85.62	80.37	76.25
conversion [g]	*d*	4.81	17.24	34.36	65.37

Table A-I footnote on next page

Table A-I. Footnote

---

[a] FVP conditions: system pressure = 1 x 10^{-5} torr, sample temperature = 0 °C. [b] Amounts determined by GC with a known quantity of biphenyl added as standard. Data represent the average of triplicate runs. Products identified by comparison with authentic samples or those that could be identified by retention time and GCMS are indicated by name. Products that were identified by GCMS only are indicated by code: XY-nnn, where 'X' corresponds to the system studied (T = pyrolysis of **1**), 'Y' to the individual unknown product (A, B, C, etc.), and 'nnn' to the nominal mass. [c] Moles of product divided by total moles of recovered material. [d] Starting material purity assay. [e] Unidentified product which constitutes ≤0.05% total area by GC. [f] Total moles of recovered material divided by moles of starting material used. [g] Total moles of recovered material minus moles of recovered starting material divided by total moles of recovered material.

Table A-II. Products and recovered starting material, total recovery of material, and conversion from the FVP of tetralin (**1**) at 0.10 torr and various oven temperatures [a,b,c]

	yield, % [d]			
entry	750 °C	800 °C	850 °C	900 °C
toluene	—	—	—	0.18
ethylbenzene	—	—	—	0.12
o-xylene	—	—	0.07	0.42
styrene (**6**)	0.06	0.24	1.71	7.34
benzocyclobutene (**3**)	0.28	1.08	3.87	8.10
o-ethyltoluene	—	—	—	0.08
o-methylstyrene	—	—	0.08	0.34
butylbenzene	—	—	0.03	0.05
o-allyltoluene (**4**)	0.08	0.31	0.85	1.32
indene (**8**)	0.02	0.10	0.65	2.45
2-methylindan (**7**)	—	0.12	0.65	1.24
1-methylindan	—	—	—	0.07
TD-130 [$C_{10}H_{10}$]	—	—	0.05	0.13
TF-130 [$C_{10}H_{10}$]	—	—	—	0.03
o-(1-propenyl)toluene	—	—	0.10	0.26
TH-130 [$C_{10}H_{10}$]	—	—	—	0.07
TI-132 [$C_{10}H_{12}$]	—	—	—	0.03
TJ-132 [$C_{10}H_{12}$]	—	—	—	0.06
tetralin (**1**)	98.63	96.31	85.69	65.73
2-methyl-1*H*-indene	—	—	0.33	0.45
TK-130 [$C_{10}H_{10}$]	—	—	0.27	0.38

Table A-II continues on next page

Table A-II. Continued

	yield, % [d]			
entry	750 °C	800 °C	850 °C	900 °C
1,2-dihydronaphthalene (**2**)	0.68	1.44	3.56	4.73
TL-128 [$C_{10}H_8$]	—	—	—	0.08
1,4-dihydronaphthalene	—	—	—	—
TM	*e*	*e*	*e*	—
naphthalene (**5**)	0.24	0.42	2.09	6.34
TN	*e*	*e*	—	*e*
recovery [f]	91.78	91.98	83.75	85.21
conversion [g]	1.37	3.69	14.31	34.27

[a] FVP conditions: system pressure = 0.10 torr, sample temperature = 0 °C. [b] See Table A-I, footnote *b*. [c] See Table A-I for sample purity assay. [d] See Table A-I, footnote *c*. [e] Unidentified product which constitutes ≤0.10% total area by GC. [f] See Table A-I, footnote *f*. [g] See Table A-I, footnote *g*.

Table A-III. Products and recovered starting material, total recovery of material, and conversion from the FVP of tetralin (**1**) at 10^{-5} torr and various sample temperatures [a,b,c]

	yield, % [d]		
entry	-30 °C	0 °C	RT
toluene	—	0.08	0.13
ethylbenzene	—	0.05	0.10
o-xylene	—	0.18	0.32
styrene (**6**)	1.76	3.04	3.31
benzocyclobutene (**3**)	5.30	5.65	4.20
o-ethyltoluene	—	—	0.11
o-methylstyrene	0.06	0.14	0.32
o-allyltoluene (**4**)	1.40	1.21	1.10
indene (**8**)	0.77	1.29	2.41
2-methylindan (**7**)	0.87	0.71	0.57
1-methylindan	0.06	0.05	0.05
TD-130 [$C_{10}H_{10}$]	—	0.05	0.16
TF-130 [$C_{10}H_{10}$]	—	0.03	0.08
o-(1-propenyl)toluene	0.21	0.16	0.12
TH-130 [$C_{10}H_{10}$]	—	0.05	0.11
tetralin (**1**)	86.62	79.29	69.84
2-methyl-1*H*-indene	—	0.34	0.60
TK-130 [$C_{10}H_{10}$]	0.18	0.35	0.63
1,2-dihydronaphthalene (**2**)	1.69	4.17	8.98
TL-128 [$C_{10}H_8$]	—	—	0.12
naphthalene (**5**)	1.06	3.15	6.75

Table A-III continues on next page

Table A-III. Continued

	yield, % [d]		
entry	-30 °C	0 °C	RT
recovery [e]	85.17	86.72	80.84
conversion [f]	13.38	20.71	30.16

[a] FVP conditions: oven temperature = 900 °C, system pressure = 1 x 10^{-5} torr. [b] See Table A-I, footnote *b*. [c] See Table A-II, footnote *c*. [d] See Table A-I, footnote *c*. [e] See Table A-I, footnote *f*. [f] See Table A-I, footnote *g*.

Table A-IV. Products and recovered starting material, total recovery of material, and conversion from the flow pyrolysis of tetralin (**1**) at various oven temperatures [a,b,c]

	yield, % [d]			
entry	805 °C	853 °C	905 °C	952 °C
toluene	—	—	—	0.12
ethylbenzene	—	—	—	0.13
o-xylene	—	—	—	0.24
styrene (**6**)	0.02	1.07	4.64	20.66
benzocyclobutene (**3**)	0.89	4.73	9.92	13.94
o-methylstyrene	—	—	—	0.17
o-allyltoluene (**4**)	0.23	1.07	1.92	2.21
indene (**8**)	—	0.21	1.02	4.32
2-methylindan (**7**)	—	0.60	1.69	2.86
TD-130 [$C_{10}H_{10}$]	—	—	—	0.52
o-(1-propenyl)toluene	—	—	0.34	0.95
TJ-132 [$C_{10}H_{12}$]	—	—	—	0.14
3-methyl-1*H*-indene	—	—	—	0.32
tetralin (**1**)	98.49	90.70	77.34	46.08
2-methyl-1*H*-indene	—	—	—	0.19
1,2-dihydronaphthalene (**2**)	0.36	1.11	1.74	2.18
naphthalene (**5**)	—	0.52	1.40	4.97
recovery [e]	88.96	89.18	93.44	85.31
conversion [f]	1.51	9.30	22.66	53.92

[a] Flow pyrolysis conditions: system pressure = 1 x 10^{-2} torr, flow rate = 24 mL min^{-1} (Ar), residence time = 0.31 s. [b] See Table A-I, footnote *b*. Data at 850 °C represent the average of six runs. [c] See Table A-II, footnote *c*. [d] See Table A-I, footnote *c*. [e] See Table A-I, footnote *f*. [f] See Table A-I, footnote *g*.

Table A-V. Products and recovered starting material, total recovery of material, and conversion from the flow pyrolysis of *o*-allyltoluene (**4**) at various oven temperatures [a,b]

	yield, % [c]						
entry	RT [d]	700 °C	757 °C	796 °C	850 °C	900 °C	950 °C
toluene	—	—	—	0.17	0.26	0.81	1.06
ethylbenzene	—	—	—	0.08	0.36	1.09	1.17
m/p-xylene	—	—	—	—	—	0.09	0.13
o-xylene	—	—	—	0.07	0.21	0.47	0.60
styrene (**6**)	—	—	—	—	0.39	2.26	5.74
benzocyclobutene (**3**)	—	—	0.15	0.48	1.36	2.79	2.17
allylbenzene	—	—	—	—	—	0.15	0.07
propylbenzene	—	—	—	—	—	0.09	0.08
o-ethyltoluene	—	—	—	0.07	0.31	0.33	0.13
o-methylstyrene	—	0.15	0.21	0.44	1.60	2.47	3.09
benzaldehyde	—	—	—	0.09	0.20	0.19	0.16
indan	—	—	—	—	—	0.16	0.38
m/p-allyltoluene	1.63	1.57	1.38	1.37	1.35	0.92	0.51
AA	—	—	—	*e*	—	—	—
o-allyltoluene (**4**)	98.07	94.03	83.60	71.00	30.92	12.74	5.77
indene (**8**)	—	0.68	1.44	1.99	9.71	23.93	39.88
2-methylindan (**7**)	—	2.10	8.37	17.80	34.85	28.68	13.07
1-methylindan	—	0.17	0.62	1.31	1.86	1.30	0.57
AB-132 [$C_{10}H_{12}$]	—	—	—	—	0.14	0.29	0.30
TD-130 [$C_{10}H_{10}$]	—	—	—	—	0.40	1.74	4.26
o-methylbenzaldehyde	—	0.10	0.11	0.07	0.16	—	—

Table A-V continues on next page

Table A-V. Continued

	yield, % [c]						
entry	RT [d]	700 °C	757 °C	796 °C	850 °C	900 °C	950 °C
o-(1-propenyl)toluene	—	0.16	0.79	1.91	6.35	7.92	5.86
TH-130 [$C_{10}H_{10}$]	—	—	—	—	—	—	0.07
TI-132 [$C_{10}H_{12}$]	—	—	—	—	0.27	0.59	0.65
3-methyl-1*H*-indene	—	—	—	—	0.83	2.12	5.93
tetralin (**1**)	—	0.27	0.83	1.95	5.18	5.37	3.86
2-methyl-1*H*-indene	—	0.11	0.29	0.19	0.45	0.47	0.39
TK-130 [$C_{10}H_{10}$]	—	—	0.47	0.35	1.00	1.04	0.85
1,2-dihydronaphthalene (**2**)	—	0.56	1.38	0.54	0.95	0.80	0.50
TL-128 [$C_{10}H_8$]	—	—	—	—	—	—	0.14
naphthalene (**5**)	0.30	0.11	0.34	0.12	0.89	1.12	2.51
TO-148 [$C_{11}H_{16}$]	—	—	—	—	—	0.06	0.08
recovery [f]	93.99	84.00	81.25	88.33	74.00	80.14	69.83
conversion [g]	*d*	5.97	16.40	29.00	69.08	87.26	94.23

[a] Flow pyrolysis conditions: system pressure = 1 x 10^{-2} torr, flow rate = 24 mL min^{-1} (Ar), residence time = 0.31 s. [b] Amounts determined by GC with a known quantity of biphenyl added as standard. Data represent the average of triplicate runs. Products identified by comparison with authentic samples or those that could be identified by retention time and GCMS are indicated by name. Products that were identified by GCMS only are indicated by code: XY-nnn, where 'X' corresponds to the system studied (A = pyrolysis of **4**, T = pyrolysis of **1**), 'Y' to the individual unknown product (A, B, C, etc.), and 'nnn' to the nominal mass. [c] See Table A-I, footnote *c*. [d] See Table A-I, footnote *d*. [e] See Table A-II, footnote *e*. [f] See Table A-I, footnote *f*. [g] See Table A-I, footnote *g*.

Table A-VI. Products and recovered starting material, total recovery of material, and conversion from the flow pyrolysis of 1,2-dihydronaphthalene (**2**) at various oven temperatures [a,b]

	yield, % [c]			
entry	RT [d]	800 °C	850 °C	903 °C
indene (**8**)	—	0.11	0.73	2.43
TD-130 [$C_{10}H_{10}$]	—	0.10	0.52	1.45
TF-130 [$C_{10}H_{10}$]	—	0.27	0.27	—
TH-130 [$C_{10}H_{10}$]	—	0.34	0.77	0.72
3-methyl-1*H*-indene	—	0.21	0.69	1.86
tetralin (**1**)	0.28	0.31	0.31	0.28
2-methyl-1*H*-indene	—	—	0.10	0.33
1,2-dihydronaphthalene (**2**)	99.72	89.91	73.23	31.09
TL-128 [$C_{10}H_8$]	—	0.06	—	0.12
naphthalene (**5**)	—	8.68	23.38	61.72
recovery [e]	92.59	80.10	90.33	83.07
conversion [f]	*d*	10.09	26.77	68.91

[a] Flow pyrolysis conditions: system pressure = 1 x 10^{-2} torr, flow rate = 22 mL min^{-1} (Ar), residence time = 0.31 s. [b] See Table A-I, footnote *b*. [c] See Table A-I, footnote *c*. [d] See Table A-I, footnote *d*. [e] See Table A-I, footnote *f*. [f] See Table A-I, footnote *g*.

APPENDIX 2

SUPPLEMENTARY PROCEDURES AND CALCULATIONS

Detailed procedure for flow pyrolysis

Initially, the flow pyrolysis apparatus (Figure 2, Paper 1) was filled with Ar. The pyrolysis portion of the apparatus was isolated from the sample chamber and flow control assembly with the three-way ball valve nearest the pyrolysis oven. After the pyrolysis portion of the apparatus had been evacuated, both the flow and bypass lines of the flow control assembly were pumped down. (CAUTION: Open the three-way ball valve **slowly** whenever a pressure difference exists. If released suddenly, the gas at higher pressure in the flow and bypass lines of the flow assembly or the sample chamber will push the hot chips from the pyrolysis oven into the trap. The ball valve is **not** designed to be a metering valve and should be left **fully open** or **fully closed**.) When both branches of the flow control assembly had reached the minimum pressure, the sample chamber was evacuated to *ca.* 15 in. vacuum (*ca.* $\frac{1}{2}$ total volume) through the flow line (needle valve fully open) and then the rest of the Ar was removed through the bypass line (CAUTION: Pressure difference across three-way ball valve). This procedure was repeated at least three times and the entire apparatus was evacuated for at least 12 hr (flow assembly on bypass).

A weighed sample in a 5-mL 14/20 round-bottom flask flushed with Ar was attached to the sample inlet with a small amount of vacuum grease. The sample was frozen with liquid N_2 and the sample inlet opened. After the system had returned to the minimum pressure (30–60 min), the sample inlet was closed and the sample allowed to warm to room temperature. The sample was refrozen with liquid N_2 and opened to the

pump for an additional 15–30 min. The sample chamber was isolated from the flow assembly and pyrolysis apparatus with the three-way ball valve nearest the sample chamber. The sample inlet was opened and the sample was allowed to warm to room temperature. No liquid sample remained in the flask. The sample chamber was filled with Ar to atmospheric pressure through the gas inlet. The gas inlet was closed and the gas mixture was allowed to equilibrate for 15 min. The pyrolysis trap was cooled with liquid N_2. The flow of gas mixture into the previously equilibrated pyrolysis oven was maintained at a fixed rate of 20–25 mL min^{-1} (Ar/1 atm/flow tube = 60 (glass), 30 (SS)) until the sample chamber was evacuated to 15 in. vacuum (*ca.* $\frac{1}{2}$ total volume). When the pyrolysis was complete (*ca.* 5 hr), the sample chamber and flow control assembly were isolated from the pyrolysis apparatus with the three-way ball valve nearest the pyrolysis oven. The pyrolysis portion of the apparatus was then filled with N_2. After the trap had warmed to near room temperature, the trap was removed and 0.5 mL biphenyl in CH_2Cl_2 (*ca.* 2 mg mL^{-1}) and an additional 0.5 mL CH_2Cl_2 was added to the trap. The trap was thoroughly rinsed with the solution, which was immediately analyzed by GC.

After a clean trap was put in place, the pyrolysis portion of the apparatus was filled with N_2 and evacuated several times. The remaining sample in the sample chamber was removed through the bypass line (CAUTION: Pressure difference across three-way ball valve). The apparatus was filled with Ar and evacuated as described above and allowed to pump down at least 12 h (flow assembly on bypass) before repeat use.

Calculation of residence time for flow pyrolysis

To calculate the residence time, the volume of the pyrolysis oven was measured. The pyrolysis run time is an average of many runs and represents the time necessary to evacuate the sample chamber from 0 to 15 in. vacuum at 20–25 mL min^{-1} (Ar/1 atm).

Volume of oven (V_{oven})

Mass of chips + mass of graduated cylinder = m_i	171.25	g
Mass of water + mass of chips + mass of graduated cylinder = m_f	248.92	g
Mass of water = $m_w = m_f - m_i$	77.76	g
Volume of water = $V_w = m_w$	77.76	mL
Volume of chips + volume of water = V_f	100.0	mL
Volume of chips = $V_{chips} = V_f - V_w$	22.3	mL
Volume of tube = $V_{tube} = \pi r^2 h = \pi(1.2\text{ cm})^2(30\text{ cm})$	135.7	mL
Volume of oven = $V_{oven} = V_{tube} - V_{chips}$	113.4	mL

Volume of sample at 760 torr and 300 K (V_{S1})

Pressure of sample (from Bourdon gauge)

Initial pressure of sample = P_i	P_i	= 0	in. vacuum
Final pressure of sample = P_f	P_f	= 15	in. vacuum
Minimum pressure of system = P_{min}	P_{min}	= 28	in. vacuum

Total volume of sample = V_T	12	L
Volume of sample = $V_{S1} = \frac{P_f - P_i}{P_{min} - P_i} V_T$	6.4	L

Volume of sample at 0.78 torr and 1100 K (V_{S2})

Initial pressure of sample = P_1	760	torr
Final pressure of sample = P_2	0.78	torr
Initial temperature of sample = T_1	300	K
Final temperature of sample = T_2	1100	K
Initial volume of sample = V_{S1}	6.4	L
Volume of sample = $V_{S2} = \frac{P_1 T_2}{P_2 T_1} V_{S1}$	2.3×10^7	mL

Flow rate (R_f)

Average run time = t_s	276	min
Flow rate = $R_f = V_{S2}/t_s$	8.3×10^4	mL min^{-1}

Residence time (t_r)

Residence time = $t_r = V_{oven}/R_f$	0.08	s

APPENDIX 3

ADDITIONAL DATA ON THE PYROLYSIS OF TETRALIN

In addition to the data on the flow pyrolysis of tetralin (**1**) presented in Paper 1 of this dissertation, additional experiments were performed. The effects of flow rate, carrier gas, and pyrolysis tube size were examined and these data are reported here. Data on the flash vacuum pyrolysis of **1** in the presence of diluents is also presented in this appendix.

Flow rate in flow pyrolysis

The results of the pyrolysis of tetralin (**1**) at 850 °C and various flow rates are presented in Table A3-I. The data at 25 mL min^{-1} can also be found in Table VIII of Paper 1 in this dissertation. A drop in conversion from *ca.* 8% to 4% and recovery from near quantitative to 60% with increasing flow rate is observed. The dehydrogenation to ethylene loss ratio increased from 0.3 to 0.7 with increasing flow rate. The reproducibility was less at higher flow rate. The range in the dehydrogenation to ethylene loss ratio at 25 mL min^{-1} was 0.23 to 0.31, while at 95 mL min^{-1} the ratio ranged from 0.48 to 0.99.

As the flow rate increases, the residence time of the sample in the pyrolysis oven decreases. The drop in conversion with increasing flow rate is expected. The decreasing recovery is most likely due to the difficulty in trapping out all of the pyrolysate at faster flow rates. The increasing dehydrogenation to ethylene loss ratio may be caused by bimolecular reactions or could be an artifact resulting from poor reproducibility between

Table A3-I. Products and recovered starting material, total recovery of material, conversion, and dehydrogenation to ethylene loss ratio from flow pyrolysis of tetralin (**1**) at various flow rates [a,b]

	yield, % [c]				
entry	10 mL min^{-1}	25 mL min^{-1}	45 mL min^{-1}	95 mL min^{-1}	390 mL min^{-1}
tetralin (**1**)	92.7	90.7	96.1	95.5	95.9
1,2-dihydronaphthalene (**2**)	0.9	1.1	1.0	1.1	0.9
naphthalene (**5**)	0.3	0.5	0.2	0.3	0.1
benzocyclobutene (**3**)	3.9	4.7	1.7	1.9	2.2
styrene (**6**)	0.7	1.1	0.2	0.2	0.3
o-allyltoluene (**4**)	0.9	1.1	0.7	0.7	0.6
2-methylindan (**7**)	0.4	0.6	0.1	0.2	—
indene (**8**)	0.2	0.2	—	0.1	—
recovery [d]	98.8	89.2	72.4	66.1	59.6
conversion [e]	7.3	9.3	3.9	4.5	4.1
ratio (**2** + **5**)/(**3** + **6**)	0.26	0.28	0.65	0.68	0.38

[a] Flow pyrolysis conditions: oven temperature = 850 °C, system pressure = 1 x 10^{-2} torr. [b] Amounts determined by GC with a known quantity of biphenyl added as standard. flow rates are for sample (Ar) volume at 1 atm. Data represent the average of triplicate runs at 95 mL min^{-1} and the average of six runs at 25 mL min^{-1}. Data for other runs are from a single experiment. [c] Moles of product divided by total moles of recovered material. [d] Total moles of recovered material divided by moles of starting material used. [e] Total moles of recovered material minus moles of recovered starting material divided by total moles of recovered material.

runs at the higher flow rates. The flow rate of 25 mL min^{-1} was chosen for the study of the flow pyrolysis of **1** at various oven temperatures presented in Table VIII of Paper 1 in this dissertation because of the high reproducibility and convenient temperature (conversion) range at this flow rate.

Carrier gas in flow pyrolysis

Two types of experiments were done to assess the effect of carrier gas on the flow pyrolysis of **1**: the use of helium as a carrier gas and the addition of hydrogen to the argon carrier gas. The data for flow pyrolysis with helium carrier gas at 850 °C are presented in Table A3-II. The recovery is only *ca.* 40–50% and the conversion *ca.* 5% for these runs. The dehydrogenation to ethylene loss ratio is between 0.1 and 0.25. The results of the flow pyrolysis of **1** at 850 °C with 18% and 36% hydrogen (by volume) in argon as carrier gas (Table A3-III) show a recovery of 80–100% and a conversion *ca.* 10%. The dehydrogenation to ethylene loss ratio is near 0.3.

The flow pyrolysis of **1** was not as convenient with helium as a carrier gas as with argon. Not only was the pyrolysate recovery with helium far lower (50% with He vs. 90% with Ar), the annoyance of listening to the roughing pump's high pitched gurgling with helium bubbling through it all day cannot be underestimated. The dehydrogenation to ethylene loss ratios are similar with the two carrier gasses but the effect of flow rate is less pronounced with helium than with argon. There were no apparent advantages of using helium as a carrier gas and argon was used for other experiments.

We also attempted to induce dehydrogenation by adding hydrogen to the argon carrier gas. The flow pyrolysis of **1** with up to 36% hydrogen (by volume) in argon is for all intents and purposes identical to pyrolysis with 100% argon (25 mL min^{-1}, Table

Table A3-II. Products and recovered starting material, total recovery of material, conversion, and dehydrogenation to ethylene loss ratio from flow pyrolysis of tetralin (**1**) with helium carrier gas [a,b]

	yield, % [c]	
entry	20 mL min^{-1}	150 mL min^{-1}
tetralin (**1**)	95.4	95.4
1,2-dihydronaphthalene (**2**)	0.5	0.7
benzocyclobutene (**3**)	2.9	2.9
styrene (**6**)	0.4	0.3
o-allyltoluene (**4**)	0.7	0.6
2-methylindan (**7**)	0.2	—
recovery [d]	40.8	52.2
conversion [e]	4.6	4.6
ratio **2**/(**3** + **6**)	0.14	0.21

[a] Flow pyrolysis conditions: oven temperature = 850 °C, system pressure = 1 x 10^{-2} torr. [b] Amounts determined by GC with a known quantity of biphenyl added as standard. flow rates are for sample (He) volume at 1 atm. Data are from a single experiment at each flow rate. [c] See Table A3-I, footnote *c*. [d] See Table A3-I, footnote *d*. [e] See Table A3-I, footnote *e*.

Table A3-III. Products and recovered starting material, total recovery of material, conversion, and dehydrogenation to ethylene loss ratio from flow pyrolysis of tetralin (**1**) with hydrogen in argon carrier gas [a,b]

	yield, % [c]	
entry	18% H_2 in Ar	36% H_2 in Ar
tetralin (**1**)	88.8	91.7
1,2-dihydronaphthalene (**2**)	1.2	1.0
naphthalene (**5**)	0.6	0.6
benzocyclobutene (**3**)	6.0	4.4
styrene (**6**)	1.3	0.8
o-allyltoluene (**4**)	1.2	1.1
2-methylindan (**7**)	0.6	0.4
indene (**8**)	0.2	0.1
o-(1-propenyl)toluene	0.1	—
recovery [d]	100	84.7
conversion [e]	11.2	8.3
ratio (**2** + **5**)/(**3** + **6**)	0.24	0.28

[a] Flow pyrolysis conditions: oven temperature = 850 °C, system pressure = 1 x 10^{-2} torr. [b] Amounts determined by GC with a known quantity of biphenyl added as standard. flow rates are for sample (H_2 in Ar) volume at 1 atm. Data are from a single experiment with each gas mixture. [c] See Table A3-I, footnote *c*. [d] See Table A3-I, footnote *d*. [e] See Table A3-I, footnote *e*.

A3-I). The recovery and conversion data are similar and no increase in dehydrogenation was observed. flow pyrolysis with larger amounts of hydrogen was not attempted because of the potential explosive hazard associated with this experiment.

Pyrolysis tube size in flow pyrolysis

We also have studied the effect of a narrow 3 mm (id) pyrolysis tube on the flow pyrolysis of **1** (Table A3-IV). The recovery is between 10% and 50% and the conversion from 1% to 15% for pyrolysis at 800–940 °C. The dehydrogenation to ethylene loss ratio is *ca.* 0.3, except for the run at 850 °C, where the conversion is <1%, the ratio is >1.

The results of the flow pyrolysis of **1** with the 3 mm pyrolysis tube are very similar to those with the normal pyrolysis tube with chip packing. The recovery was generally lower with the 3 mm tube but the dehydrogenation to ethylene loss ratios and product distributions were comparable, except for the run at 850 °C. However, the conversion is so low for this run that the ratio will have a large error. This tube is so narrow that it is difficult to work with. Note that the flow rates were markedly different at 850 °C and 940 °C even though the setting on the flow meter was the same. This experiment should be more practical with a tube of slightly larger diameter, perhaps 5–6 mm (id).

Copyrolysis with diluents in FVP

We have also copyrolyzed **1** in the presence of diluents, some of which are expected to act as hydrogen atom chain terminators. The dehydrogenation to ethylene loss ratios for the FVP of **1** at 900 °C (system pressure = 10^{-5} torr, sample temperature = RT) with *ca.* 5, 10, and 20 fold excess by mass of toluene are 0.90, 0.68, and 0.50,

Table A3-IV. Products and recovered starting material, total recovery of material, and conversion from flow pyrolysis of tetralin (**1**) with 3 mm (id) pyrolysis tube [a,b]

	yield, % [c]		
entry	800 °C [d]	850 °C [e]	940 °C [e]
tetralin (**1**)	84.1	99.1	94.0
1,2-dihydronaphthalene (**2**)	2.3	0.4	1.2
naphthalene (**5**)	0.7	—	—
benzocyclobutene (**3**)	7.9	0.3	3.6
styrene (**6**)	1.7	—	—
o-allyltoluene (**4**)	2.0	0.2	1.2
2-methylindan (**7**)	0.8	—	—
indene (**8**)	0.5	—	—
recovery [f]	30.5	46.4	13.6
conversion [g]	15.9	0.93	6.0
ratio (**2** + **5**)/(**3** + **6**)	0.32	1.29	0.33

[a] Flow pyrolysis conditions: system pressure = 1 x 10^{-2} torr. [b] Amounts determined by GC with a known quantity of biphenyl added as standard. flow rates are for sample (Ar) volume at 1 atm. Data are from a single experiment at each temperature. [c] See Table A3-I, footnote *c*. [d] Flow rate = 10 mL min^{-1} (Ar/1 atm). [e] The flow setting on the flow meter was identical for these two runs but the flow rate was substantially different: flow rate (850 °C) = 57 mL min^{-1}, flow rate (940 °C) = 84 mL min^{-1}. [f] See Table A3-I, footnote *d*. [g] See Table A3-I, footnote *e*.

respectively. Similar experiments with 5, 10, and 20 fold excess by mass of benzene leads to dehydrogenation to ethylene loss ratios of 0.96, 0.58, and 0.82, respectively. When the less volatile diluent 2-chloro-*p*-xylene is copyrolyzed in a 5 fold excess by mass with **1** the dehydrogenation to ethylene loss ratio is 0.39. By comparison, the dehydrogenation to ethylene loss ratio for the FVP of **1** alone at 900 °C under these conditions is 1.04. When less volatile diluents 2-chloro-*p*-xylene and mesitylene are copyrolyzed in a 5 fold excess by mass with **1** at 800 °C (system pressure = 10^{-5} torr, sample temperature = RT), the dehydrogenation to ethylene loss ratios are 0.71 and 0.57, respectively. By comparison, the dehydrogenation to ethylene loss ratio for the FVP of **1** alone at 800 °C under these conditions is 1.08.

The experiments with toluene and benzene were designed to differentiate between the dilution effect of the addition of these compounds to the sample and the hydrogen atom chain terminating effect of toluene. The results show that both pyrolyses are nearly identical up to a 10 fold excess of diluent. There is no evidence that toluene is reducing dehydrogenation more than benzene, indicating that the main effect is dilution rather than hydrogen atom chain termination. The likely cause of the reversal at 20 fold excess of diluent is crystallization of the benzene sample when it is cooled prior to pyrolysis. At 20 fold excess of benzene, the tetralin (**1**) in the mixture may be located between crystal planes and, therefore, easily removed by the vacuum leaving the benzene behind in the sample chamber. The toluene sample, on the other hand, forms a glass when cooled and the same effect is not observed.

The high volatility of toluene in comparison to **1** may have made it an ineffective hydrogen atom chain terminator so we chose some less volatile methylated benzene rings as diluents. When 2-chloro-*p*-xylene and mesitylene were copyrolyzed with **1**, dehydrogenation was reduced more than in copyrolysis with either toluene or benzene.

with mesitylene reducing dehydrogenation more than 2-chloro-*p*-xylene. This could be interpreted as a hydrogen atom chain termination being proportional to the number of methyl groups on the benzene rings.

The data presented above could be the result of heat transfer effects. The diluents may be acting as heat transfer agents effectively raising the temperature of the pyrolysis and reducing the dehydrogenation to ethylene loss ratio. The greater the excess of diluent the greater the effect, with the anomalous benzene result at 20 fold excess explained as above. The greater effect of 2-chloro-*p*-xylene and mesitylene could be due to their lower volatility making them more effective heat transfer agents. The apparent difference between the two could be to due to dehydrogenation induced by chlorine atoms produced by hydrodehalogenation from 2-chloro-*p*-xylene.

PAPER 2. THE FLASH VACUUM PYROLYSIS OF 3-BENZOCYCLOHEPTENONE AND 1,3,4,5-TETRAHYDRO-2-BENZOTHIEPIN-2,2-DIOXIDE: MODEL SYSTEMS FOR THE GAS-PHASE PYROLYSIS OF TETRALIN

INTRODUCTION

The gas-phase thermal decomposition of tetralin (**1**) gives rise to several products (Scheme I).[1,2] The major products include primary products 1,2-dihydronaphthalene (**2**), benzocyclobutene (**3**), and *o*-allyltoluene (**4**). Secondary products, naphthalene (**5**) from **2**, styrene (**6**) from **3**, 2-methylindan (**7**)[3] from **4**, and indene (**8**) primarily from **7**, have been identified along with various minor products.

The thermal decomposition of **1** is believed to involve cleavage of the weak benzylic carbon-carbon bond to form diradical **9**. As part of our effort to understand the

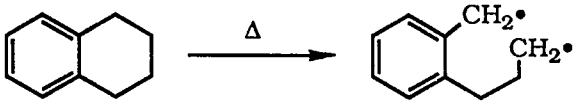

1 **9**

thermal decomposition of **1**, we have studied the flash vacuum pyrolysis (FVP) of some model systems that could produce **9**. It was hoped that the loss of carbon monoxide from 3-benzocycloheptenone (**10**) and sulfur dioxide from 1,3,4,5-tetrahydro-2-benzothi-

Scheme I

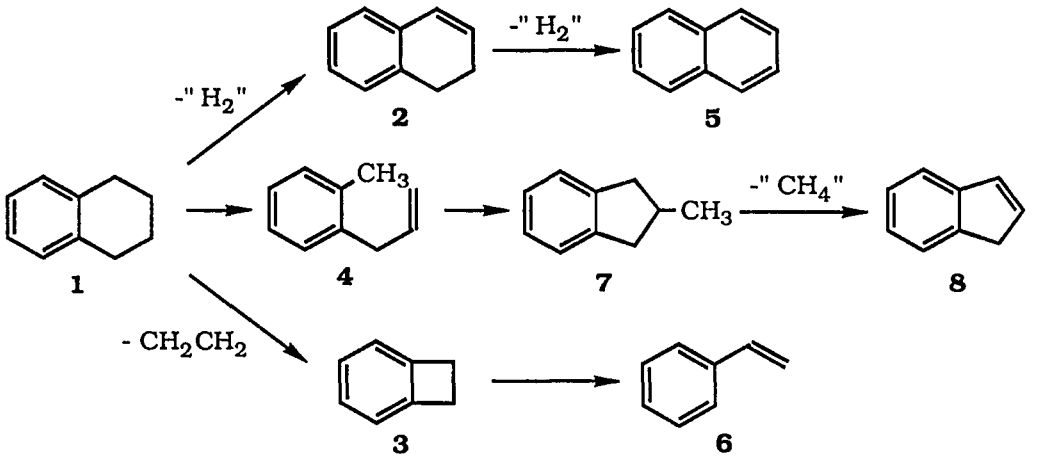

epin-2,2-dioxide (**11**) would involve the formation of intermediate **9**. Our studies of the

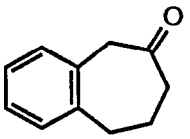

10

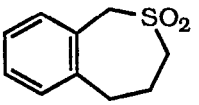

11

FVP of ketone **10** and sulfone **11** and the photolysis of ketone **10** are presented in this paper. We also present a study of the pyrolysis of **10** under flow pyrolysis conditions that was conducted to discover to what extent the chemistry observed from FVP involves bimolecular reactions.

RESULTS

3-Benzocycloheptenone (**10**) and 1,3,4,5-tetrahydro-2-benzothiepin-2,2-dioxide (**11**) were prepared by the reaction sequences shown in Scheme II.

When 3-benzocycloheptenone (**10**) was pyrolyzed at 10^{-5} torr, the major products were tetralin (**1**), 1,2-dihydronaphthalene (**2**), naphthalene (**5**), indene (**8**), 1-methylnaphthalene (**12**), and 2-methylnaphthalene (**13**). At 700 °C, no benzocyclobutene (**3**) or styrene (**6**) was detected; only at 850–900 °C were more substantial amounts of **3** and **6** observed. These results are summarized in Table I.

Ketone **10** was also pyrolyzed under flow conditions (Table II) to investigate the possibility that bimolecular reactions were occurring in the FVP experiments. Comparable amounts of the major FVP products were also produced in the flow pyrolysis.

The results of the photolysis of **10** ($\lambda > 280$ nm) in the presence of methanol are presented in Table III. The major products produced were **1** and **4**. A small amount of methyl ester **14** was also detected. We could not isolate this compound because of the

Scheme II

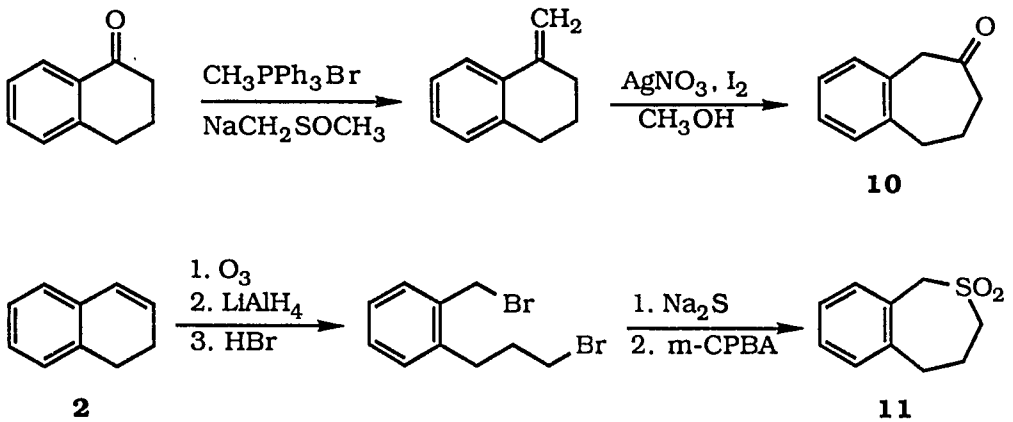

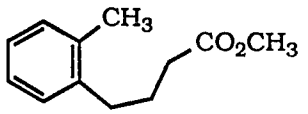

14

limited quantity, but the mass spectrum is consistent with structure **14** and none of the other products detected have the formula $C_{12}H_{16}O_2$.

The results from the FVP of sulfone **11** are strikingly different from those for ketone **10** (Table IV). The major product observed was tetralin (**1**), but some *o*-allyltoluene (**4**) was also detected. All the other products were produced in only minor amounts.

Table I. Products and recovered starting material from FVP of 3-benzocycloheptenone (**10**) at various oven temperatures [a,b]

	yield, % [c]				
entry	700 °C	750 °C	800 °C	850 °C	900 °C
3-benzocycloheptenone (**10**)	93.3	88.6	63.6	38.6	11.9
tetralin (**1**)	0.2	1.1	6.5	14.9	19.9
1,2-dihydronaphthalene (**2**)	0.7	1.3	3.4	5.7	5.6
naphthalene (**5**)	0.4	0.6	2.2	4.7	10.2
benzocyclobutene (**3**)	—	0.1	0.7	2.0	4.2
styrene (**6**)	—	0.2	0.4	1.1	4.0
o-allyltoluene (**4**)	—	0.2	0.8	1.8	1.9
2-methylindan (**7**)	—	—	0.2	0.8	1.6
indene (**8**)	0.2	0.7	3.3	8.2	15.3
1-methylnaphthalene (**12**)	1.5	2.6	8.1	8.4	6.6
2-methylnaphthalene (**13**)	0.6	1.1	3.1	3.5	3.0
other products	2.9 [d]	3.4 [d]	7.6 [d]	10.3 [d]	15.4 [d]
recovery [e]	90.1	83.7	84.0	78.4	66.7
conversion [f]	6.7	11.4	36.4	61.5	88.1

[a] FVP conditions: system pressure = 2 x 10^{-5} torr, sample temperature = 30–40 °C. [b] Amounts determined by GC with a known quantity of biphenyl added as standard. Data represent the average of triplicate runs. [c] Moles of product divided by total moles of recovered material. [d] See Table A-I in the Appendix of Paper 2, this dissertation, for a more detailed analysis. [e] Total moles of recovered material divided by moles of starting material used. [f] Total moles of recovered material minus moles of recovered starting material divided by moles of recovered material.

Table II. Products and recovered starting material from flow pyrolysis of 3-benzocycloheptenone (**10**) at various oven temperatures [a,b]

	yield, % [c]			
entry	750 °C	800 °C	850 °C	900 °C
3-benzocycloheptenone (**10**)	90.2	79.8	49.8	12.2
tetralin (**1**)	2.1	6.3	18.7	29.3
1,2-dihydronaphthalene (**2**)	1.0	1.1	2.4	3.2
naphthalene (**5**)	0.7	0.8	2.0	3.7
benzocyclobutene (**3**)	—	0.5	1.7	8.0
styrene (**6**)	—	—	0.4	4.1
o-allyltoluene (**4**)	0.6	1.0	2.1	3.9
2-methylindan (**7**)	—	—	0.7	2.6
indene (**8**)	0.4	1.3	4.2	10.4
1-methylnaphthalene (**12**)	1.9	3.5	7.8	8.6
2-methylnaphthalene (**13**)	0.8	1.4	3.2	3.6
other products	2.4 [d]	4.5 [d]	6.9 [d]	10.4 [d]
recovery [e]	54.0	50.4	52.3	45.9
conversion [f]	9.8	20.2	50.2	87.8

[a] Flow pyrolysis conditions: system pressure = 0.010 torr, sample. temperature = 26 °C, flow rate = 450 mL min^{-1} (Ar/1 atm) for 10 h, residence time = 0.28 s. [b] See Table I, footnote *b*. [c] See Table I, footnote *c*. [d] See Table A-II in the Appendix of Paper 2, this dissertation, for a more detailed analysis. [e] See Table I, footnote *e*. [f] See Table I, footnote *f*.

Table III. Products and recovered starting material from photolysis of 3-benzocycloheptenone (**10**) [a,b]

		yield, % [c]				
recovery, % [d]	conversion, % [e]	**10**	**1**	**4**	**14** [f]	other prods.
72.4	15.8	84.2	8.1	2.7	1.4	3.7 [g]

[a] Photolysis conditions: [**10**] = 0.33 mM in 11:1 (v:v) pentanes:methanol, medium pressure Hg lamp with Pyrex filter (λ > 280 nm), 2 h at room temperature. [b] See Table I, footnote *b*. [c] See Table I, footnote *c*. [d] See Table I, footnote *e*. [e] See Table I, footnote *f*. [f] GCMS (EI, 70 eV) *m/e* (% base peak) 192 (28.1), 161 (16.1), 119 (29.1), 118 (100), 117 (33.6), 105 (55.5), 77 (20.6), 74 (47.1). [g] See Table A-III in the Appendix of Paper 2, this dissertation, for a more detailed analysis.

Table IV. Products and recovered starting material from FVP of 1,3,4,5-tetrahydro-2-benzothiepin-2,2-dioxide (**11**) at various oven temperatures [a,b]

	yield, % [c]			
entry	600 °C	700 °C	800 °C	900 °C
1,3,4,5-tetrahydro-2-benzothiepin-2,2-dioxide (**11**)	84.0	8.5	0.1	—
tetralin (**1**)	13.2	75.8	79.1	62.5
1,2-dihydronaphthalene (**2**)	0.3	0.9	2.0	3.4
naphthalene (**5**)	—	0.3	0.9	4.6
benzocyclobutene (**3**)	0.3	1.1	2.1	7.8
styrene (**6**)	0.3	0.6	0.4	3.6
o-allyltoluene (**4**)	2.0	12.5	11.3	5.4
2-methylindan (**7**)	—	0.2	2.6	5.2
indene (**8**)	—	0.1	0.6	4.4
other products	*d*	*d*	0.7 [d]	2.9 [d]
recovery [e]	83.5	79.0	72.6	69.4
conversion [f]	29.9	93.2	99.9	100

[a] FVP conditions: system pressure = 2 x 10^{-5} torr, sample temperature = RT. [b] See Table I, footnote *b*. [c] See Table I, footnote *c*. [d] See Table A-IV in the Appendix of Paper 2, this dissertation, for a more detailed analysis. [e] See Table I, footnote *e*. [f] See Table I, footnote *f*.

DISCUSSION

A comparison of the pyrolysis chemistry of 3-benzocycloheptenone (**10**) and tetralin (**1**) reveals three major differences. First, the pyrolysis of ketone **10** produces primarily 1,2-dihydronaphthalene (**2**) and naphthalene (**5**) while, flow pyrolysis of **1** produces primarily benzocyclobutene (**3**) and styrene (**6**).[5a] Second, the amount of indene (**8**) produced from the pyrolysis of ketone **10** is much larger than the amounts of *o*-allyltoluene (**4**) and 2-methylindan (**7**), but these products are obtained in comparable yields from **1**.[5] We have identified the pathway **4** to **7** to **8** as the major source of **8** in the decomposition of **1**;[5] therefore, in the decomposition of ketone **10**, **8** is unlikely to have resulted from the secondary pyrolysis of **4** and **7** and must have been produced by an alternate pathway. Finally, the pyrolysis of **10** leads to several $C_{11}H_{10}$ products, most prominently 1-methyl (**12**) and 2-methylnaphthalene (**13**), that constitute a net loss of H_2O from ketone **10** ($C_{11}H_{12}O$) and obviously have no parallel in the decomposition of **1**.

The initial step in the decomposition of 3-benzocycloheptenone (**10**) is expected to be breakage of the weak benzylic carbon-carbon bond leading to the formation of diradical **15** that could lose CO to form diradical **9**. It is reasonable to expect diradical **9**

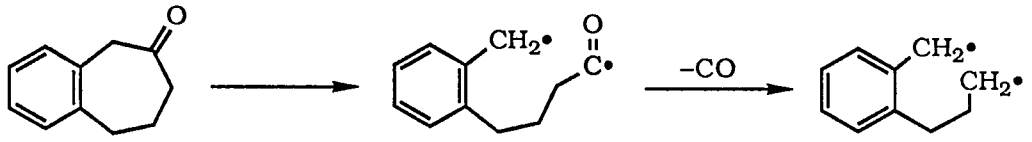

10 **15** **9**

to close to form tetralin (**1**) and disproportionate to form *o*-allyltoluene (**4**), and both are produced in the decomposition of **10** under FVP (Table I) and flow pyrolysis (Table II) conditions. Photolysis of ketone **10** also yields **1** and **4**. Further support for the production of **1** and **4** from diradical **9** comes from study of the pyrolysis of the strained

hydrocarbon **16** that produces **1** and **4** as the major products and probably involves **9** as an intermediate.[6]

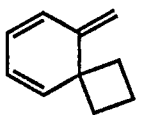

16

The production of a small amount of methyl ester **14** in the photolysis of **10** in the presence of methanol is explained by the addition of methanol to ketene **7**. This

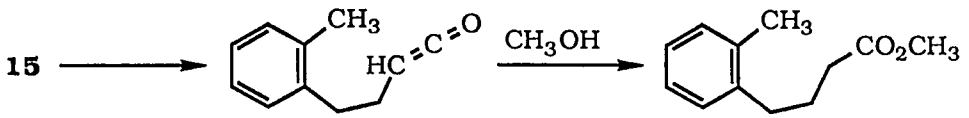

17 **14**

ketene could be formed from the disproportionation of carbonyl diradical **15**. The observation of **14** supports the assumption that the loss of CO is stepwise and shows that **15** has an appreciable lifetime at room temperature in dilute solution.

The relative amounts of dehydrogenation products, 1,2-dihydronaphthalene (**2**) and naphthalene (**5**), to ethylene-loss products, benzocyclobutene (**3**) and styrene (**6**), produced in the pyrolysis of ketone **10** are also of interest. We have previously observed that ethylene loss is the lowest energy gas-phase unimolecular reaction of **1**.[5a] The flow pyrolysis of **1** produces an ethylene loss to dehydrogenation ratio of between 3 and 5 to 1 over the entire temperature range studied (750–900 °C). However, bimolecular dehydrogenation of **1** is the predominate reaction under some FVP conditions.

The FVP of **10** clearly produces greater amounts of dehydrogenation than ethylene loss (Table I). No **3** or **6** was detected at 700 °C; although, larger amounts are produced at 850–900 °C. This increase corresponds to a leveling off of the amount of **1** that indicates secondary pyrolysis is occurring. Even at 900 °C, the ratio of ethylene loss to dehydrogenation is *ca.* 0.5:1.

We studied the decomposition of **10** under flow pyrolysis conditions (Table II) to eliminate possible bimolecular reactions. Both FVP and flow pyrolysis produced an excess of dehydrogenation except at the highest flow pyrolysis temperature. At 900 °C, substantially less **2** and **5** is produced than in the corresponding FVP experiments. This is consistent with bimolecular dehydrogenation in the secondary decomposition of **1** during FVP. In both the FVP and flow pyrolysis of **10**, the increase in the amount of **3** and **6** corresponds to a leveling off of the amount of **1**. This indicates that the ethylene-loss products appear to result from secondary decomposition of **1**. Thus, the unimolecular thermal decomposition of **10** appears to produce more dehydrogenation products **2** and **5** than are produced by the unimolecular decomposition of **1**. Possibly **2** and **5** are produced from diradical **15** by a route that does not involve loss of CO to form diradical **9**.

The pyrolysis of ketone **10**, whether under FVP or flow conditions, also produces more indene (**8**) relative to *o*-allyltoluene (**4**) and 2-methylindan (**7**) than is produced by tetralin (**1**) under similar conditions. We have shown[5] that **8** produced in the decomposition of **1** is a secondary product ultimately derived from **4** that cyclizes to **7**. The subsequent loss of a methyl group from **7** leads to the formation of **8**. We can therefore conclude that **8** produced directly from **10** derives from another reaction path. Of course, at 900–950 °C where secondary pyrolysis of **1** takes place, some **8** no doubt comes from **4** and **7**. It is difficult to quantify how much **8** is produced by the new reaction and how much from the **4** to **7** to **8** pathway at the higher pyrolysis temperatures.

The most surprising products of the pyrolysis of ketone **10** are the $C_{11}H_{10}$ isomers that constitute an elimination of water from ketone **10**. The major water-loss products produced in the pyrolysis of **10**, under both FVP and flow conditions, are

1-methyl (**12**) and 2-methylnaphthalene (**13**). Several minor $C_{11}H_{10}$ products were also observed in the pyrolysis of **10**. These products are produced in diminishing amounts as the temperature is increased and appear to be precursor products to **12** and **13**. These precursor products were produced in amounts too small to be isolated but literature precedence for the transformation of $C_{11}H_{10}$ isomers to **12** and **13** was found.[7] Previous workers had found that benzocycloheptatrienes **18** and **19** (Scheme III) were formed in the pyrolysis of benzonorbornene.[7a] At higher pyrolysis temperatures, **18** and **19** were converted to **12** and **13**.[7a] One could speculate that **18** and **19** may be formed from ketone **10** through enol **20**. A [1,5] hydrogen shift of **20** would form *o*-quinodimethane **21**. The loss of H_2O from **21** would give *o*-quinodimethane **22** and subsequent [1,5] hydrogen shifts would give **18** and **19**. Benzocycloheptatriene **18** could provide a source of indene (**8**) if cyclization to **23** followed by the loss of acetylene occurred.

The pyrolysis of 1,3,4,5-tetrahydro-2-benzothiepin-2,2-dioxide (**11**) is as simple as the pyrolysis of 3-benzocycloheptenone (**10**) is complex. The FVP of sulfone **11** produces tetralin (**1**) and a small amount of *o*-allyltoluene (**4**). At higher temperatures, the products appear to derive from secondary pyrolysis of **1**.

At a given temperature, sulfone **11** decomposes to a greater extent than ketone **10**. This is consistent with the benzylic-sulfonyl bond being weaker than the benzylic-carbonyl bond that is supported by bond energies.[8] The ratio of tetralin (**1**) to *o*-allyltoluene (**4**) from sulfone **11** at lower pyrolysis temperatures (7.0 at 800 °C) is close to that produced from the pyrolysis of ketone **10** (6.3 at 800 °C) and may reflect the ratio of **1** to **4** that diradical **9** produces at this temperature. It is possible that some **1** from sulfone **11** may result from a concerted extrusion of SO_2 with concurrent

carbon-carbon bond formation. Alternately, formation of diradical **24** followed by direct conversion of **24** to **1** with concurrent loss of SO_2 may be responsible.

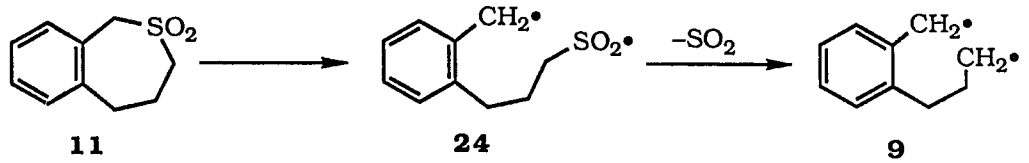

11 **24** **9**

Scheme III

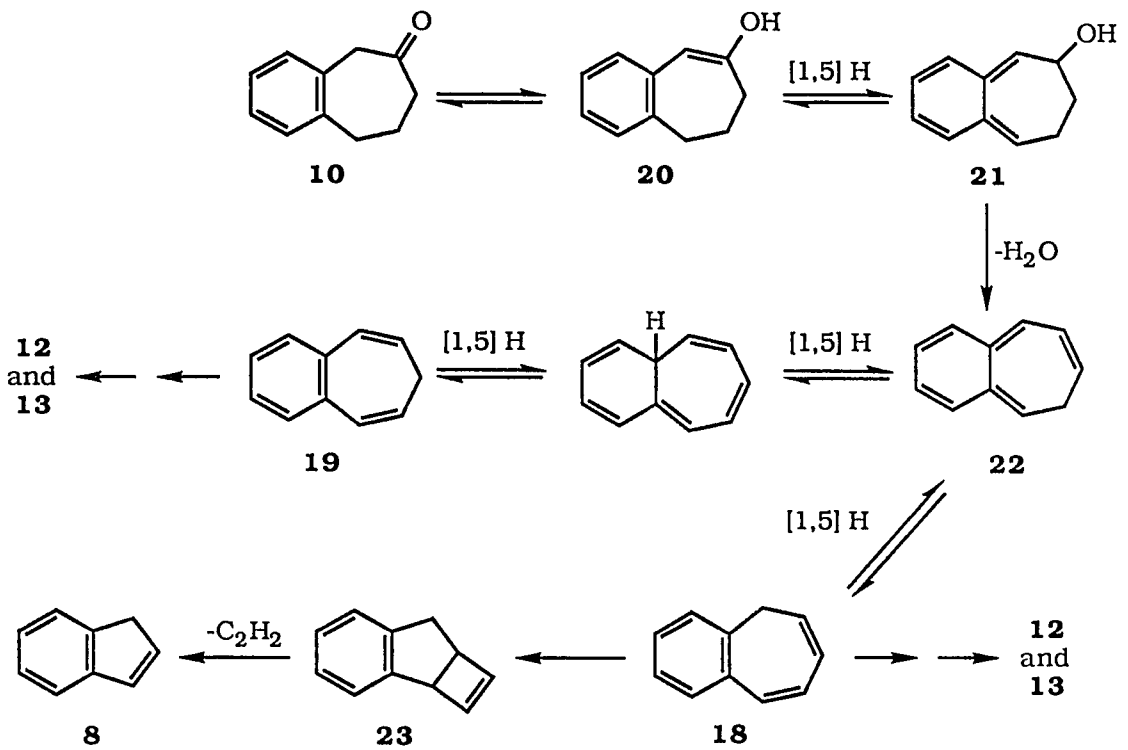

10 **20** **21** **19** **22** **8** **23** **18**

CONCLUSION

Several conclusions can be drawn from this study. First the thermal decomposition of ketone **10** in the gas-phase does produce diradical **9** but other reactions not involving **9** produce dehydration products (**12**, **13**, and other minor products), dehydrogenation products (**2** and **5**), and indene (**8**). Second, the major reaction in the photochemical decomposition of **10** at room temperature involves diradical **9**. Third, the major pathway of the thermal decomposition of sulfone **11** in the gas-phase also involves diradical **9**. Fourth, in all three cases presented here and in a previous study,[6] where **9** was produced from strained hydrocarbon **16**, the major products were tetralin (**1**) and *o*-allyltoluene (**4**). The ratio of **1** to **4** increases with temperature and is between 1 and 8 to 1 over a temperature range of 25 to 950 °C. Fifth, diradical **9** produces little or no dehydrogenation products (**2** and **5**) or ethylene-loss products (**3** and **6**). This conclusion supports the argument that ethylene loss from the thermal decomposition of tetralin (**1**) proceeds by a concerted mechanism and this argument has received support from other experiments.[2n]

EXPERIMENTAL

General Procedures

Methods and materials

Some general methods have been described previously.[9] Photolysis was performed using a water-cooled 450 W medium pressure Conrad-Hanovia lamp. ^1H NMR spectra were recorded on a Nicolet NT-300 spectrometer. FTIR spectra were obtained on an IBM IR/98 or a Digilab FTS-7 spectrophotometer. GCMS were performed on a Finnegan 4000 mass spectrometer. HRMS were performed on a Kratos MS-50 mass spectrometer. All materials were commercially available and used as received, except where indicated.

3-Benzocycloheptenone (10) 1-Methylene-1,2,3,4-tetrahydronaphthalene was prepared by a modified literature procedure.[10] Dry DMSO (50 mL) was added to NaH (4.0 g, 0.165 mol) in a 250-mL three-neck round-bottom flask fitted with a 125-mL dropping funnel and condenser under Ar atmosphere with a magnetic stirrer. The solution was heated to 70–75 °C for 1 h (until H_2 evolution had ceased). DMSO (100 mL) was added to methyltriphenylphosphonium bromide (53.6 g, 0.15 mol) that was then heated to *ca.* 70 °C until the salt completely dissolved. This solution was transferred to the dropping funnel and was added dropwise to $NaCH_2SOCH_3$/DMSO, forming a red-brown solution. After stirring for an additional 1 h, 1-tetralone (14.6 g, 0.10 mol) was added dropwise with a syringe and the solution was stirred for 2 h. H_2O (250 mL) was added to the reaction mixture that was then extracted with hexanes (4 x 150 mL). The combined hexanes portions was washed with H_2O (2 x 150 mL) and dried ($MgSO_4$). The hexanes solution was filtered through neutral alumina to remove residual triphen-

ylphosphine oxide and color. The solvent was removed *in vacuo*. The product was purified by flash chromatography on a silica gel column (50 x 150 mm) with hexanes to yield 1-methylene-1,2,3,4-tetrahydronaphthalene (13.5 g, 0.093 mol, 93% yield). bp 60–61 °C (0.8 torr) [lit.[11] 103 °C (14 mm)]; ^{1}H NMR ($CDCl_3$) δ 7.66–7.63 (m, 1 H), 7.17–7.05 (m, 3 H), 5.47 (br s, 1 H), 4.94 (d, J = 1.3 Hz, 1 H), 2.84 (t, J = 6.3 Hz, 2 H), 2.55 (pseudo t, J = 6.2 Hz, 2 H), 1.88 (quintet, J = 6.2 Hz, 2 H) [lit.[11] ^{1}H NMR (benzene-d_6) δ 7.83–7.53 (m, 1 H), 7.46–7.03 (m, 3 H), 5.50 (br s, 1 H), 4.96 (br s, 1 H), 3.00–1.60 (m, 6 H)]; GCMS (EI, 70 eV) *m/e* (% base peak) 144 (46.4), 129 (100), 128 (46.5), 115 (15.6).

The following procedure was adapted from the previously published procedure.[12] $AgNO_3$ (4.7 g, 0.028 mol) was added to a dry 500-mL three-neck round-bottom flask fitted with a 125-mL pressure-equalizing dropping funnel and condenser under Ar. Dry CH_3OH (2 Na, 150 mL) was added to the $AgNO_3$ and the solution was refluxed until the salt dissolved (<1 h). Care was taken to avoid exposure of this solution to light. I_2 (3.6 g, 0.014 mol) was dissolved in dry CH_3OH (2 Na, 100 mL). After the $AgNO_3$ had dissolved, 1-methylene-1,2,3,4-tetrahydronaphthalene (2.0 g, 0.014 mol) was added to the I_2 solution in CH_3OH. The stopper was removed from the dropping funnel and the alkene/I_2 solution was immediately transferred ALL AT ONCE. The funnel was restoppered and the alkene/I_2 solution was added RAPIDLY to the refluxing $AgNO_3$ in CH_3OH over a period of a few minutes with rapid stirring. After the addition was complete, the reaction mixture was refluxed for an additional 5 h. When the solution had cooled to room temperature, the AgI was filtered off and washed with CH_3OH (2 x 25 mL). H_2O (150 mL) and saturated NaCl (150 mL) were added to the filtrate. The reaction mixture was extracted with ether (4 x 150 mL) and the combined organic fractions was washed with H_2O (2 x 150 mL) and saturated NaCl (150 mL). The organic phase was dried ($MgSO_4$), concentrated, and the crude ketone was purified by flash

chromatography on a silica gel column (50 x 160 mm) with 1:9 ethyl acetate to hexanes to yield 3-benzocycloheptenone (1.3 g, 8.2 mmol, 59% yield). mp (2,4-DNP derivative) 170–170.3 °C [lit.[13] 169–170.5 °C]; FTIR (KBr) 2941, 1713, 787, 756; ^{1}H NMR ($CDCl_3$) δ 7.23–7.15 (m, 4 H), 3.73 (s, 2 H), 2.95 (t, J = 6.3 Hz, 2 H), 2.57 (t, J = 6.9 Hz, 2 H), 1.99 (quintet, J = 6.6 Hz, 2 H) [lit.[13] ^{1}H NMR ($CDCl_3$) δ 7.16 (s, 4 H), 3.7 (s, 2 H), 3.1–2.8 (pseudo t, 2 H), 2.7–2.4 (pseudo t, 2 H), 2.2–1.6 (m, 2 H)]; GCMS (EI, 70 eV) *m/e* (% base peak) 160 (82.1), 105 (88.0), 104 (66.8), 55 (100).

1,3,4,5-Tetrahydro-2-benzothiepin-2,2-dioxide (11) 1,2-Dihydronaphthalene (2.6 g, 0.020 mol) was dissolved in CH_2Cl_2 (100 mL) and the solution was cooled to -78 °C. O_3 (*ca.* 2% in O_2) was bubbled through the solution until a blue color developed. Excess O_3 was then removed by bubbling N_2 through the solution until the blue color had dissipated. The reaction mixture was warmed to room temperature and the solvent was removed *in vacuo*. The ozonide was dissolved in THF (15 mL) and added dropwise to a slurry of $LiAlH_4$ (0.8 g, 0.022 mol) in THF (100 mL) at 0 °C. After the addition was complete, the reaction mixture was stirred overnight at room temperature. A slurry of wet Na_2SO_4 was added to the reaction mixture until evolution of H_2 ceased. The white solid was filtered off and washed with ethyl acetate. The filtrate was dried ($MgSO_4$) and the solvent was removed *in vacuo*. The crude diol was distilled at 150 °C (0.2 torr) to yield *o*-(3-hydroxypropyl)benzyl alcohol (2.54 g, 0.015 mol, 75% yield). FTIR (thin film) 3375 (br), 2937, 1032, 758; ^{1}H NMR ($CDCl_3$) δ 7.33–7.14 (m, 4 H), 4.67 (s, 2 H), 3.50 (t, J = 6.0 Hz, 2 H), 2.82 (t, J = 6.9 Hz, 2 H), 1.90 (quintet, J = 6.6 Hz, 2 H).

Hydrobromic acid (48%, 4 mL, 0.035 mol) was added to *o*-(3-hydroxypropyl)benzyl alcohol (0.62 g, 3.8 mmol) and the reaction mixture was heated to 100 °C for 8 h. After it had cooled to room temperature, the reaction mixture was extracted with ether (3 x 20 mL). The combined organic phases was washed with saturated

$NaHCO_3$ (20 mL), H_2O (20 mL) and saturated NaCl (20 mL). The organic phase was dried ($MgSO_4$) and the solvent was removed *in vacuo*. The dibromide was purified by flash chromatography on a silica gel column (40 x 80 mm) with hexanes to yield *o*-(3-bromopropyl)benzyl bromide (0.88 g, 3.0 mmol, 79% yield). ^1H NMR ($CDCl_3$) δ 7.37–7.20 (m, 4 H), 4.56 (s, 2 H), 3.48 (t, J = 6.8 Hz, 2 H), 2.91 (t, J = 7.2 Hz, 2 H), 2.29–2.18 (m, 2 H); GCMS (EI, 70 eV) *m/e* (% base peak) 294 (3.1), 292 (6.0), 290 (2.8), 213 (49.5), 211 (52.9), 131 (84.9), 105 (100).

$Na_2S{\bullet}9H_2O$ (0.82 g, 3.4 mmol) was dissolved in absolute ethanol (500 mL). Five portions of *o*-(3-bromopropyl)benzyl bromide (50 mg, 0.17 mmol, *ca.* 30 μL) were added at 1 $\frac{1}{2}$ h intervals and then the reaction mixture was stirred overnight.[14] This procedure was repeated with five additional portions of dibromide. After the reaction mixture was again stirred overnight, most of the ethanol (*ca.* 450 mL) was removed by distillation. H_2O (100 mL) was added to the residue that was then extracted with ether (3 x 50 mL). The combined organic layers was washed with H_2O (2 x 50 mL) and saturated NaCl (50 mL), then dried ($MgSO_4$). The solvent was removed *in vacuo* and the crude product was purified by flash chromatography on a silica gel column (30 x 150 mm) with 5:1 hexanes to CH_2Cl_2 to yield 1,3,4,5-tetrahydro-2-benzothiepin (0.18 g, 1.1 mmol, 65% yield). mp 46–48 °C [lit.[15] 49–50 °C]; FTIR (thin film) 3014, 2937, 2918, 2842, 1449, 747; ^1H NMR ($CDCl_3$) δ 7.15–7.10 (m, 4 H), 3.83 (s, 2 H), 2.86–2.95 (m, 4 H), 2.03–1.94 (m, 2 H) [lit.[15] ^1H NMR ($CDCl_3$) δ 7.04 (m, 4 H), 3.76 (s, 2 H), 2.85 (t, J = 6 Hz, 2 H), 1.75 (t, 2 H), 1.15 (m, 2 H)]; GCMS (EI, 70 eV) *m/e* (% base peak) 164 (100), 131 (51.9), 117 (46.5), 115 (37.9), 91 (32.0).

1,3,4,5-Tetrahydro-2-benzothiepin (0.18 g, 1.1 mmol) was dissolved in CH_2Cl_2 (5 mL). *m*-CPBA (80%, 0.52 g, 2.4 mmol) was added and the reaction mixture was stirred overnight. The reaction mixture was washed with saturated sodium bisulfite (10 mL), 1

M KOH (3 x 10 mL) and H_2O (10 mL) and then dried ($MgSO_4$). The solvent was removed *in vacuo* to yield 1,3,4,5-tetrahydro-2-benzothiepin-2,2-dioxide (0.21 g, 1.1 mmol, 100% yield). mp 179–180 °C (dec); FTIR (thin film) 2973, 2916, 2861, 1284, 1254, 1110, 858, 781, 750; ^1H NMR ($CDCl_3$) δ 7.33–7.15 (m, 4 H), 4.39 (s, 2 H), 3.28 (t, J = 6.0 Hz, 2 H), 3.01–2.95 (m, 2 H), 2.25–2.15 (m, 2 H); GCMS (EI, 70 eV) *m/e* (% base peak) 196 (18.7), 132 (16.0), 104 (100), 91 (26.8); HRMS (EI, 70 eV) calculated for $C_{10}H_{12}O_2S$, 196.05580; measured, 196.05604 (error +1.21 ppm).

Flash vacuum pyrolysis Flash vacuum pyrolysis (FVP) was performed as previously described.[16]

Flow pyrolysis Flow pyrolysis was performed on the same apparatus described previously[5a] except that the sample inlet was modified. An attachment was made that consisted of a Pyrex tube with 24/40 inner and outer joints attached to each end. The attachment also had glass tube that extended below the inner joint and passed through the side wall to a ground glass stopcock. The attachment was placed on the sample inlet of the flow pyrolysis apparatus and the sample, in a round-bottom flask, was placed on the other end of the attachment. After the usual degassing, Ar was flowed over the sample through the side tube on the attachment. The sample temperature was maintained for the entire pyrolysis time with a thermostatic oil bath. Other aspects of the flow pyrolysis were as previously described.[5a]

Photolysis 3-Benzocycloheptenone (**10**, 32 mg, 0.20 mmol) was dissolved in 550 mL of spectrophotometric grade pentanes and 50 mL methanol. After deæration for 2 h with Ar, the sample was photolyzed for 2 h with a Pyrex filter (λ > 280 nm). The solution was extracted with H_2O (500 mL), saturated NaCl (500 mL), and dried ($MgSO_4$). The pentanes was removed by distillation until a few milliliters of solution remained. The

reaction mixture was analyzed as described below after 1 mL of *ca.* 5 mg mL^{-1} solution of biphenyl in CH_2Cl_2 was added.

Product analysis FVP and flow pyrolysis reaction mixtures were analyzed by capillary gas chromatography on a Hewlett-Packard HP5840A gas chromatograph equipped with a 30-m (0.25-μm film thickness) DB-1701 capillary column using the analytical procedure previously described.[5a] Photolysis reaction mixtures were analyzed on a Hewlett-Packard HP5890 gas chromatograph equipped with a 30-m (0.25-μm film thickness) DB-1 capillary column following the same analytical procedure used for FVP and flow pyrolysis reaction mixtures.

REFERENCES

(1) Poutsma, M. L. *A Review of Thermolysis Studies of Model Compounds Relevant to Processing of Coal*; ORNL/TM-10673, Oak Ridge National Laboratory, Oak Ridge, TN 37831. This review is available from National Technical Information Service, U. S. Dept. of Commerce, 5285 Port Royal Rd., Springfield, VA 22161.

(2) (a) Badger, G. M.; Kimber, R. W. L. *J. Chem. Soc.* **1960**, 266. (b) Badger, G. M.; Kimber, R. W. L.; Novotny, J. *Aust. J. Chem.* **1962**, *15*, 616. (c) Loudon, A. G.; Maccoll, A.; Wong, S. K. *J. Chem. Soc. B* **1970**, 1733. (d) Penninger, J. M. L.; Slotboom, H. W. *Recl. Trav. Chim. Pays-bays* **1973**, *92*, 513. (e) Penninger, J. M. L.; Slotboom, H. W. *Ibid.* **1973**, *92*, 1089. (f) Tominaga, H.; Yahagi, U. *J. Fac. Eng., Univ. Tokyo, Ser. A* **1977**, *15*, 68. (g) Bredael, P.; Vinh, T. H. *Fuel* **1979**, *58*, 211. (h) Gangwer, T.; MacKenzie, D.; Casano, S. *J. Phys. Chem.* **1979**, *83*, 2013. (i) Berman, M. R.; Comita, P. B.; Moore, C. B.; Bergman, R. G. *J. Amer. Chem. Soc.* **1980**, *102*, 5692. (j) Cyprès, R.; Bredael, P. *Fuel Process. Tech.* **1980**, *3*, 297. (k) Trushkova, L. V.; Magaril, R. Z.; Korzun, N. V.; Bulatov, R. A. *Russ. J. Phys. Chem.* **1980**, *54*, 1062. (l) Comita, P. B.; Berman, M. R.; Moore, B. C.; Bergman, R. G. *J. Phys. Chem.* **1981**, *85*, 3266. (m) Takahashi, K.; Ogino, Y. *Fuel* **1981**, *60*, 975. (n) Trahanovsky, W. S.; Swenson, K. E. *J. Org. Chem.* **1981**, *46*, 2984. (o) Bajus, M.; Baxa, J. *Coll. Czech. Chem. Commun.* **1982**, *47*, 1838. (p) Penninger, J. M. L. *Int. J. Chem. Kinetics* **1982**, *14*, 761. (q) Hillebrand, W.; Hodek, W.; Kölling, G. *Fuel* **1984**, *63*, 756. (r) Korzun, N. V.; Trushkova, L. V. *Kinetics Catal.* **1985**, *26*, 195. (s) Tsang, W.; Cui, J. P. *J. Amer. Chem. Soc.* **1990**, *112*, 1665.

(3) In the liquid-phase pyrolysis of **1**, the major ring-contracted product has been identified as 1-methylindan,[4] but we have conclusively identified the major methylindan in gas-phase pyrolysis of **1** as the 2-methyl isomer (**7**). Some workers have incorrectly reported 1-methylindan as the gas-phase pyrolysis product.[2d,e,p]

(4) Benjamin, B. M.; Hagaman, E. W.; Raaen, V. F.; Collins, C. J. *Fuel* **1979**, *58*, 386.

(5) (a) Malandra, J. L.; Zhu, J.; Lee, S.-K.; Spurlin, S. R.; Tunkel, J. L.; Fischer, D. R.; Yeung, E. S.; Trahanovsky, W. S., manuscript in preparation. [Paper 1, this dissertation] (b) Trahanovsky, W. S.; Malandra, J. L.; Ferguson, J. M. *J. Amer. Chem. Soc.* **1993**, *115*, 0000. [Paper 5, this dissertation]

(6) Gajewski, J. J.; Paul, G. C. *J. Org. Chem.* **1990**, *55*, 4575.

(7) (a) Cristol, S. J.; Caple, R. *J. Org. Chem.* **1966**, *31*, 585. (b) Scott, L. T.; Erden, I. *J. Amer. Chem. Soc.* **1982**, *104*, 1147. (c) Brinker, U. H.; Wilk, G.; Gomann, K. *Angew. Chem.* **1983**, *95*, 892; *Angew. Chem., Int. Ed. Engl.* **1983**, *22*, 868.

(8) Bond energies in kcal mol^{-1} for: $PhCH_2$–SO_2CH_3, 52.9; $PhCH_2$–$COCH_2Ph$, 65.4. From *CRC Handbook of Chemistry and Physics, 66th Edition*; Weast, R. C., Ed.; CRC Press, Inc.: Boca Raton, FL, 1985.

(9) (a) Trahanovsky, W. S.; Cassady, T. J.; Woods, T. L. *J. Amer. Chem. Soc.* **1981**, *103*, 6691. (b) Chou, C.-H.; Trahanovsky, W. S. *J. Amer. Chem. Soc.* **1986**, *108*, 4138.

(10) Greenwald, R.; Chaykovsky, M.; Corey, E. J. *J. Org. Chem.* **1963**, *28*, 1128.

(11) Meyers, A. I.; Ford, M. E. *J. Org. Chem.* **1976**, *41*, 1735.

(12) El-Hossini, M. S.; McCullough, K. J.; McKay, R.; Proctor, G. R. *Tetrahedron Lett.* **1986**, *27*, 3783.

(13) Fristad, W. E.; Bailey, T. R.; Paquette, L. A. *J. Org. Chem.* **1980**, *45*, 3028.

(14) It was necessary to do this procedure at high dilution. At higher concentrations, sulfide dimer **25** was formed. We oxidized **25** to sulfone dimer **26**.

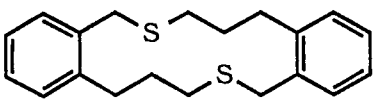

25

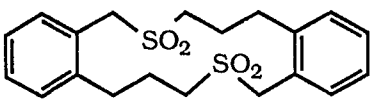

26

1,8-Dithia-3,10-dibenzocyclotetradecadiene (25). mp 142–143 °C; FTIR (thin film) 2920, 1489, 1462, 1259, 1047, 748, 708; ^1H NMR ($CDCl_3$) δ 7.35–7.30 (m, 2 H), 7.23–7.11 (m, 6 H), 3.96 (s, 4 H), 2.87–2.80 (m, 4 H), 2.72–2.65 (t, J = 6 Hz, 4 H), 2.06–1.95 (m, 4 H); MS (EI, 70 eV) *m/e* (% base peak) 328 (52.5), 164 (100), 163 (59.8), 162 (42.7), 131 (48.4), 130 (36.5), 129 (37.4), 117 (33.8), 115 (30.3), 105 (38.9), 91 (40.3).

1,8-Dithia-3,10-dibenzocyclotetradecadiene-1,1,8,8-tetroxide (26). mp 345–346 °C; FTIR (thin film) 2943, 1283, 1148, 1117, 756; ^1H NMR (CD_2Cl_2) δ 7.65–7.61 (m, 2 H), 7.40–7.26 (m, 6 H), 4.73 (s, 4 H), 3.17–3.11 (m, 4 H), 3.00 (t, J = 6 Hz, 4 H), 2.37–2.25 (m, 4 H); MS (EI, 70 eV) *m/e* (% base peak) 392 (1.4), 328 (30.9), 144 (27.0), 131 (100), 117 (30.3), 104 (49.5), 91 (38.4).

(15) Pellicciari, R.; Natalini, B. *J. Chem. Soc., Perkin Trans. 1* **1977**, 1822.

(16) (a) Trahanovsky, W. S.; Ong, C. C.; Pataky, J. G.; Weitl, F. L.; Mullen, P. W.; Clardy, J. C.; Hansen, R. S. *J. Org. Chem.* **1971**, *36*, 3575. Commercial apparatus is available from Kontes Scientific Glassware, Vineland, NJ 08360. (b) For review, see Brown, R. C. F. *Pyrolysis Methods in Organic Chemistry*; Academic: New York, 1980, Chapter 2.

APPENDIX 1

SUPPLEMENTARY DATA TABLES

Table A-I. Products and recovered starting material, total recovery of material, and conversion from the FVP of 3-benzocycloheptenone (**10**) at various oven temperatures [a,b]

	yield, % [c]				
entry	700 °C	750 °C	800 °C	850 °C	900 °C
toluene	—	—	—	—	1.46
ethylbenzene	—	—	0.28	0.68	1.34
o-xylene	—	—	0.36	1.15	2.68
styrene (**6**)	—	0.15	0.40	1.10	4.04
benzocyclobutene (**3**)	—	0.11	0.71	2.05	4.17
o-ethyltoluene	—	—	0.42	1.33	1.53
o-methylstyrene	—	—	—	—	0.96
o-allyltoluene (**4**)	—	0.17	0.85	1.76	1.92
indene (**8**)	0.17	0.71	3.32	8.15	15.28
2-methylindan (**7**)	—	—	0.21	0.83	1.60
TD-130 [$C_{10}H_{10}$]	—	—	—	—	0.29
o-(1-propenyl)toluene	—	—	—	—	0.45
3-methyl-1*H*-indene	—	0.12	0.26	0.51	0.93
tetralin (**1**)	0.25	1.09	6.49	14.88	19.93
2-methyl-1*H*-indene	—	—	0.15	—	0.50
TK-130 [$C_{10}H_{10}$]	—	—	0.28	0.63	0.81

Table A-I continues on next page

Table A-I. Continued

	yield, % [c]				
entry	700 °C	750 °C	800 °C	850 °C	900 °C
1,2-dihydronaphthalene (**2**)	0.68	1.34	3.41	5.71	5.58
TL-128 [$C_{10}H_8$]	—	—	—	—	0.22
naphthalene (**5**)	0.36	0.64	2.20	4.72	10.24
KA-142 [$C_{11}H_{10}$]	1.47	1.10	1.14	0.59	0.24
KB-142 [$C_{11}H_{10}$]	0.20	0.32	0.66	0.58	0.29
KC-142 [$C_{11}H_{10}$]	0.74	0.50	0.49	—	—
2-methylnaphthalene (**13**)	0.63	1.06	3.12	3.47	3.04
1-methylnaphthalene (**12**)	1.47	2.62	8.09	8.41	6.64
KD-142 [$C_{11}H_{10}$]	—	—	0.27	0.35	0.21
KE-142 [$C_{11}H_{10}$]	—	—	0.37	0.56	0.49
KF-160 [$C_{11}H_{12}O$]	—	0.07	0.11	—	—
KG-160 [$C_{11}H_{12}O$]	—	0.08	0.11	—	—
KH-146 [$C_{10}H_{10}O$]	0.19	0.19	0.12	—	—
KI-160 [$C_{11}H_{12}O$]	0.11	0.27	0.75	1.06	0.63
KJ	*d*	*d*	—	—	—
3-benzocycloheptenone (**10**)	93.26	88.55	63.57	38.55	11.90
KK-160 [$C_{11}H_{12}O$]	0.14	0.35	1.15	1.81	1.49
KL-160 [$C_{11}H_{12}O$]	0.33	0.47	0.38	0.32	0.09
KM	—	—	—	—	*d*
KN-144 [$C_{10}H_8O$]	—	0.09	0.32	0.87	1.11
KO	—	—	—	—	*d*
KP	*d*	*d*	*d*	—	—

Table A-I continues on next page

Table A-I. Continued

	yield, % [c]				
entry	700 °C	750 °C	800 °C	850 °C	900 °C
KQ	—	—	*d*	—	*d*
recovery [e]	90.07	83.73	84.03	78.40	66.67
conversion [f]	6.74	11.45	36.43	61.47	88.10

[a] FVP conditions: system pressure = 2 x 10^{-5} torr, sample temperature = 30–40 °C. [b] Amounts determined by GC with a known quantity of biphenyl added as standard. Data represent the average of triplicate runs. Products identified by comparison with authentic samples or those that could be identified by retention time and GCMS are indicated by name. Products that were identified by GCMS only are indicated by code: XY-nnn, where 'X' corresponds to the system studied (K = pyrolysis of **10**, T = pyrolysis of **1**), 'Y' to the individual unknown product (A, B, C, etc.), and 'nnn' to the nominal mass. [c] Moles of product divided by total moles of recovered material. [d] Product which constitutes ≤0.25% total area by GC. [e] Total moles of recovered material divided by moles of starting material used. [f] Total moles of recovered material minus moles of recovered starting material divided by total moles of recovered material.

Table A-II. Products and recovered starting material, total recovery of material, and conversion from the flow pyrolysis of 3-benzocycloheptenone (**10**) at various oven temperatures [a,b]

	yield, % [c]			
entry	754 °C	800 °C	851 °C	900 °C
toluene	—	—	—	0.56
ethylbenzene	—	—	—	0.29
o-xylene	—	—	0.22	0.82
styrene (**6**)	—	—	0.36	4.12
benzocyclobutene (**3**)	—	0.54	1.69	7.98
o-ethyltoluene	—	—	—	0.52
benzaldehyde	—	—	—	0.33
o-allyltoluene (**4**)	0.58	0.95	2.13	3.87
indene (**8**)	0.40	1.29	4.15	10.43
2-methylindan (**7**)	—	—	0.70	2.57
TD-130 [$C_{10}H_{10}$]	—	—	—	0.60
o-(1-propenyl)toluene	—	0.57	0.92	0.81
TH-130 [$C_{10}H_{10}$]	—	—	—	0.94
tetralin (**1**)	2.08	6.28	18.74	29.26
1,2-dihydronaphthalene (**2**)	0.95	1.09	2.45	3.19
naphthalene (**5**)	0.70	0.76	2.01	3.74
siloxane $((CH_3)_2SiO)_6$	—	—	*d*	—
KA-142 [$C_{11}H_{10}$]	0.50	0.36	0.30	—
KB-142 [$C_{11}H_{10}$]	—	0.31	0.40	0.37
2-methylnaphthalene (**13**)	0.75	1.37	3.20	3.59
1-methylnaphthalene (**12**)	1.91	3.48	7.85	8.63

Table A-II continues on next page

Table A-II. Continued

	yield, % [c]			
entry	754 °C	800 °C	851 °C	900 °C
KD-142 [$C_{11}H_{10}$]	—	—	0.28	0.60
KF-160 [$C_{11}H_{12}O$]	—	0.17	0.48	1.56
KH-146 [$C_{10}H_{10}O$]	0.50	0.50	0.41	0.13
KI-160 [$C_{11}H_{12}O$]	0.31	0.76	1.03	0.60
3-benzocycloheptenone (**10**)	90.15	79.79	49.76	12.22
KK-160 [$C_{11}H_{12}O$]	0.73	1.32	2.64	2.61
KL-160 [$C_{11}H_{12}O$]	0.44	0.45	0.27	—
recovery [e]	54.04	50.36	52.26	45.87
conversion [f]	9.85	20.21	50.24	87.78

[a] Flow pyrolysis conditions: system pressure = 0.010 torr, sample temperature = 26 °C, flow rate = 450 mL min^{-1} (Ar/1 atm) for 10 h, residence time = 0.28 s. [b] See Table A-I, footnote *b*. [c] See Table A-I, footnote *c*. [d] Product which constitutes ≤0.50% total area by GC. [e] See Table A-I, footnote *e*. [f] See Table A-I, footnote *f*.

Table A-III. Products and recovered starting material, total recovery of material, and conversion from the photolysis of 3-benzocycloheptenone (**10**) [a,b]

entry	yield, % [c]	entry	yield, % [c]
LA-142 [$C_{11}H_{12}$]	0.12	LH-192 [$C_{12}H_{16}O_2$] (**14**)	1.44
LB-142 [$C_{11}H_{12}$]	0.58	LI-160 [$C_{11}H_{12}O$]	0.65
LC-142 [$C_{11}H_{12}$]	0.35	LJ-160 [$C_{11}H_{12}O$]	0.49
LD-142 [$C_{11}H_{12}$]	0.39	LK	*d*
o-allyltoluene (**4**)	2.67	LL	*d*
LE	*d*	LM	*d*
tetralin (**1**)	8.06	LN	*d*
LF-160 [$C_{11}H_{12}O$]	0.67		
LG-160 [$C_{11}H_{12}O$]	0.38	recovery [e]	72.38
3-benzocycloheptenone (**10**)	84.20	conversion [f]	15.80

[a] Photolysis conditions: [**10**] = 0.33 mM in 11:1 (v:v) pentanes:methanol, medium pressure Hg lamp with Pyrex filter ($\lambda > 280$ nm), 2 h at room temperature. [b] Amounts determined by GC with a known quantity of biphenyl added as standard. Data represent the average of triplicate runs. Products identified by comparison with authentic samples or those that could be identified by retention time and GCMS are indicated by name. Products that were identified by GCMS only are indicated by code: XY-nnn, where 'X' corresponds to the system studied (L = photolysis of **10**), 'Y' to the individual unknown product (A, B, C, etc.), and 'nnn' to the nominal mass. [c] See Table A-I, footnote *c*. [d] Product which constitutes ≤0.75% total area by GC. [e] See Table A-I, footnote *e*. [f] See Table A-I, footnote *f*.

Table A-IV. Products and recovered starting material, total recovery of material, and conversion from the FVP of 1,3,4,5-tetrahydro-2-benzothiepin-2,2-dioxide (**11**) at various oven temperatures [a,b]

	yield, % [c]			
entry	600 °C	700 °C	800 °C	900 °C
ethylbenzene	—	—	0.32	0.52
o-xylene	—	—	0.14	0.42
styrene (**6**)	0.25	0.58	0.45	3.61
benzocyclobutene (**3**)	0.29	1.13	2.07	7.79
siloxane $((CH_3)_2SiO)_4$	—	—	*d*	—
o-methylstyrene	—	—	0.13	0.49
o-allyltoluene (**4**)	2.04	12.48	11.34	5.40
indene (**8**)	—	0.13	0.61	4.43
2-methylindan (**7**)	—	0.17	2.60	5.25
siloxane $((CH_3)_2SiO)_5$	*d*	*d*	—	—
o-(1-propenyl)toluene	—	—	0.21	1.13
tetralin (**1**)	13.18	75.77	79.10	62.53
2-methyl-1*H*-indene	—	—	—	0.36
1,2-dihydronaphthalene (**2**)	0.28	0.94	1.98	3.44
naphthalene (**5**)	—	0.27	0.91	4.63
siloxane $((CH_3)_2SiO)_6$	*d*	*d*	*d*	—
SA	—	*d*	—	—
SB	—	*d*	—	—
SC	—	*d*	*d*	—
SD	—	—	*d*	—
SE	—	*d*	—	—

Table A-IV continues on next page

Table A-IV. Continued

	yield, % [c]			
entry	600 °C	700 °C	800 °C	900 °C
SF	*d*	—	—	—
1,3,4,5-tetrahydro-2-benzo-thiepin-2,2-dioxide (**11**)	83.96	8.54	0.14	—
recovery [e]	83.54	79.01	72.56	69.40
conversion [f]	29.86	93.25	99.90	100.0

[a] FVP conditions: system pressure = 2 x 10^{-5} torr, sample temperature = RT. [b] Amounts determined by GC with a known quantity of biphenyl added as standard. Data represent the average of triplicate runs. Products identified by comparison with authentic samples or those that could be identified by retention time and GCMS are indicated by name. Products that were identified by GCMS only are indicated by code: XY-nnn, where 'X' corresponds to the system studied (S = pyrolysis of **11**), 'Y' to the individual unknown product (A, B, C, etc.), and 'nnn' to the nominal mass. [c] See Table A-I, footnote *c*. [d] See Table A-II, footnote *d*. [e] See Table A-I, footnote *e*. [f] See Table A-I, footnote *f*.

APPENDIX 2

SUPPLEMENTARY PROCEDURES AND CALCULATIONS

Detailed procedure for flow pyrolysis of ketone (10)

Flow pyrolysis was performed on the same apparatus (Figure 2, Paper 1) described in the Experimental Section of Paper 1 in this dissertation except that the sample inlet was modified. An attachment was made that consisted of a Pyrex tube with 24/40 inner and outer joints attached to each end. The attachment also has a glass tube that extends below the inner joint and passes through the side wall to a ground glass stopcock. The attachment was placed on the sample inlet of the flow pyrolysis apparatus with a small amount of vacuum grease. The weighed sample (*ca.* 50 mg) in a 5-mL round-bottom flask was placed on the other end of the attachment with a small amount of vacuum grease.

The apparatus and sample were degassed as described in Appendix 2 of Paper 1 in this dissertation prior to pyrolysis. During the pyrolysis, Ar was flowed over the sample through the side tube on the attachment. The sample temperature was maintained for the entire pyrolysis time with a thermostatic oil bath (26–27 °C). A flow rate of 450 mL min^{-1} (Ar/1 atm/flow tube = 100 (SS)) was maintained for 10 h to allow enough sample to pyrolyze for analysis (*ca.* 2–3 mg). Initially, *ca.* 50 mg of sample was used. The sample was weighed before and after pyrolysis to determine how much had pyrolyzed. The same sample could be used for several runs. However, since the sample size effects the amount of substance pyrolyzed, the total size of the sample was not allowed to drop below *ca.* 35 mg. Other aspects of the flow pyrolysis were as described in Appendix 2 of Paper 1 in this dissertation.

Calculation of residence time for flow pyrolysis of ketone (10)

This calculation of residence time is similar to the one in Appendix 2 of Paper 1 in this dissertation. The same oven volume was used here. The pyrolysis time was determined in separate runs where the time necessary to evacuate the sample chamber from 0 to 15 in. vacuum at 450 mL min^{-1} (Ar/1 atm) was measured.

Volume of argon at 760 torr at 300 K (V_{A1})

Pressure of sample (from Bourdon gauge)

Initial pressure of argon = P_i	P_i	= 0	in. vacuum
Final pressure of argon = P_f	P_f	= 15	in. vacuum
Minimum pressure of system = P_{min}	P_{min}	= 28	in. vacuum

Total volume of argon = V_T	12	L
Volume of argon = $V_{A1} = \frac{P_f - P_i}{P_{max} - P_i} V_T$	6.4	L

Volume of argon at 15 torr at 1100 K (V_{A2})

Initial pressure of sample = P_1	760	torr
Final pressure of sample = P_2	15	torr
Initial temperature of sample = T_1	300	K
Final temperature of sample = T_2	1100	K
Initial volume of argon = V_{A1}	6.4	L
Volume of argon = $V_{A2} = \frac{P_1 T_2}{P_2 T_1} V_{A1}$	1.2×10^6	mL

Flow rate (R_f)

Average time = t_s	14	min
Flow rate = $R_f = V_{A2}/t_s$	8.6×10^4	mL min^{-1}

Residence time (t_r)

Volume of oven = V_{oven}	113	mL
Residence time = $t_r = V_{oven}/R_f$	0.08	s

PAPER 3. THE HIGH-TEMPERATURE GAS-PHASE REACTIONS OF *o*-ALLYLBENZYL RADICALS GENERATED BY FLASH VACUUM PYROLYSIS OF BIS(*o*-ALLYLBENZYL) OXALATE

INTRODUCTION

In the gas-phase thermal decomposition of tetralin (**1**),[1,2] the major products include 1,2-dihydronaphthalene (**2**) and naphthalene (**3**), derived by the loss of hydrogen, and benzocyclobutene (**4**) and styrene (**5**), derived by the loss of ethylene (Scheme I). Several other significant products such as indene (**6**), formed by the loss of the equivalent of methane from **1**, are also produced. One of the mechanisms proposed[21] for the formation of **2** involves the *o*-allylbenzyl radical (**7**) formed from diradical **8** by loss of a hydrogen atom. Conversion of **7** to **2** is reasonable, but previous studies[3] of

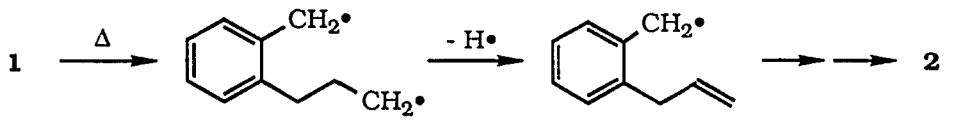

8 **7**

related radicals indicate that **7** could produce other products such as **6**. In an attempt to determine the fate of radical **7** under high-temperature gas-phase conditions, we have studied the flash vacuum pyrolysis (FVP) of bis(*o*-allylbenzyl) oxalate (**9**). Oxalates have

Scheme I

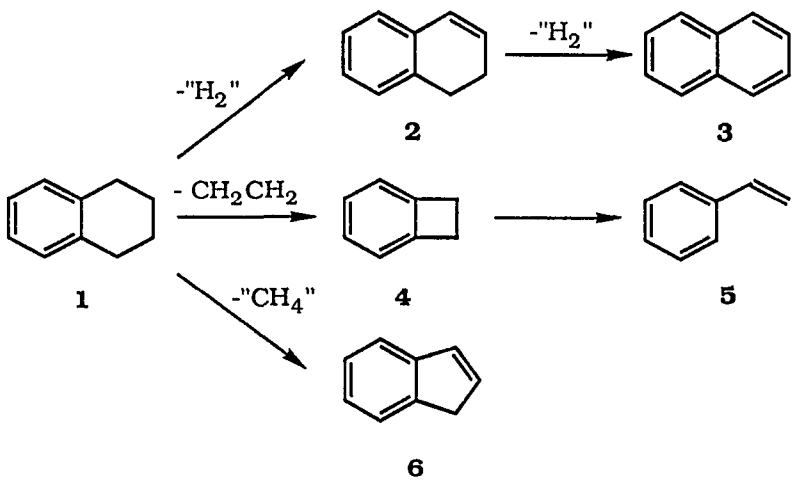

been shown to be good precursors of benzyl radicals under FVP conditions[4] and we expected **9** to produce **7** in good yield. The results of the study of the FVP of **9** are

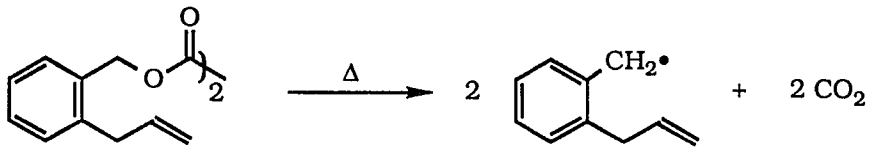

9 **7**

presented in this paper.

RESULTS

Oxalate **9** was prepared from 1,2-dihydronaphthalene (**2**) by the following reaction sequence.

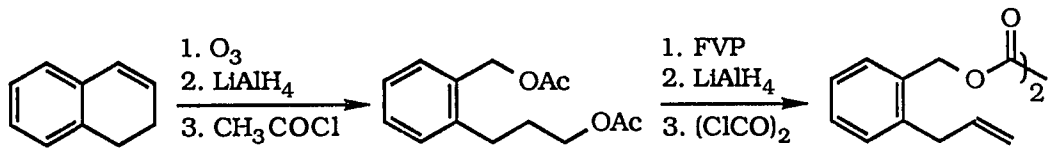

2 **9**

The FVP of **9** (Table I) leads primarily to the formation of 1,2-dihydronaphthalene (**2**), naphthalene (**3**), indene (**6**), 3-methyl-1*H*-indene (**10**), and 2-methyl-1*H*-indene (**11**). Small amounts (<2 %) of tetralin (**1**), benzocyclobutene (**4**), styrene (**5**), *o*-allyltoluene (**12**), and 2-methylindan (**13**)[5] were produced. The dimer of **7**, 1,2-di(2-allylphenyl)ethane (**14**), was detected (<1 %) at 700–750 °C.

Table I. Products and recovered starting material from FVP of bis(*o*-allylbenzyl) oxalate (**9**) at various oven temperatures [a,b]

	yield, % [c]				
entry	700 °C	750 °C	800 °C	850 °C	900 °C
bis(*o*-allylbenzyl) oxalate (**9**)	3.4	1.7	1.2	0.3	—
1,2-dihydronaphthalene (**2**)	62.6	62.2	60.5	55.2	46.4
naphthalene (**3**)	5.3	7.5	11.1	16.5	27.1
indene (**6**)	6.3	6.9	8.2	10.1	12.3
3-methyl-1*H*-indene (**10**)	4.2	4.4	3.6	2.9	2.2
2-methyl-1*H*-indene (**11**)	1.4	1.5	1.8	1.7	1.8
1,2-di(2-allylphenyl)ethane (**14**)	0.7	0.2	—	—	—
other products	16.0 [d]	15.5 [d]	13.6 [d]	13.2 [d]	10.2 [d]
recovery [e]	71.5	65.1	68.7	67.1	59.9
conversion [f]	96.6	98.3	98.8	99.7	100

[a] FVP conditions: system pressure = 1 x 10^{-5} torr, sample temperature = 60-80 °C. [b] Amounts determined by GC with a known quantity of triphenylmethane added as standard. Data represent the average of triplicate runs. [c] Moles of product divided by total moles of recovered material. [d] See Table A-I in the Appendix of Paper 3, this dissertation, for a more detailed analysis. [e] Total moles of recovered material divided by moles of starting material used. [f] Total moles of recovered material minus moles of recovered starting material divided by moles of recovered material.

DISCUSSION

The gas-phase chemistry of *o*-allylbenzyl radical (**7**) and other related radicals (Scheme II), such as 1-tetryl (**15**), 2-tetryl (**16**), 1-indanylmethyl (**17**), and 2-indanylmethyl (**18**), has been studied;[3] although, the high-temperature gas-phase chemistry of **7** was not investigated directly.[3a,b]

The FVP of bis oxalate ester **9** leads primarily to the formation of 1,2-dihydronaphthalene (**2**) produced by loss of the ß hydrogen from **16**. Significant amounts of naphthalene (**3**), from the secondary pyrolysis of **2**, were also observed. The thermal behavior of **7** appears to be similar to that of 5-hexenyl radicals. There may be a kinetic preference of *ca.* 2 kcal mol^{-1} for the formation of the five-membered 2-indanylmethyl radical (**18**) over the six-membered 2-tetryl radical (**16**), but under pyrolysis conditions,

Scheme II

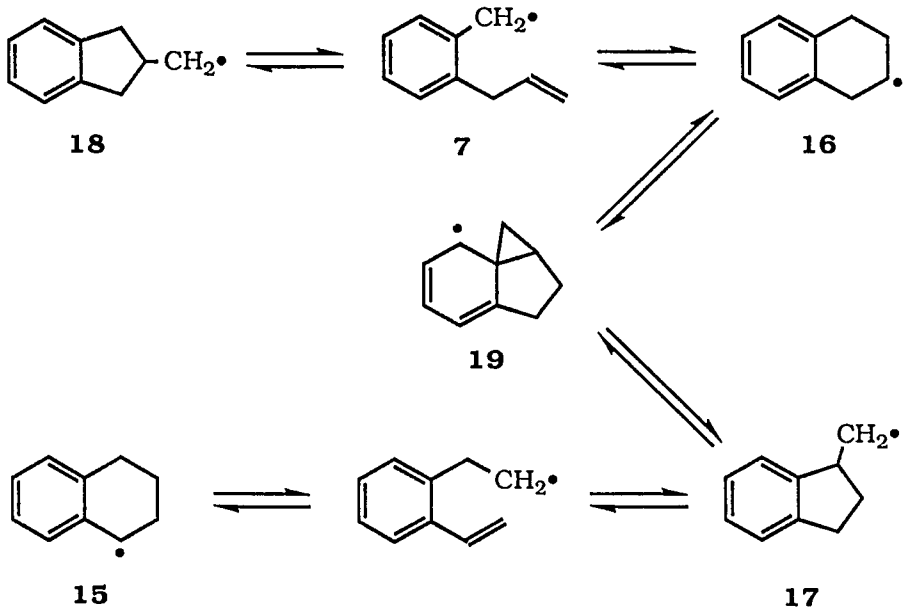

the initial closure will be reversible and the chemistry of the more stable **16** should predominate.

Consistent with the previously reported results,[3] expected products such as **10** and **11**, formed from radicals **17** and **18**, respectively, were also observed. Indene (**6**), as well as small amounts of **12** and **13** were also formed. The ratio of **6** to dehydrogenation products **2** and **3** was low, less than 0.17 to 1. In the pyrolysis of tetralin (**1**), this ratio is much higher, 0.6 to 1 at higher temperatures, and therefore the major route to **6** in the decomposition of **1** cannot involve radical **7**. Other recent work in our laboratory[7] indicates that the major source of **6** involves the pathway **1** to **12** to **13** to **6**. In the pyrolysis of oxalate **9**, any of all of the radicals **17**, **18**, or **19** could be the source of **6**.

Another minor product at lower pyrolysis temperatures is **14**, the dimer of radical **7**. Production of **14** offers further support for the formation of **7** in the pyrolysis of **9**.

CONCLUSION

The results of the FVP of bis(*o*-allylbenzyl) oxalate (**9**) are consistent with the formation of *o*-allylbenzyl radical (**7**). The major product from **7** is 1,2-dihydronaphthalene (**2**) which is readily explained by closure of **7** to **16** followed by the loss of a ß hydrogen atom. Other products which could come from radical **7** are formed in relatively low yields.

EXPERIMENTAL

General Procedures

Methods and materials

Some general methods have been described previously.[8] ^{1}H NMR spectra were recorded on a Nicolet NT-300 spectrometer. FTIR spectra were obtained on an IBM IR/98 spectrophotometer. GCMS were performed on a Finnegan 4000 mass spectrometer. HRMS were performed on a Kratos MS-50 mass spectrometer. All materials were commercially available and used as received, except where indicated.

Bis(*o*-allylbenzyl) oxalate (9) *o*-(3-Hydroxypropyl)benzyl alcohol (3.0 g, 0.018 mol), prepared as described previously,[9] was dissolved in dry ether (50 mL) and triethylamine (4.0 g, 0.040 mol, *ca.* 5.5 mL) was added. The mixture was cooled to 0 °C and a solution of acetyl chloride (3.1 g, 0.040 mol, *ca.* 2.8 mL) in ether (20 mL) was added dropwise. After the addition was complete, the reaction mixture was stirred for 10 min at 0 °C and then overnight at room temperature. The reaction mixture was washed with H_2O (20 mL), saturated $NaHCO_3$ (20 mL) and H_2O (20 mL) and then dried ($MgSO_4$). The solvent was removed *in vacuo* to yield *o*-(3-acetoxypropyl)benzyl acetate (4.1 g, 0.016 mol, 89% yield). FTIR (thin film) 2960, 1749, 1454, 1383, 1367, 1259, 1034, 758; ^{1}H NMR ($CDCl_3$) δ 7.37–7.18 (m, 4 H), 5.14 (s, 2 H), 4.11 (t, J = 6.4 Hz, 2 H), 2.74 (t, J = 7.8 Hz, 2 H), 2.11 (s, 3 H), 2.07 (s, 3 H), 2.01–1.90 (m, 2 H).

o-(3-Acetoxypropyl)benzyl acetate (3.9 g, 0.016 mol) was pyrolyzed at 700 °C and 1 x 10^{-5} torr with a sample temperature of 80 °C.[10] The pyrolysate was dissolved in ether and treated with K_2CO_3. The solvent was removed *in vacuo* and the crude product was purified by flash chromatography on a silica gel column (50 x 150 mm) with 1:1 hexanes

to CH_2Cl_2 to yield *o*-allylbenzyl acetate (1.5 g, 7.9 mmol, 49% yield). FTIR (thin film) 2924, 1742, 1229, 1026, 754; ^1H NMR ($CDCl_3$) δ 7.37–7.18 (m, 4 H), 5.96 (ddt, J_d = 16.8 Hz, J_d = 10.3 Hz, J_t = 6.3 Hz, 1 H), 5.07 (dd, J_d = 10.2 Hz, J_d = 1.1 Hz, 1 H), 4.99 (dd, J_d = 17.1 Hz, J_d = 1.1 Hz, 1 H), 5.13 (s, 2 H), 3.44 (d, J = 6.2 Hz, 2 H), 2.09 (s, 3 H).

o-Allylbenzyl acetate (1.5 g, 7.9 mmol) was dissolved in THF (10 mL) and added dropwise to a slurry of $LiAlH_4$ (0.4 g, 0.010 mol) in THF (50 mL) at 0 °C. The reaction mixture was allowed to warm to room temperature and stirred for 2 h. A slurry of wet Na_2SO_4 was added to the reaction mixture until evolution of H_2 ceased. The white solid was filtered off and washed with ethyl acetate. The filtrate was dried ($MgSO_4$) and the solvent was removed *in vacuo* to yield *o*-allylbenzyl alcohol (1.1 g, 7.4 mmol, 94% yield). FTIR (thin film) 3333 (br), 2918, 1040; ^1H NMR ($CDCl_3$) δ 7.41–7.36 (m, 1 H), 7.34–7.18 (m, 3 H), 6.01 (ddt, J_d = 16.8 Hz, J_d = 10.4 Hz, J_t = 6.3 Hz, 1 H), 5.07 (dq, J_d = 10.1 Hz, J_q = 1.5 Hz, 1 H), 5.00 (dd, J_d = 17.2 Hz, J_d = 1.5 Hz, 1 H), 4.71 (d, J = 5.9 Hz, 2 H), 3.48 (dt, J_d = 6.2 Hz, J_t = 1.4 Hz, 2 H), 1.26 (t, J = 6.0 Hz, 1 H) [lit.[6c] ^1H NMR ($CDCl_3$) δ 7.6–7.1 (m, 4 H), 6.02 (ddt, J_d = 16.6 Hz, J_d = 10.5 Hz, J_t = 6.1 Hz, 1 H), 5.05 (m, 1 H (*cis*)), 5.0 (m, 1 H (*trans*)), 4.70 (s, 2 H), 3.47 (dt, 2 H), 1.6 (s, 1 H)].

o-Allylbenzyl alcohol (1.2 g, 8.0 mmol) was dissolved in ether (150 mL) and triethylamine (1.1 g, 0.011 mol) was added. The reaction mixture was cooled to 0 °C and oxalyl chloride (0.8 g, 6.0 mmol) in ether (10 mL) was added dropwise. After the reaction mixture was stirred for 1 h at room temperature, it was extracted with H_2O (50 mL), saturated $NaHCO_3$ (2 x 50 mL), H_2O (50 mL), and saturated NaCl (50 mL) and then dried ($MgSO_4$). The solvent was removed *in vacuo* and the crude product was purified by flash chromatography on a silica gel column (30 x 150 mm) with 1:1 CH_2Cl_2 to hexanes to yield bis(*o*-allylbenzyl) oxalate (1.1 g, 3.2 mmol, 80% yield). FTIR (thin film) 2957, 2924, 1767, 1744, 1155; ^1H NMR ($CDCl_3$) δ 7.41–7.19 (m, 4 H), 5.94 (ddt, J_d = 16.8 Hz, J_d =

10.4 Hz, J_t = 6.3 Hz, 1 H), 5.33 (s, 2 H), 5.02 (dq, J_d = 10.1 Hz, J_q = 1.5 Hz, 1 H), 4.95 (dd, J_d = 17.0 Hz, J_d = 1.7 Hz, 1 H), 3.45 (dt, J_d = 6.2 Hz, J_t = 1.4 Hz, 2 H); GCMS (CI, NH_3) *m/e* 368 (M + NH_4); GCMS (EI, 70 eV) *m/e* (% base peak) 260 (5.5), 219 (4.8), 131 (100), 130 (98.6), 116 (15.6), 115 (22.0), 91 (45.6); Analysis calculated for $C_{22}H_{22}O_4$, C 75.41%, H 6.33%; measured, C 75.42%, H 6.36%.

Flash vacuum pyrolysis Flash vacuum pyrolysis (FVP) was performed as previously described.[3c,9]

Product analysis FVP reaction mixtures were analyzed by capillary gas chromatography on a Hewlett-Packard HP5840A gas chromatograph equipped with a 30-m (0.25-μm film thickness) DB-1701 capillary column using the analytical procedure previously described except that the standard used was triphenylmethane instead of biphenyl.[7a]

REFERENCES

(1) Poutsma, M. L. *A Review of Thermolysis Studies of Model Compounds Relevant to Processing of Coal*; ORNL/TM-10673, Oak Ridge National Laboratory, Oak Ridge, TN 37831. This review is available from National Technical Information Service, U. S. Dept. of Commerce, 5285 Port Royal Rd., Springfield, VA 22161.

(2) (a) Badger, G. M.; Kimber, R. W. L. *J. Chem. Soc.* **1960**, 266. (b) Badger, G. M.; Kimber, R. W. L.; Novotny, J. *Aust. J. Chem.* **1962**, *15*, 616. (c) Loudon, A. G.; Maccoll, A.; Wong, S. K. *J. Chem. Soc. B* **1970**, 1733. (d) Penninger, J. M. L.; Slotboom, H. W. *Recl. Trav. Chim. Pays-bays* **1973**, *92*, 513. (e) Penninger, J. M. L.; Slotboom, H. W. *Ibid.* **1973**, *92*, 1089. (f) Tominaga, H.; Yahagi, U. *J. Fac. Eng., Univ. Tokyo, Ser. A* **1977**, *15*, 68. (g) Bredael, P.; Vinh, T. H. *Fuel* **1979**, *58*, 211. (h) Gangwer, T.; MacKenzie, D.; Casano, S. *J. Phys. Chem.* **1979**, *83*, 2013. (i) Berman, M. R.; Comita, P. B.; Moore, C. B.; Bergman, R. G. *J. Amer. Chem. Soc.* **1980**, *102*, 5692. (j) Cyprès, R.; Bredael, P. *Fuel Process. Tech.* **1980**, *3*, 297. (k) Trushkova, L. V.; Magaril, R. Z.; Korzun, N. V.; Bulatov, R. A. *Russ. J. Phys. Chem.* **1980**, *54*, 1062. (l) Comita, P. B.; Berman, M. R.; Moore, B. C.; Bergman, R. G. *J. Phys. Chem.* **1981**, *85*, 3266. (m) Takahashi, K.; Ogino, Y. *Fuel* **1981**, *60*, 975. (n) Trahanovsky, W. S.; Swenson, K. E. *J. Org. Chem.* **1981**, *46*, 2984. (o) Bajus, M.; Baxa, J. *Coll. Czech. Chem. Commun.* **1982**, *47*, 1838. (p) Penninger, J. M. L. *Int. J. Chem. Kinetics* **1982**, *14*, 761. (q) Hillebrand, W.; Hodek, W.; Kölling, G. *Fuel* **1984**, *63*, 756. (r) Korzun, N. V.; Trushkova, L. V. *Kinetics Catal.* **1985**, *26*, 195. (s) Tsang, W.; Cui, J. P. *J. Amer. Chem. Soc.* **1990**, *112*, 1665.

(3) (a) Franz, J. A.; Camaioni, D. M. *Fuel* **1980**, *59*, 803. (b) Franz, J. A.; Camaioni, D. M. *J. Org. Chem.* **1980**, *45*, 5247. (c) Franz, J. A.; Barrows, R. D.; Camaioni, D. M. *J. Am. Chem. Soc.* **1984**, *106*, 3964. (d) Franz, J. A.; Suleman, N. K.; Alnajjar, M. S. *J. Org. Chem.* **1986**, *51*, 19. (e) Franz, J. A.; Alnajjar, M. S.; Barrows, R. D.; Camaioni, D. M.; Suleman, N. K. *J. Org. Chem.* **1986**, *51*, 1446.

(4) (a) Trahanovsky, W. S.; Ong, C. C.; Lawson, J. A. *J. Amer. Chem. Soc.* **1968**, *90*, 2839. (b) Trahanovsky, W. S.; Ong, C. C. *J. Amer. Chem. Soc.* **1970**, *92*, 7174. (c) Trahanovsky, W. S.; Ong, C. C.; Pataky, J. G.; Weitl, F. L.; Mullen, P. W.; Clardy, J. C.; Hansen, R. S. *J. Org. Chem.* **1971**, *36*, 3575.

(5) In the liquid-phase pyrolysis of **1**, the major ring-contracted product has been identified as 1-methylindan,[6] but we have conclusively identified the major methylindan in gas-phase pyrolysis of **1** as the 2-methyl isomer (**7**). Some workers have incorrectly reported 1-methylindan as the gas-phase pyrolysis product.[2d,e,p]

(6) Benjamin, B. M.; Hagaman, E. W.; Raaen, V. F.; Collins, C. J. *Fuel* **1979**, *58*, 386.

(7) (a) Malandra, J. L.; Zhu, J.; Lee, S.-K.; Spurlin, S. R.; Tunkel, J. L.; Fischer, D. R.; Yeung, E. S.; Trahanovsky, W. S., manuscript in preparation. [Paper 1, this dissertation] (b) Trahanovsky, W. S.; Malandra, J. L.; Ferguson, J. M. *J. Amer. Chem. Soc.* **1993**, *115*, 0000. [Paper 5, this dissertation]

(8) (a) Trahanovsky, W. S.; Cassady, T. J.; Woods, T. L. *J. Amer. Chem. Soc.* **1981**, *103*, 6691. (b) Chou, C.-H.; Trahanovsky, W. S. *J. Amer. Chem. Soc.* **1986**, *108*, 4138.

(9) Malandra, J. L.; Trahanovsky, W. S., manuscript in preparation. [Paper 2, this dissertation]

(10) Commercial apparatus is available from Kontes Scientific Glassware, Vineland, NJ 08360. For review, see Brown, R. C. F. *Pyrolysis Methods in Organic Chemistry*; Academic: New York, 1980, Chapter 2.

APPENDIX

SUPPLEMENTARY DATA TABLE

Table A-I. Products and recovered starting material, total recovery of material, and conversion from the FVP of bis(*o*-allylbenzyl) oxalate (**9**) at various oven temperatures [a,b]

	yield, % [c]				
entry	700 °C	750 °C	800 °C	850 °C	900 °C
toluene	0.84	0.81	0.66	1.78	0.95
ethylbenzene	0.64	0.52	0.55	0.82	0.82
o-xylene	0.41	0.64	0.58	0.90	0.79
styrene (**5**)	0.44	0.40	0.43	0.61	0.68
benzocyclobutene (**4**)	0.21	0.26	0.29	0.37	0.40
allylbenzene	0.23	0.19	0.19	0.20	0.15
o-ethyltoluene	0.27	0.36	0.45	0.50	0.42
o-methylstyrene	0.57	0.68	0.68	0.84	0.81
o-allyltoluene (**12**)	1.42	1.03	0.84	0.65	0.32
indene (**6**)	6.29	6.89	8.15	10.06	12.32
2-methylindan (**13**)	0.22	0.24	0.32	0.36	0.35
TD-130 [$C_{10}H_{10}$]	0.96	1.02	0.88	0.75	0.62
TE-130 [$C_{10}H_{10}$]	—	0.08	—	0.17	0.22
TF-130 [$C_{10}H_{10}$]	—	—	—	0.21	0.26
o-methylbenzaldehyde	0.17	0.20	—	—	—
o-(1-propenyl)toluene	0.20	0.18	—	0.16	0.14

Table A-I continues on next page

Table A-I. Continued

	yield, % [c]				
entry	700 °C	750 °C	800 °C	850 °C	900 °C
TH-130 [$C_{10}H_{10}$]	0.48	0.78	0.83	0.84	0.84
3-methyl-1*H*-indene (**10**)	4.19	4.35	3.57	2.88	2.18
tetralin (**1**)	0.97	1.15	1.11	1.16	1.01
2-methyl-1*H*-indene (**11**)	1.45	1.52	1.79	1.70	1.81
1,2-dihydronaphthalene (**2**)	62.63	62.20	60.54	55.23	46.44
TL-128 [$C_{10}H_8$]	—	—	—	0.11	0.22
1,4-dihydronaphthalene	1.59	1.02	0.35	0.22	—
OA-144 [$C_{11}H_{12}$]	—	0.08	—	—	—
naphthalene (**3**)	5.30	7.54	11.12	16.54	27.11
1-methyltetralin	0.62	0.69	0.86	0.74	0.63
siloxane $((CH_3)_2SiO)_6$	*d*	*d*	—	—	—
OB-144 [$C_{11}H_{12}$]	0.10	0.15	0.33	—	—
TO-148 [$C_{11}H_{16}$]	1.65	1.98	2.10	1.09	0.52
OC-146 [$C_{11}H_{14}$ or $C_{10}H_{10}O$]	0.67	0.35	0.31	0.11	—
OD-146 [$C_{11}H_{14}$ or $C_{10}H_{10}O$]	0.56	0.40	0.26	—	—
OE-146 [$C_{11}H_{14}$ or $C_{10}H_{10}O$]	1.26	0.56	0.73	0.13	—
OF-220 [$C_{12}H_{12}O_4$]	0.13	0.09	0.16	0.13	—
OG	*d*	*d*	*d*	—	—
bis(*o*-allylbenzyl) oxalate (**9**)	3.44	1.72	1.22	0.33	—
OH-148 [$C_{11}H_{16}$ or $C_{10}H_{12}O$]	0.33	1.45	0.45	—	—
1-tetralone	0.32	0.24	0.23	0.39	—
OI	—	—	*d*	—	—

Table A-I continues on next page

Table A-I. Continued

	yield, % [c]				
entry	700 °C	750 °C	800 °C	850 °C	900 °C
1,2-diphenylethane	0.49	—	—	—	—
1,2-di(2-methylphenyl)ethane	0.25	—	—	—	—
OJ	—	—	—	—	*d*
OK	—	—	*d*	—	*d*
OL	—	—	—	—	*d*
OM	—	—	—	—	*d*
1,2-di(2-allylphenyl)ethane (**14**)	0.69	0.24	—	—	—
recovery [e]	71.49	65.07	68.72	67.12	59.93
conversion [f]	96.56	98.28	98.78	99.67	100.0

[a] FVP conditions: system pressure = 1 x 10^{-5} torr, sample temperature = 60–80 °C. [b] Amounts determined by GC with a known quantity of triphenylmethane added as standard. Data represent the average of triplicate runs. Products identified by comparison with authentic samples or those that could be identified by retention time and GCMS are indicated by name. Products that were identified by GCMS only are indicated by code: XY-nnn, where 'X' corresponds to the system studied (O = pyrolysis of **9**, T = pyrolysis of **1**), 'Y' to the individual unknown product (A, B, C, etc.), and 'nnn' to the nominal mass. [c] Moles of product divided by total moles of recovered material. [d] Product which constitutes ≤0.50% total area by GC. [e] Total moles of recovered material divided by moles of starting material used. [f] Total moles of recovered material minus moles of recovered starting material divided by total moles of recovered material.

PAPER 4. THE FLASH VACUUM PYROLYSIS OF 1,4-DIPHENYLBUTANE

INTRODUCTION

We have concluded from our study of the gas-phase decomposition of tetralin (**1**) that the lowest energy unimolecular reaction of **1** is ethylene loss to form benzocyclobutene (**2**),[1] a conclusion that has also been reached from a study of the laser-induced decomposition of **1**.[2] One of the mechanisms proposed[2b] for the thermal decomposition of **1** to **2** involves cleavage of the weak benzylic carbon-carbon bond to form diradical **3** followed by loss of ethylene from **3** to form *o*-xylylene (**4**) which is known to

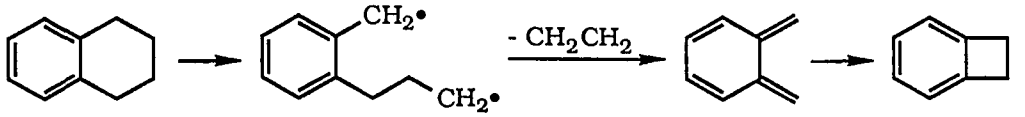

1 **3** **4** **2**

close to **2** at high temperatures.[3] From our study of the pyrolysis of ketone **5** and sulfone **6**,[4] we have concluded that diradical **3** is produced by both of these compounds. The results show, however, that the major reactions of **3** are coupling to form **1** and disproportionation to form *o*-allyltoluene (**7**). Little or no cleavage of the ß carbon-car-

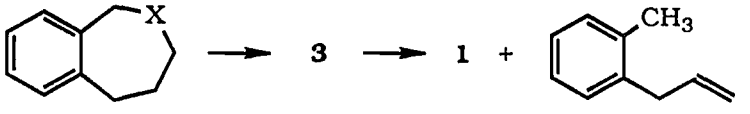

5 X = CO
6 X = SO_2

7

bon bond of diradical **3** to form **4** and subsequently **2** is observed.

Cleavage of the ß carbon-carbon bond in alkyl radicals is common,[5] but this does not seem to be a favorable reaction for diradical **3**. It is conceivable that under high-temperature gas-phase pyrolysis conditions that a 3-arylpropyl radical losses a ß hydrogen atom or undergoes cyclization in preference to cleavage of the ß carbon-carbon bond. In order to determine the fate of a simple arylpropyl radical under these

conditions, we have studied the products of the 3-phenylpropyl radical (**8**) produced by

$$\underset{\mathbf{9}}{PhCH_2CH_2CH_2CH_2Ph} \longrightarrow \underset{\mathbf{8}}{PhCH_2CH_2CH_2\bullet} + \bullet CH_2Ph \qquad (1)$$

the pyrolysis of 1,4-diphenylbutane (**9**). The results of this study are reported in this paper.

RESULTS

FVP of **9** at 10^{-5} torr (700–900 °C) produces 1,2-diphenylethane (**10**) as the major product (Table I). At higher temperatures (850–900 °C), *ca.* 10% toluene (**11**) is formed. Small amounts (<2.5%) of indan (**12**), styrene (**13**), ethylbenzene (**14**), allylbenzene (**15**), butylbenzene (**19**), and diphenylmethane (**20**) are also produced.

Table I. Products and recovered starting material from the FVP of 1,4-diphenylbutane (**9**) at various oven temperatures [a,b]

	yield, % [c]				
entry	700 °C	750 °C	800 °C	850 °C	900 °C
1,4-diphenylbutane (**9**)	98.2	91.1	65.7	23.4	7.1
1,2-diphenylethane (**10**)	1.6	7.8	30.4	62.9	71.9
toluene (**11**)	—	0.1	0.8	6.4	11.2
indan (**12**)	—	0.1	0.8	1.9	2.2
styrene (**13**)	—	0.1	0.6	1.9	2.3
ethylbenzene (**14**)	—	—	0.1	0.7	1.5
allylbenzene (**15**)	—	—	0.2	0.4	0.4
butylbenzene (**19**)	0.1	0.2	0.4	0.4	0.5
diphenylmethane (**20**)	—	—	<0.1	0.3	0.8
other products	—	0.6 [d]	1.1 [d]	1.7 [d]	2.2 [d]
recovery [e]	98.9	98.6	96.4	94.0	85.5
conversion [f]	1.8	8.9	34.3	76.6	92.9

[a] FVP conditions: system pressure = 2 x 10^{-5} torr, sample temperature = RT. [b] Amounts determined by GC with a known quantity of triphenylmethane added as standard. Data represent the average of triplicate runs. [c] Moles of product divided by total moles of recovered material. [d] See Table A-I in the Appendix of Paper 3, this dissertation, for a more detailed analysis. [e] Total moles of recovered material divided by moles of starting material used. [f] Total moles of recovered material minus moles of recovered starting material divided by total moles of recovered material.

DISCUSSION

The major product from the FVP of **9**, 1,2-diphenylethane (**10**), is consistent with the expected mechanism: cleavage of the benzylic carbon-carbon bond to form a benzyl radical and **8** (eq 1) followed by the loss of ethylene from **8** to form another benzyl

$$\mathbf{8} \longrightarrow CH_2{=}CH_2 + {\bullet}CH_2Ph \qquad (2)$$

radical (eq 2). Benzyl radicals produced under these conditions couple to form **10** (eq 3).[6]

$$2\ PhCH_2{\bullet} \longrightarrow \underset{\mathbf{10}}{PhCH_2CH_2Ph} \qquad (3)$$

The production of indan (**12**) supports the formation of **8** (eq 4) and the low yield of **12**

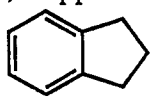

$$\mathbf{8} \longrightarrow \underset{\mathbf{12}}{\text{[indan]}} + H{\bullet} \qquad (4)$$

shows that under these conditions cleavage of the ß carbon-carbon bond of **8** is favored over cyclization. Loss of a ß hydrogen atom from **8** could account for the production of allylbenzene (**15**) (eq 5) but **15** could also arise from radical induced decomposition of **9**

$$\mathbf{8} \longrightarrow \underset{\mathbf{15}}{PhCH_2CH{=}CH_2} + H{\bullet}$$

as discussed below. The low yield of **15**, whatever its source, means that cleavage of the ß carbon-carbon bond is much more important than ß carbon-hydrogen bond cleavage.

In liquid-phase studies of the decomposition of **9**,[5,7] radical chain reactions account for the decomposition products. The reaction of a benzyl radical with **9** leads to the formation of radical **16** or **17** (eq 6,7). Radical **16** decomposes to the 2-phenylethyl

$$\mathbf{9} + PhCH_2{\bullet} \longrightarrow \underset{\mathbf{16}}{PhC{\bullet}HCH_2CH_2CH_2Ph} + \underset{\mathbf{11}}{PhCH_3} \qquad (6)$$

$$\mathbf{9} + PhCH_2{\bullet} \longrightarrow \underset{\mathbf{17}}{PhCH_2C{\bullet}HCH_2CH_2Ph} + \mathbf{11} \qquad (7)$$

radical (**18**) and styrene (**13**) (eq 8) and radical **17** fragments to benzyl radical and

$$\underset{\mathbf{16}}{\longrightarrow} \underset{\mathbf{13}}{PhCH{=}CH_2} + \underset{\mathbf{18}}{{\bullet}CH_2CH_2Ph} \qquad (8)$$

allylbenzene (**15**) (eq 9). Abstraction of a hydrogen atom from **9** by a benzyl radical

$$\underset{\mathbf{17}}{\longrightarrow} \underset{\mathbf{15}}{PhCH_2CH{=}CH_2} + {\bullet}CH_2Ph \qquad (9)$$

forms toluene (**11**) and radical **16** or **17** (eq 6, 7) and abstraction of a hydrogen atom from **9** by radical **18** forms ethylbenzene (**14**) and radical **16** or **17** (eq 10).

$$\mathbf{18} + \mathbf{9} \longrightarrow \mathbf{16} + \mathbf{17} + \underset{\mathbf{14}}{CH_3CH_2Ph} \qquad (10)$$

Two other minor products are butylbenzene (**19**) and diphenylmethane (**20**). A reasonable pathway to these products is addition of a benzyl radical to a phenyl ring of **9** to form radical **21** followed by decomposition of radical **21** to the 4-phenylbutyl radical (**22**) and **20** (eq 11). Abstraction of a hydrogen atom by radical **22** from **9** gives **19** and radical **16** or **17** (eq 12).

$$\mathbf{9} + PhCH_2{\bullet} \longrightarrow \underset{\mathbf{21}}{\text{ 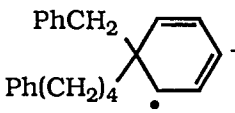 }} \longrightarrow \underset{\mathbf{22}}{Ph(CH_2)_3CH_2{\bullet}} + \underset{\mathbf{20}}{PhCH_2Ph} \qquad (11)$$

$$\mathbf{9} + \mathbf{22} \longrightarrow \underset{\mathbf{19}}{PhCH_2CH_2CH_2CH_3} + \mathbf{16} + \mathbf{17} \qquad (12)$$

The detection of increasing amounts of **11** with higher pyrolysis temperatures and the observation of minor products **13**, **14**, **19**, and **20** indicate some induced decomposition of **9** is occurring. However, these reactions occur to a significant extent only at high conversion where a high concentration of benzyl radicals is expected.

CONCLUSION

In conclusion, our results show that the major reaction of the 3-phenylpropyl radicals (**8**) in the gas-phase at high temperature is cleavage of the ß carbon-carbon bond to produce ethylene and benzyl radical; loss of a ß hydrogen atom to form allylbenzene (**15**) and cyclization to form indan (**12**) are minor reactions under these conditions. Thus, the small amount of ß carbon-carbon bond cleavage of diradical **3** appears to be characteristic of that system, rather than a consequence of the method of generation. Apparently for diradical **3**, the two reactions which involve interaction of the two radical sites, coupling to form **1** and disproportionation to form **7**, are much faster than ß carbon-carbon bond cleavage.

EXPERIMENTAL

General Procedures

Methods and materials

Some general methods have been described previously.[8] ^{1}H NMR spectra were recorded on a Nicolet NT-300 spectrometer. GCMS were performed on a Finnegan 4000 mass spectrometer. All materials were commercially available and used as received, except where indicated.

1,4-Diphenylbutane (9) 1,4-Diphenylbutane was prepared as previously described.[6a] mp 51–53 °C; ^{1}H NMR ($CDCl_3$) δ 7.30–7.12 (m, 10 H), 2.68–2.57 (m, 4 H), 1.74–1.62 (m, 4 H) [lit.[9] ^{1}H NMR δ 7.05 (s, 5 H), 2.60 (m, 2 H), 1.65 (m, 2 H)]; GCMS (EI, 70 eV) *m/e* (% base peak) 210 (32.4), 92 (53.1), 91 (100) [lit.[9] GCMS (EI, 70 eV) *m/e* (% base peak) 210 (27.5), 92 (57), 91 (100)].

Flash vacuum pyrolysis Flash vacuum pyrolysis (FVP) was performed as previously described.[1,10]

Product analysis FVP reaction mixtures were analyzed by capillary gas chromatography on a Hewlett-Packard HP5840A gas chromatograph equipped with a 30-m (0.25-μm film thickness) DB-1701 capillary column using the analytical procedure previously described.[1]

REFERENCES

(1) Malandra, J. L.; Zhu, J.; Lee, S.-K.; Spurlin, S. R.; Tunkel, J. L.; Fischer, D. R.; Yeung, E. S.; Trahanovsky, W. S., manuscript in preparation. [Paper 1, this dissertation]

(2) (a) Berman, M. R.; Comita, P. B.; Moore, C. B.; Bergman, R. G. *J. Amer. Chem. Soc.* **1980**, *102*, 5692. (b) Comita, P. B.; Berman, M. R.; Moore, B. C.; Bergman, R. G. *J. Phys. Chem.* **1981**, *85*, 3266.

(3) Martin, N.; Seoane, C.; Hanack, M. *Org. Prep. Proc. Int.* **1991**, *23*, 239.

(4) Malandra, J. L.; Trahanovsky, W. S., manuscript in preparation. [Paper 2, this dissertation]

(5) Poutsma, M. L. *A Review of Thermolysis Studies of Model Compounds Relevant to Processing of Coal*; ORNL/TM-10673, Oak Ridge National Laboratory, Oak Ridge, TN 37831. This review is available from National Technical Information Service, U. S. Dept. of Commerce, 5285 Port Royal Rd., Springfield, VA 22161.

(6) Trahanovsky, W. S.; Ong, C. C. *J. Amer. Chem. Soc.* **1970**, *92*, 7174.

(7) (a) Poutsma, M. L.; Dyer, C. W. *J. Org. Chem.* **1982**, *47*, 4903. (b) Hung, M.-H.; Stock, L. M. *Fuel* **1982**, *61*, 1161. (c) King, H.-H.; Stock, L. M. *Fuel* **1984**, *63*, 810.

(8) (a) Trahanovsky, W. S.; Cassady, T. J.; Woods, T. L. *J. Amer. Chem. Soc.* **1981**, *103*, 6691. (b) Chou, C.-H.; Trahanovsky, W. S. *J. Amer. Chem. Soc.* **1986**, *108*, 4138.

(9) Rupprecht, R.; Zilliox, J.-G.; Franta, E.; Brossas, J. *Eur. Polym. J.* **1979**, *15*, 11.

(10) (a) Trahanovsky, W. S.; Ong, C. C.; Pataky, J. G.; Weitl, F. L.; Mullen, P. W.; Clardy, J. C.; Hansen, R. S. *J. Org. Chem.* **1971**, *36*, 3575. Commercial apparatus is available from Kontes Scientific Glassware, Vineland, NJ 08360. (b) For review, see Brown, R. C. F. *Pyrolysis Methods in Organic Chemistry*; Academic: New York, 1980, Chapter 2.

APPENDIX

SUPPLEMENTARY DATA TABLE

Table A-I. Products and recovered starting material, total recovery of material, and conversion from the FVP of 1,4-diphenylbutane (**9**) at various oven temperatures [a,b]

	yield, % [c]				
entry	700 °C	750 °C	800 °C	850 °C	900 °C
toluene (**11**)	—	0.08	0.75	6.38	11.16
ethylbenzene (**14**)	—	—	0.08	0.71	1.46
styrene (**13**)	—	0.10	0.56	1.87	2.33
allylbenzene (**15**)	—	—	0.15	0.39	0.43
butylbenzene (**19**)	0.13	0.23	0.35	0.41	0.46
indan (**12**)	—	0.13	0.79	1.94	2.15
indene	—	—	0.06	0.11	0.18
BA	—	*d*	*d*	*d*	*d*
diphenylmethane (**20**)	—	—	0.04	0.28	0.76
1,2-diphenylethane (**10**)	1.63	7.82	30.44	62.93	71.86
BB	—	—	*e*	*e*	*e*
BC	—	—	—	—	*d*
BD	*d*	*d*	*d*	*d*	—
BE	—	—	—	—	*d*
1,4-diphenylbutane (**9**)	98.24	91.09	65.73	23.43	7.13
BF	—	—	*d*	*d*	*d*

Table A-I continues on next page

Table A-I. Continued

	yield, % [c]				
entry	700 °C	750 °C	800 °C	850 °C	900 °C
BG-196 [$C_{15}H_{16}$]	—	0.06	0.32	0.32	0.40
BH-196 [$C_{15}H_{16}$]	—	—	0.09	0.08	0.11
BI-196 [$C_{15}H_{16}$]	—	0.06	0.25	0.19	0.30
BJ	—	—	*d*	—	—
BK	—	—	—	*d*	—
BL	—	*d*	*d*	—	*d*
BM	—	—	—	*d*	*d*
BN-272 [$C_{21}H_{20}$]	—	0.10	0.11	0.26	0.29
BO	—	—	—	—	*d*
BP	—	—	—	—	*d*
BQ-272 [$C_{21}H_{20}$]	—	0.08	—	0.08	0.13
BR-272 [$C_{21}H_{20}$]	—	0.26	0.28	0.62	0.84
recovery [f]	98.94	98.55	96.36	94.01	85.47
conversion [g]	1.76	8.91	34.27	76.57	92.87

[a] FVP conditions: system pressure = 2 x 10^{-5} torr, sample temperature = RT. [b] Amounts determined by GC with a known quantity of triphenylmethane added as standard. Data represent the average of triplicate runs. Products identified by comparison with authentic samples or those that could be identified by retention time and GCMS are indicated by name. Products that were identified by GCMS only are indicated by code: XY-nnn, where 'X' corresponds to the system studied (B = pyrolysis of **9**), 'Y' to the individual unknown product (A, B, C, etc.), and 'nnn' to the nominal mass. [c] Moles of product divided by total moles of recovered material. [d] Product which constitutes ≤0.30% total area by GC. [e] Product which constitutes between 0.35% to 0.90% total area by GC. [f] Total moles of recovered material divided by moles of starting material used. [g] Total moles of recovered material minus moles of recovered starting material divided by total moles of recovered material.

PAPER 5. THE FLASH VACUUM PYROLYSIS OF *o*-ALLYLTOLUENE, *o*-(3-BUTENYL)TOLUENE AND *o*-(4-PENTENYL)TOLUENE

INTRODUCTION

In our study of the gas-phase decomposition of tetralin (**1**),[1] flow pyrolysis was used to limit bimolecular and heterogeneous surface reactions. Under these conditions, we found that *o*-allyltoluene (**4**) was one of the primary decomposition products, with 1,2-dihydronaphthalene (**2**) and benzocyclobutene (**3**). It was previously known (Scheme I) that, at higher temperatures, **2** would be converted to naphthalene (**5**) and **3** to styrene (**6**). The fate of **4** had not been previously explored. We pyrolyzed **4** under flow conditions and found that 2-methylindan (**7**) was formed and that **7** could be further pyrolyzed to indene (**8**) at higher temperatures.

Scheme I

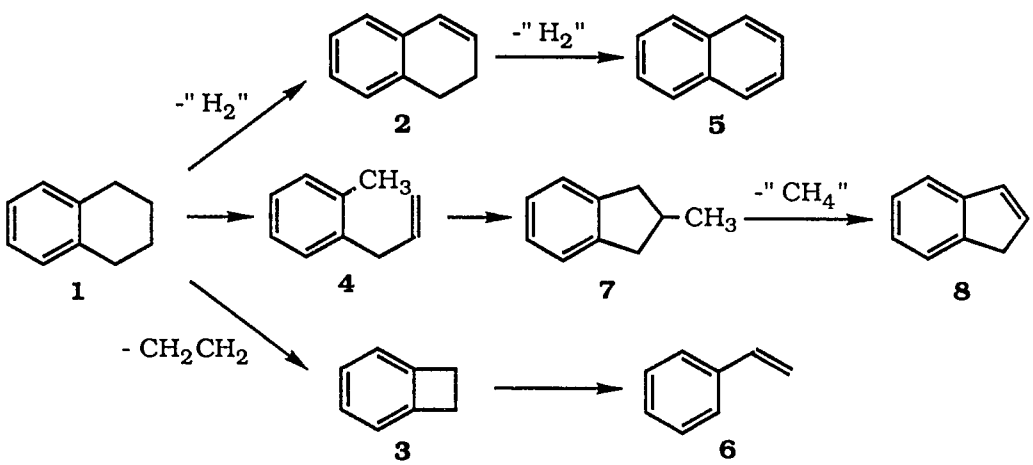

In this study, we have examined the flash vacuum pyrolysis (FVP) of **4** in order to determine if the conversion to **7** and **8** will occur under standard FVP conditions. The FVP of two homologous compounds, *o*-(3-butenyl)toluene (**9**) and *o*-(4-pentenyl)toluene

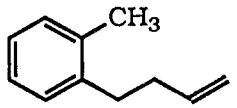

9

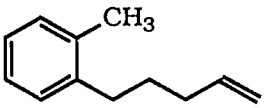

10

(**10**), was also studied for comparison purposes.

RESULTS

The results of the FVP of *o*-allyltoluene (**4**) at 0.10 torr (700–900 °C) are presented in Table I. The major products are 2-methylindan (**7**) and indene (**8**). Small amounts (<4%) of tetralin (**1**), 1,2-dihydronaphthalene (**2**), and naphthalene (**5**) are also produced at 700–800 °C. At 900 °C, *ca.* 8% **5** is formed.

The FVP of *o*-(3-butenyl)toluene (**9**) under similar conditions produces 1,2-di(*o*-tolyl)ethane (**11**) in good yield (*ca.* 40%) at 700–800 °C. At 900 °C, significant amounts (*ca.* 10–20%) of *o*-xylene (**12**), benzocyclobutene (**3**), *o*-ethyltoluene (**13**), and styrene (**6**) are formed.

The FVP of *o*-(4-pentenyl)toluene (**10**) results in the formation of *o*-methylstyrene (**14**). Numerous side products, each produced in small amounts, were detected at high conversion (900 °C). These results are presented in Table III.

Table I. Products and recovered starting material from the FVP of *o*-allyltoluene (**4**) at various oven temperatures [a,b]

	yield, % [c]		
entry	700 °C	800 °C	900 °C
o-allyltoluene (**4**) [d]	90.9	45.4	6.6
2-methylindan (**7**)	4.1	25.3	14.1
indene (**8**)	0.8	6.9	32.0
tetralin (**1**)	0.3	2.7	3.3
1,2-dihydronaphthalene (**2**)	0.6	1.4	1.1
naphthalene (**5**)	—	1.0	8.1
other products	3.3 [e]	17.3 [e]	34.9 [e]
recovery [f]	83.3	88.8	72.8
conversion [g]	9.1	54.6	93.4

[a] FVP conditions: system pressure = 0.10 torr, sample temperature = 0 °C. [b] Amounts determined by GC with a known quantity of biphenyl added as standard. Data represent the average of triplicate runs. [c] Moles of product divided by total moles of recovered material. [d] Starting material (yield, %): *o*-allyltoluene (96.5), *m*/*p*-allyltoluene (1.9), toluene (0.6), unidentified product TL-128 with formula $C_{10}H_8$ (0.4), naphthalene (0.4), 2,2'-dimethylbiphenyl (0.2). [e] See Table A-I in the Appendix of Paper 5, this dissertation, for a more detailed analysis. [f] Total moles of recovered material divided by moles of starting material used. [g] Total moles of recovered material minus moles of recovered starting material divided by total moles of recovered material.

Table II. Products and recovered starting material from the FVP of *o*-(3-butenyl)toluene (**9**) at various oven temperatures [a,b]

	yield, % [c]		
entry	700 °C	800 °C	900 °C
o-(3-butenyl)toluene (**9**) [d]	64.2	41.7	15.9
1,2-di(*o*-tolyl)ethane (**11**)	34.4	39.4	7.6
o-xylene (**12**)	0.4	4.7	18.6
benzocyclobutene (**3**)	0.4	3.5	15.2
o-ethyltoluene (**13**)	—	3.0	10.4
styrene (**6**)	—	0.5	6.8
other products	0.6 [e]	7.3 [e]	25.5 [e]
recovery [f]	97.8	88.7	110.0
conversion [g]	35.8	58.3	84.1

[a] FVP conditions: system pressure = 0.010 torr, sample temperature = 0 °C. [b] See Table I, footnote *b*. [c] See Table I, footnote *c*. [d] Starting material (yield, %): *o*-(3-butenyl)toluene (100.0). [e] See Table A-II in the Appendix of Paper 5, this dissertation, for a more detailed analysis. [f] See Table I, footnote *f*. [g] See Table I, footnote *g*.

Table III. Products and recovered starting material from the FVP of *o*-(4-pentenyl)toluene (**10**) at various oven temperatures [a,b]

	yield, % [c]		
entry	600 °C	700 °C	800 °C
o-(4-pentenyl)toluene (**10**) [d]	90.4	52.9	3.0
o-methylstyrene (**14**)	1.5	30.6	59.8
other products	8.1 [e]	16.5 [e]	37.0 [e]
recovery [f]	96.2	86.6	70.4
conversion [g]	9.6	47.1	97.0

[a] FVP conditions: see Table II, footnote *a*. [b] See Table I, footnote *b*. [c] See Table I, footnote *c*. [d] Starting material (yield, %): *o*-(4-pentenyl)toluene (92.4), 2,2'-dimethylbiphenyl (7.6), unidentified impurity PC which constitutes <0.35% total area by GC. [e] See Table A-III in the Appendix of Paper 5, this dissertation, for a more detailed analysis. [f] See Table I, footnote *f*. [g] See Table I, footnote *g*.

DISCUSSION

FVP of *o*-allyltoluene (**4**) clearly results in the formation of 2-methylindan (**7**), which then further decomposes to indene (**8**). Even at 900 °C, **4**, **7** and **8** constitute over 50% of the products. These FVP results are similar to the flow pyrolysis results obtained earlier.[1] However, the FVP of **4** results in the formation of more side products at high temperature than flow pyrolysis.

We propose that **7** is produced by a two-step mechanism involving diradical **15** formed by an intramolecular hydrogen atom transfer. Although there are examples of

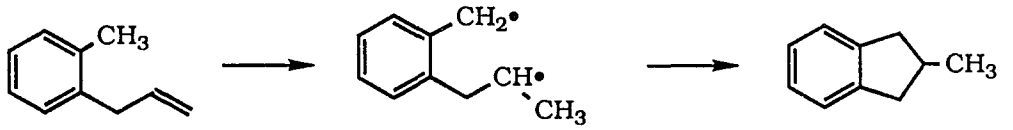

4 **15** **7**

the formation of hydrocarbon radicals by intramolecular hydrogen atom transfers,[2,3]

$$RH + R'H \longrightarrow R\bullet + R'H_2$$

we are not aware of any intramolecular examples of this reaction. The calculated[4] enthalpies of formation of radicals **4** and **15** have a $\Delta H°$ of 45 kcal mol^{-1}. This indicates that the conversion of **4** to **7** is reasonable at FVP temperatures ≥700 °C.

Conversion of 2-methylindan (**7**) to indene (**8**) at higher temperatures is readily explained by the loss of a methyl group form **7** to form the 2-indanyl radical which would rapidly lose a ß hydrogen atom to give **8**.[5]

The FVP of **4** also gives some tetralin (**1**) and this may arise from the 1,6-diradical (**16**) produced by a hydrogen atom transfer reaction to the internal olefinic

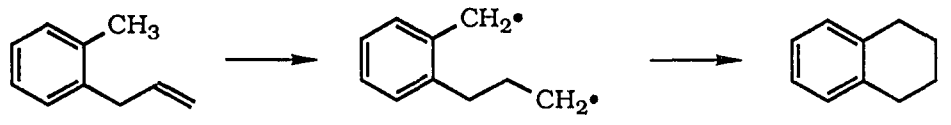

4 **16** **1**

carbon atom. The 1,2-dihydronaphthalene (**2**), naphthalene (**5**), and other products may simply be products of the secondary pyrolysis of **1**.

In the FVP of *o*-(3-butenyl)toluene (**9**), the main reaction is homolytic cleavage of the weak benzylic-allylic carbon-carbon bond (Table II). The dimerization of *o*-methylbenzyl radicals (**17**), produced from this bond cleavage, results in the formation of 1,2-di(*o*-tolyl)ethane (**11**). The allyl radicals (**18**) should dimerize to form 1,5-hexadiene

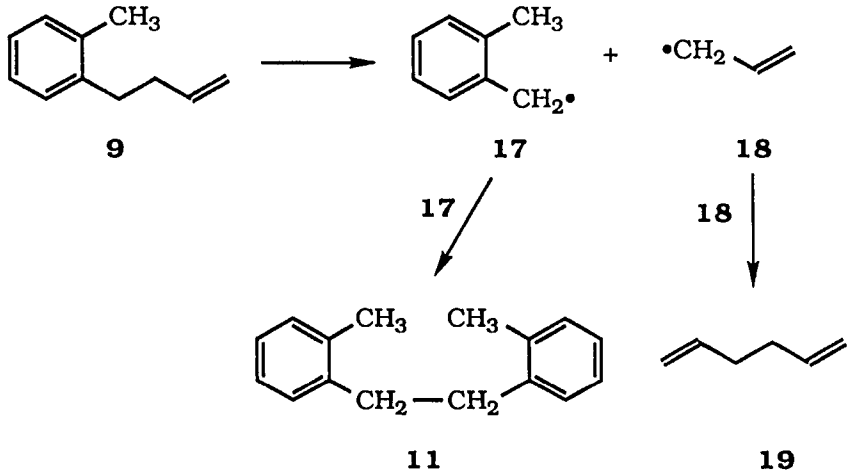

(**19**), however, this product was not detected due to its high volatility. At 900 °C, the major products are *o*-xylene (**12**), benzocyclobutene (**3**), *o*-ethyltoluene (**13**), and styrene (**6**). These products all appear to be formed from **17**.

The results of the pyrolysis of *o*-(4-pentenyl)toluene (**10**) are presented in Table III. The main product from the pyrolysis of *o*-(4-pentenyl)toluene (**10**) is *o*-methylstyrene (**14**) formed by a retro-ene reaction. Numerous minor side products are formed at high temperature (800 °C).

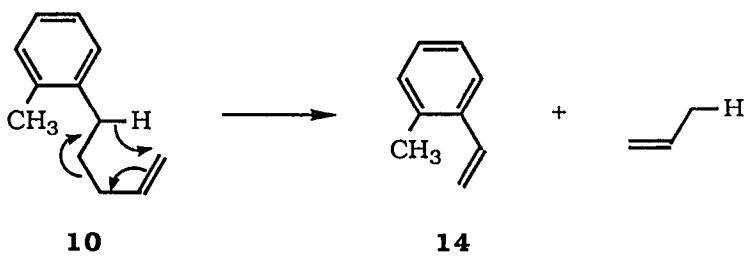

The $\Delta H^{\ddagger}$ for the conversion of **4** to **7** and **8** (Table I) was estimated from the FVP data for **9** (Table II) and **10** (Table III) by the method of Schiess.[6] The 50% conversion temperature (T 50%) was determined for **4**, **9** and **10** from a linear least squares line of a temperature vs. conversion plot (Figure 1, Table IV). The $\Delta H^{\ddagger}$ for the homolytic bond cleavage of **9** was calculated[4] ($\Delta H^{\ddagger} \approx \Delta H^{o}$) and the $\Delta H^{\ddagger}$ for the retro-ene reaction of **10** was estimated from the previously studied retro-ene reaction of 1,6-heptadiene[7] (Table IV). In this way, the $\Delta H^{\ddagger}$ for the conversion of **4** to **7** and **8** was estimated to be *ca.* 64 kcal mol^{-1} (Table IV).

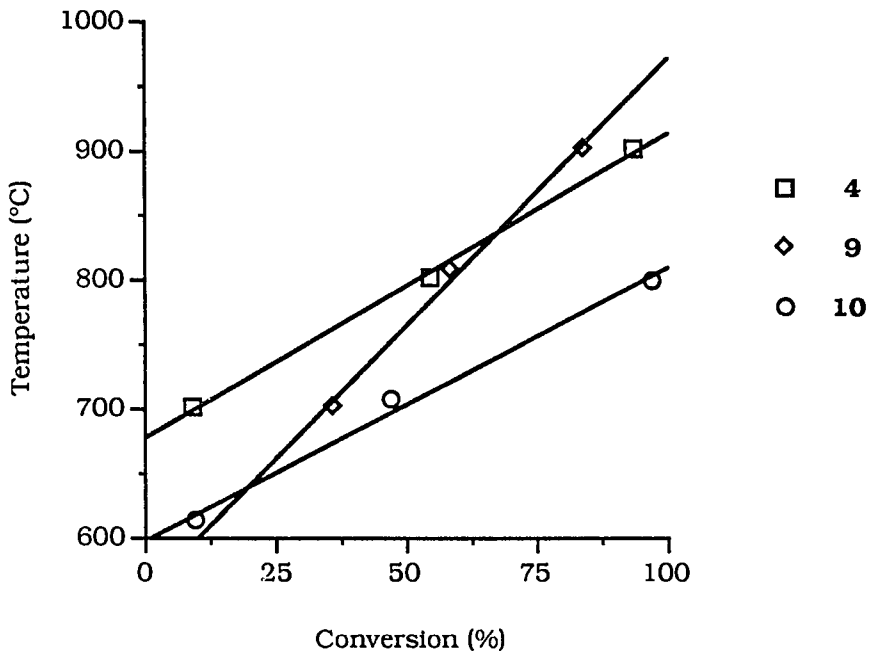

Figure 1. Plot of temperature vs. conversion for the FVP of *o*-allyltoluene (**4**), *o*-(3-butenyl)toluene (**9**), and *o*-(4-pentenyl)toluene (**10**) (system pressure, 0.10–0.010 torr; sample temperature, 0 °C)

Table IV. Linear least squares line for temperature vs. conversion and $\Delta H^{\ddagger}$ for the FVP of *o*-allyltoluene (**4**), *o*-(3-butenyl)toluene (**9**), and *o*-(4-pentenyl)toluene (**10**)

	linear least squares line temperature vs. conversion				
entry	slope, °C $\%^{-1}$	y-intercept, °C	r^2	T 50%, °C	$\Delta H^{\ddagger}$, kcal mol^{-1}
o-allyltoluene (**4**)	2.37	677	0.998	796	64 [a]
o-(3-butenyl)toluene (**9**)	4.13	559	0.995	765	58.4 [b]
o-(4-pentenyl)toluene (**10**)	2.12	598	0.993	704	47.5 [c]

[a] Estimated from the FVP data of **9** and **10** (ref 6). [b] Calculated (ref 4). [c] Estimated from $\Delta H^{\ddagger}$ of retro-ene reaction of 1,6-heptadiene (45.6 kcal mol^{-1}, ref 7) adjusted for the decreased thermodynamic stability of **10** (1.9 kcal mol^{-1}, ref 4).

CONCLUSION

We have observed the conversion of *o*-allyltoluene (**4**) to 2-methylindan (**7**) and indene (**8**) under both FVP and flow pyrolysis conditions. We believe the **4** to **7** reaction involves intramolecular benzylic hydrogen atom transfer to the double bond to form diradical **15**. The calculated $\Delta H°$ for this reaction is 45 kcal mol^{-1}. We have also pyrolyzed *o*-(3-butenyl)toluene (**9**) which undergoes homolytic bond cleavage and *o*-(4-pentenyl)toluene (**10**) which forms *o*-methylstyrene (**14**) through a retro-ene reaction. From the $\Delta H^{\ddagger}$ of these reactions, we estimate the $\Delta H^{\ddagger}$ for the **4** to **7** conversion is 65 kcal mol^{-1}.

EXPERIMENTAL

General Procedures

Methods and materials

Some general methods have been described previously.[8] ^{1}H NMR spectra were recorded on a Nicolet NT-300 spectrometer. FTIR spectra were obtained on an IBM IR/98 spectrophotometer. GCMS were performed on a Finnegan 4000 mass spectrometer. HRMS were performed on a Kratos MS-50 mass spectrometer. All materials were commercially available and used as received, except where indicated.

***o*-Allyltoluene (4)** *o*-Allyltoluene (**4**) was prepared by previously published procedure.[9] ^{1}H NMR ($CDCl_3$) δ 7.12 (s, 4 H), 5.94 (qt, J_q = 10.3 Hz, J_t = 6.4 Hz, 1 H), 5.04 (dq, J_d = 10.1 Hz, J_q = 1.6 Hz, 1 H), 4.98 (dq, J_d = 17.0 Hz, J_q = 1.7 Hz, 1 H), 3.36 (dt, J_d = 6.3 Hz, J_t = 1.6 Hz, 1 H), 2.28 (s, 3 H) [lit.[10b] ^{1}H NMR (CCl_4) δ 6.94 (s, 4 H), 5.79 (qt, J_q = 11.3 Hz, J_t = 6.5 Hz, 1 H), 4.93 (m, 1 H), 4.79 (dq, J_d = 11.3 Hz, J_q = 2.1 Hz, 1 H), 3.24 (dt, J_d = 6.0 Hz, J_t = 1.8 Hz, 2 H), 2.20 (s, 3H)]; GCMS (70 eV) *m/e* (% base peak) 132 (77.5), 117 (100), 115 (42.3), 91 (35.6), 65 (31.6) [lit.[9b] MS (50 eV) *m/e* 132 (parent), 117 (base)].

***o*-(3-Butenyl)toluene (9)** Allylmagnesium bromide (25 mL, 1.0 M solution in ether, 0.025 mol) was added dropwise to a solution of α-chloro-*o*-xylene (3.5 g, 0.025 mol, *ca.* 3.3 mL) in ether (15 mL) at 0 °C. The reaction mixture was stirred at room temperature for 1 h, quenched with H_2O (50 mL), and the phases separated. The aqueous phase was extracted with ether (3 x 50 mL). The combined organic phases were washed with H_2O (2 x 50 mL) and saturated NaCl (50 mL), dried ($MgSO_4$), and the solvent removed *in vacuo*. HPLC purification[1] yielded.*o*-(3-butenyl)toluene (1.9 g, 0.013 mol, 64% yield). ^{1}H NMR ($CDCl_3$) δ 7.17–7.07 (m, 4 H), 5.84 (qt, J_q = 10.2 Hz, J_t = 6.6 Hz, 1 H), 5.04 (dq, J_d = 17.1 Hz, J_q = 1.5 Hz, 1 H), 4.98 (ddt, J_d = 10.2 Hz, J_d = 1.8 Hz, J_t = 1.2

Hz, 1 H), 2.73–2.65 (m, 2 H), 2.37–2.27 (m, J = 7 Hz, 2 H), 2.31 (s, 3 H); GCMS (70 eV) *m/e* (% base peak) 160 (16.4), 118 (78.4), 106 (33.8), 105 (100), 91 (40.7), 77 (26.7).

o-(4-Pentenyl)toluene (10) The following modified literature procedure[11] was used. Crushed Mg turnings (0.36 g, 0.015 mol) were added to THF (55 mL) under Ar atmosphere. 2-Bromotoluene (2.3 g, 0.013 mol, *ca.* 1.6 mL) was added and the mixture was stirred overnight. 5-Bromo-1-pentene (2.0 g, 0.013 mol, *ca.* 1.6 mL) and CuBr (0.096 g, 0.67 mmol) in HMPA (5 mL) were heated to 50–60 °C for one-half h. The Grignard reagent was transferred to an addition funnel and added dropwise to the warm HMPA solution. After the addition was complete, the reaction mixture was refluxed for 2 h, added to a mixture of ice and 1 M HCl in a beaker, and extracted with ether (3 x 50 mL). The combined ether fractions were washed with H_2O (50 mL), saturated NaCl (50 mL), dried ($MgSO_4$), and the solvent removed *in vacuo*. Flash column chromatography on a silica gel column (30 x 100 mm) with hexanes yielded *o*-(4-pentenyl)toluene (0.87 g, 5.4 mmol, 40 % yield). ^{1}H NMR ($CDCl_3$) δ 7.15–7.05 (m, 4 H), 5.85 (qt, J_q = 10.2 Hz, J_t = 6.7 Hz, 1 H), 5.04 (dq, J_d = 17.1 Hz, J_q = 1.7 Hz, 1 H), 4.98 (ddt, J_d = 10.2 Hz, J_d = 2.2 Hz, J_t = 1.2 Hz, 1 H), 2.64–2.55 (m, 2 H), 2.30 (s, 3 H), 2.19–2.11 (m, 2 H), 1.71–1.65 (m, 2 H) [lit.[12] ^{1}H NMR ($CDCl_3$) δ 7.08 (4 H), 5.88 (1 H), 5.05 (2 H), 2.60 (2 H), 2.28 (3 H), 2.6–1.3 (4 H)]; GCMS (70 eV) *m/e* (% base peak) 160 (16.4), 118 (78.4), 106 (33.8), 105 (100), 91 (40.7), 77 (26.7).

Flash vacuum pyrolysis Flash vacuum pyrolysis (FVP) was performed as previously described.[13]

Product analysis FVP reaction mixtures were analyzed by capillary gas chromatography on a Hewlett-Packard HP5840A gas chromatograph equipped with a 30-m (0.25-μm film thickness) DB-1701 capillary column using the analytical procedure previously described.[1]

REFERENCES

(1) Malandra, J. L.; Zhu, J.; Lee, S.-K.; Spurlin, S. R.; Tunkel, J. L.; Fischer, D. R.; Yeung, E. S.; Trahanovsky, W. S., manuscript in preparation. [Paper 1, this dissertation]

(2) Poutsma, M. L. *A Review of Thermolysis Studies of Model Compounds Relevant to Processing of Coal*; ORNL/TM-10673, Oak Ridge National Laboratory, Oak Ridge, TN 37831. This review is available from National Technical Information Service, U. S. Dept. of Commerce, 5285 Port Royal Rd., Springfield, VA 22161.

(3) (a) Franz, J. A.; Camaioni, D. M.; Beishline, R. R.; Dalling, D. K. *J. Org. Chem.* **1984**, *49*, 3563. (b) Billmers, R.; Griffith, L. L.; Stein, S. E. *J. Phys. Chem.* **1986**, *90*, 517.

(4) Benson, S. W. *Thermochemical Kinetics*, 2nd ed.; Wiley: 1976.

(5) Franz, J. A.; Camaioni, D. M. *J. Org. Chem.* **1980**, *45*, 5247.

(6) Schiess, P. *Thermochimica Acta* **1987**, *112*, 31.

(7) Egger, K. W.; Vitins, P. *J. Amer. Chem. Soc.* **1974**, *96*, 2714.

(8) (a) Trahanovsky, W. S.; Cassady, T. J.; Woods, T. L. *J. Amer. Chem. Soc.* **1981**, *103*, 6691. (b) Chou, C.-H.; Trahanovsky, W. S. *J. Amer. Chem. Soc.* **1986**, *108*, 4138.

(9) Hurd, C. D.; Bollman, H. T. *J. Amer. Chem. Soc.* **1934**, *56*, 447.

(10) (a) Berman, M. R.; Comita, P. B.; Moore, C. B.; Bergman, R. G. *J. Amer. Chem. Soc.* **1980**, *102*, 5692. (b) Comita, P. B.; Berman, M. R.; Moore, B. C.; Bergman, R. G. *J. Phys. Chem.* **1981**, *85*, 3266.

(11) Nishimura, J.; Yamada, N.; Horiuchi, E. U.; Ohbayashi, A.; Oku, A. *Bull. Chem. Soc. Japan* **1986**, *59*, 2035.

(12) Ellis-Davies, G. C. R.; Gilbert, A.; Heath, P.; Lane, J. C.; Warrington, J. V.; Westover, D. L. *J. Chem. Soc., Perkin Trans. 2* **1984**, 1833.

(13) (a) Trahanovsky, W. S.; Ong, C. C.; Pataky, J. G.; Weitl, F. L.; Mullen, P. W.; Clardy, J. C.; Hansen, R. S. *J. Org. Chem.* **1971**, *36*, 3575. Commercial apparatus is available from Kontes Scientific Glassware, Vineland, NJ 08360. (b) For review, see Brown, R. C. F. *Pyrolysis Methods in Organic Chemistry*; Academic: New York, 1980, Chapter 2.

APPENDIX

SUPPLEMENTARY DATA TABLES

Table A-I. Products and recovered starting material, total recovery of material, and conversion from the FVP of *o*-allyltoluene (**4**) at various oven temperatures [a,b]

	yield, % [c]			
entry	RT [d]	701 °C	802 °C	901 °C
toluene	0.57	—	1.05	3.03
ethylbenzene	—	—	0.55	1.92
m/p-xylene	—	—	0.51	0.18
o-xylene (**12**)	—	—	0.23	1.92
styrene (**6**)	—	—	0.75	3.45
benzocyclobutene (**3**)	—	—	0.35	1.19
allylbenzene	—	—	—	0.26
propylbenzene	—	—	—	0.12
o-ethyltoluene (**13**)	—	—	1.46	0.94
AA-118 [C_9H_{10}]	—	—	—	0.09
o-methylstyrene (**14**)	—	1.02	3.18	5.52
AB-118 [C_9H_{10}]	—	—	—	0.29
benzaldehyde	—	—	—	0.17
indan	—	—	—	0.68
trans-ß-methylstyrene	—	—	—	0.11
m/p-allyltoluene	1.94	1.97	1.76	0.79

Table A-I continues on next page

Table A-I. Continued

	yield, % [c]			
entry	RT [d]	701 °C	802 °C	901 °C
o-allyltoluene (**4**)	96.47	90.94	45.35	6.56
indene (**8**)	—	0.83	6.86	31.98
2-methylindan (**7**)	—	4.09	25.34	14.08
1-methylindan	—	—	1.43	0.60
TD-130 [$C_{10}H_{10}$]	—	—	0.14	0.92
TE-130 [$C_{10}H_{10}$]	—	—	—	0.11
o-methylbenzaldehyde	—	—	0.28	0.15
o-(1-propenyl)toluene	—	—	3.05	3.68
TH-130 [$C_{10}H_{10}$]	—	—	—	0.18
3-methyl-1*H*-indene	—	—	0.72	3.47
tetralin (**1**)	—	0.32	2.74	3.28
2-methyl-1*H*-indene	—	—	0.42	0.73
TK-130 [$C_{10}H_{10}$]	—	—	1.20	2.43
1,2-dihydronaphthalene (**2**)	—	0.55	1.42	1.10
TL-128 [$C_{10}H_8$]	0.40	—	—	0.98
naphthalene (**5**)	0.39	—	0.96	8.10
TN	—	—	—	*e*
TO-148 [$C_{11}H_{16}$]	—	—	—	0.10
2-methylnaphthalene	—	—	—	0.17
1-methylnaphthalene	—	—	—	0.24
2,2'-dimethylbiphenyl	0.24	0.27	0.25	0.39
AC-182 [$C_{14}H_{14}$]	—	—	—	0.10

Table A-I continues on next page

Table A-I. Continued

	yield, % [c]			
entry	RT [d]	701 °C	802 °C	901 °C
recovery [f]	94.62	83.28	88.78	72.79
conversion [g]	[d]	9.06	54.65	93.44

[a] FVP conditions: system pressure = 0.10 torr, sample temperature = 0 °C. [b] Amounts determined by GC with a known quantity of biphenyl added as standard. Data represent the average of triplicate runs. Products identified by comparison with authentic samples or those that could be identified by retention time and GCMS are indicated by name. Products that were identified by GCMS only are indicated by code: XY-nnn, where 'X' corresponds to the system studied (A = pyrolysis of **4**, T = pyrolysis of **1**), 'Y' to the individual unknown product (A, B, C, etc.), and 'nnn' to the nominal mass. [c] Moles of product divided by total moles of recovered material. [d] Starting material purity assay. [e] Unidentified product which constitutes ≤0.25% total area by GC. [f] Total moles of recovered material divided by moles of starting material used. [g] Total moles of recovered material minus moles of recovered starting material divided by total moles of recovered material.

Table A-II. Products and recovered starting material, total recovery of material, and conversion from the FVP of *o*-(3-butenyl)toluene (**9**) at various oven temperatures [a,b]

	yield, % [c]			
entry	RT [d]	702 °C	808 °C	902 °C
toluene	—	—	—	2.29
ethylbenzene	—	—	—	1.59
m/*p*-xylene	—	—	—	0.75
o-xylene (**12**)	—	0.40	4.70	18.58
styrene (**6**)	—	—	0.46	6.80
benzocyclobutene (**3**)	—	0.36	3.51	15.24
allylbenzene	—	—	—	0.23
propylbenzene	—	—	—	0.32
o-ethyltoluene (**13**)	—	—	2.97	10.37
o-methylstyrene (**14**)	—	—	0.51	2.14
indan	—	—	—	0.13
m/*p*-allyltoluene	—	—	0.95	3.83
o-allyltoluene (**4**)	—	—	0.21	0.40
HA	—	—	*e*	—
indene (**8**)	—	—	0.34	1.64
2-methylindan (**7**)	—	—	—	0.22
o-methylbenzaldehyde	—	0.33	0.39	0.21
o-(1-propenyl)toluene	—	—	—	0.15
HB-146 [$C_{11}H_{14}$]	—	—	0.16	0.43
HC-146 [$C_{11}H_{14}$]	—	—	0.16	0.22
o-(3-butenyl)toluene (**9**)	100.0	64.20	41.73	15.87

Table A-II continues on next page

Table A-II. Continued

	yield, % [c]			
entry	RT [d]	702 °C	808 °C	902 °C
HD-146 [$C_{11}H_{14}$]		0.32	0.25	0.12
2-methyl-1*H*-indene	—	—	0.23	0.10
TK-130 [$C_{10}H_{10}$]	—	—	—	0.14
1,2-dihydronaphthalene (**2**)	—	—	0.30	0.30
TM	—	—	*e*	*e*
naphthalene (**5**)	—	—	0.45	1.38
HE-146 [$C_{11}H_{14}$]	—	—	0.20	0.12
HF-156 [$C_{12}H_{12}$]	—	—	—	0.20
2-methylnaphthalene	—	—	—	0.10
1-methylnaphthalene	—	—	—	0.18
HG-182 [$C_{14}H_{14}$]	—	—	—	0.46
HH-182 [$C_{14}H_{14}$]	—	—	—	0.47
HI-196 [$C_{15}H_{16}$]	—	—	—	0.29
HJ-196 [$C_{15}H_{16}$]	—	—	2.15	4.24
HK-210 [$C_{16}H_{18}$]	—	—	0.37	0.49
1,2-di(*o*-tolyl)ethane (**11**)	—	34.38	39.36	7.59
HL-178 [$C_{14}H_{10}$]	—	—	0.63	1.46
HM-208 [$C_{16}H_{16}$]	—	—	—	0.46
HN-192 [$C_{15}H_{12}$]	—	—	—	0.47
recovery [f]	102.4	97.77	88.72	110.0
conversion [g]	*d*	35.80	58.27	84.13

Table A-II footnote on next page

Table A-II. Footnote

---

[a] FVP conditions: system pressure = 0.010 torr, sample temperature = 0 °C. [b] Amounts determined by GC with a known quantity of biphenyl added as standard. Data represent the average of triplicate runs. Products identified by comparison with authentic samples or those that could be identified by retention time and GCMS are indicated by name. Products that were identified by GCMS only are indicated by code: XY-nnn, where 'X' corresponds to the system studied (H = pyrolysis of **9**, T = pyrolysis of **1**), 'Y' to the individual unknown product (A, B, C, etc.), and 'nnn' to the nominal mass. [c] See Table A-I, footnote *c*. [d] See Table A-I, footnote *d*. [e] See Table A-I, footnote *e*. [f] See Table A-I, footnote *f*. [g] See Table A-I, footnote *g*.

Table A-III. Products and recovered starting material, total recovery of material, and conversion from the FVP of *o*-(4-pentenyl)toluene (**10**) at various oven temperatures [a,b]

	yield, % [c]			
entry	RT [d]	613 °C	707 °C	800 °C
toluene	—	—	0.26	3.24
ethylbenzene	—	—	—	1.32
o-xylene (**12**)	—	—	1.00	5.65
styrene (**6**)	—	—	—	2.54
benzocyclobutene (**3**)	—	—	0.92	3.24
o-ethyltoluene (**13**)	—		0.88	3.15
o-methylstyrene (**14**)	—	1.52	30.62	59.78
benzaldehyde	—	—	0.21	1.33
indan	—	—	—	1.07
m/*p*-allyltoluene	—	0.31	0.26	0.51
o-allyltoluene (**4**)	—	—	0.20	—
indene (**8**)	—	—	0.34	2.29
o-methylbenzaldehyde	—	—	1.67	2.56
PA	—	—	*e*	—
PB-146 [$C_{11}H_{14}$]	—	—	0.82	0.98
naphthalene (**5**)	—	—	0.11	0.52
PC	*e*	*e*	*e*	—
PD	—	—	*e*	—
2-(4-pentenyl)toluene (**10**)	92.42	90.40	52.92	2.97
PE-160 [$C_{12}H_{16}$]	—	—	0.58	0.52
PF	—	—	*e*	—

Table A-III continues on next page

Table A-III. Continued

	yield, % [c]			
entry	RT [d]	613 °C	707 °C	800 °C
PG-160 [$C_{12}H_{16}$]	—	—	0.97	1.10
2,2'-dimethylbiphenyl	7.58	7.77	8.23	7.22
recovery [e]	97.85	96.20	86.59	70.36
conversion [f]	*d*	9.60	47.08	97.03

[a] See Table A-II, footnote *a*. [b] Amounts determined by GC with a known quantity of biphenyl added as standard. Data represent the average of triplicate runs. Products identified by comparison with authentic samples or those that could be identified by retention time and GCMS are indicated by name. Products that were identified by GCMS only are indicated by code: XY-nnn, where 'X' corresponds to the system studied (P = pyrolysis of **10**), 'Y' to the individual unknown product (A, B, C, etc.), and 'nnn' to the nominal mass. [c] See Table A-I, footnote *c*. [d] See Table A-I, footnote *d*. [e] Unidentified product which constitutes ≤0.35% total area by GC. [f] See Table A-I, footnote *f*. [g] See Table A-I, footnote *g*.

GENERAL SUMMARY

In the gas-phase thermal decomposition studies of tetralin (**1**) found in paper 1, the relative amounts of dehydrogenation products, 1,2-dihydronaphthalene (**2**) and naphthalene (**5**), to ethylene loss products, benzocyclobutene (**3**) and styrene (**6**), vary with the conditions of the experiment. The multiphoton dissociation (MPD) of **1** produces mostly ethylene loss while the pulsed and continuous wave (cw) laser-sensitized decomposition of **1** produces mostly dehydrogenation. The relative amounts of dehydrogenation to ethylene loss in the flash vacuum pyrolysis (FVP) of **1** are dependent on the system pressure and the sample temperature. In the FVP of **1** at 10^{-5} torr, the ratio of dehydrogenation to ethylene loss remains *ca.* 1 (0.90–1.03) from 850 to 950 °C and finally drops to 0.73 at 1000 °C. On the other hand, when **1** is pyrolyzed at 0.10 torr a distinct drop in the dehydrogenation to ethylene loss ratio, from 2.70 to 0.72, with increasing pyrolysis temperature is observed. High sample temperature increases the proportion of dehydrogenation. When **1** is pyrolyzed under flow conditions, where sample molecules are diluted with a large excess of Ar, ethylene loss exceeds dehydrogenation by a ratio of between 3 and 5 to 1 over a wide temperature and conversion range. These flow experiments show that the lowest energy unimolecular gas-phase decomposition channel for **1** is ethylene loss. A bimolecular dehydrogenation reaction, possibly a hydrogen atom chain, is responsible for greater amounts of hydrogen-loss products observed under some conditions in the decomposition of **1**. In none of our pyrolysis experiments, whether laser-induced or under standard pyrolysis conditions, did we find any evidence of heterogeneous catalytic reactions on surfaces. We can conclude that MPD favors the lowest energy unimolecular

decomposition channel while laser-sensitized pyrolysis (cw or pulsed) can lead to homogenous bimolecular reactions as well.

We have observed the facile transformation of *o*-allyltoluene (**4**) to 2-methylindan (**7**), which we propose occurs through an intramolecular hydrogen atom transfer from the benzylic methyl group to the double bond of **4**. Loss of a methyl from **7** leads to the formation of indene (**8**). We have identified the transformation **4** to **7** to **8** as the major source of **8** in the gas-phase thermal decomposition of **1**.

Paper 2 shows that the FVP of 3-benzocycloheptenone (**10'**) leads to the formation of tetralin (**1**), 1,2-dihydronaphthalene (**2**), naphthalene (**5**), indene (**8**), 1-methylnaphthalene (**12'**), 2-methylnaphthalene (**13'**), and several other minor products. The results from the flow pyrolysis of **10'** are similar. An unusual aspect of the pyrolysis of **10'** is the formation of **12'** and **13'**, products formed by a net loss of water from ketone **10'**. The photolysis of **10'** at 25 °C in solution gives mostly **1** and some *o*-allyltoluene (**4**). In contrast to the pyrolysis of **10'**, FVP of 1,3,4,5-tetrahydro-2-benzothiepin-2,2-dioxide (**11'**) leads to the formation of large amounts of **1** and some **4** with only small amounts of other products. It is concluded that the 1,6-diradical formed by cleavage of the benzylic bond of **1** is produced in the pyrolysis and photolysis of **10'**, and the pyrolysis of **11'**. This diradical gives rise to **1** and **4** in a ratio between 3 and 8 to 1 over a temperature range of 25 to 950 °C. The pyrolysis of **10'** involves other major reactions. Mechanisms for these reactions are proposed.

In paper 3, the FVP of bis(*o*-allylbenzyl) oxalate (**9''**) at 700–900 °C gives as the major product 1,2-dihydronaphthalene (**2**). Several other minor products including naphthalene (**3''**), indene (**6''**), 3-methyl-1*H*-indene (**10''**), and 2-methyl-1*H*-indene (**11''**) are also produced. At lower temperatures the dimer of *o*-allylbenzyl radical (**7''**), 1,2-di(2-allylphenyl)ethane (**14''**), is produced in low yield. These results are consistent

with the production of radical **7''** as an intermediate in the FVP of **9''**. Formation of the major product **2** is readily explained by closure of **7''** to 2-tetryl radical (**16''**) followed by loss of a ß hydrogen atom.

Paper 4 describes the FVP of 1,4-diphenylbutane (**9'''**) (700–900 °C, 10^{-5} torr) produces 1,2-diphenylethane (**10'''**) in high yield. At higher temperatures, *ca.* 10% toluene (**11'''**) and small amounts (<2.5%) of indan (**12'''**), styrene (**13'''**), ethylbenzene (**14'''**), allylbenzene (**15'''**), butylbenzene (**19'''**), and diphenylmethane (**20'''**) are also produced. Formation of the benzyl radical coupling product **10'''** as the major product is consistent with initial cleavage of the benzylic carbon-carbon bond of **9'''** to form a benzyl radical and 3-phenylpropyl radical (**8'''**), followed by the loss of ethylene from **8'''** to produce another benzyl radical. Formation of **8'''** is supported by the detection of indan (**12'''**) as a minor product. The results show that the major reaction of **8'''** in the gas-phase is ß carbon-carbon bond cleavage to produce ethylene and benzyl radical; the loss of a ß hydrogen to form allylbenzene (**15'''**) and cyclization to indan (**12'''**) are minor reactions under these conditions. Formation of the minor products toluene (**11'''**), styrene (**13'''**), ethylbenzene (**14'''**), butylbenzene (**19'''**), and diphenylmethane (**20'''**) at higher temperatures indicates that some induced decomposition of **9'''** is occurring.

In paper 5, the FVP of *o*-allyltoluene (**4**) at 700 °C and 800 °C gives as the major product 2-methylindan (**7**). At 900 °C, **7** is still produced but the major product is indene (**8**). It is proposed that **7** is produced by a two-step mechanism involving 1,5-diradical **15''''** formed by an intramolecular hydrogen atom transfer. Conversion of **7** to indene

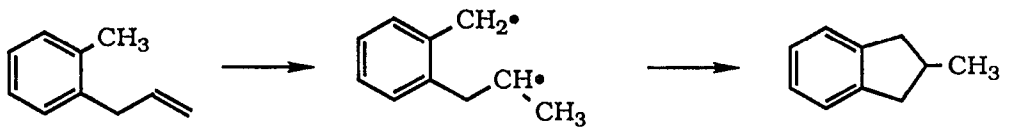

4 **15''''** **7**

(**8**) at higher temperatures is explained by the loss of a methyl group from **7** to form the 2-indanyl radical which would readily lose a ß hydrogen atom to give **8**. The calculated $\Delta H°$ for this reaction is 45 kcal mol^{-1}. We have also pyrolyzed *o*-(3-butenyl)toluene (**9''''**), which undergoes homolytic bond cleavage, and *o*-(4-pentenyl)toluene (**10''''**), which forms *o*-methylstyrene (**14''''**) through a retro-ene reaction. From the $\Delta H^{\ddagger}$ of these reactions, we estimate the $\Delta H^{\ddagger}$ for the **4** to **7** conversion is 65 kcal mol^{-1}.

In this dissertation, a clearer understanding of the high temperature gas-phase chemistry of tetralin has resulted from our decomposition studies of the simplest hydroaromatic compound and related model systems. We have demonstrated that the lowest energy unimolecular decomposition reaction of tetralin is ethylene loss and that a facile bimolecular dehydrogenation reaction occurs under some conditions. We have found no evidence of heterogeneous surface reactions in the gas-phase decomposition of tetralin. The decomposition of model systems designed to probe the pathways involved in tetralin decomposition has resulted in a greater understanding of the mechanism of tetralin decomposition and has suggested avenues for further research.

ACKNOWLEDGMENTS

I would like to thank Professor Walter S. Trahanovsky for his guidance during my graduate study at Iowa State. I would also like to thank members of the Trahanovsky research group for their friendship and assistance.

Above all, I would like to thank my parents. Their love, support, patience and example have made all that I have achieved possible.